Title
The expression of cytokeratins in the preimplantation mouse embryo

Author
Emerson, Julia Andrew

Publication Date
1988

Peer reviewed|Thesis/dissertation

The Expression of Cytokeratins in the Preimplantation Mouse Embryo

by

Julia Andrew Emerson

DISSERTATION

Submitted in partial satisfaction of the requirements for the degree of

DOCTOR OF PHILOSOPHY

in

Anatomy

in the

GRADUATE DIVISION

of the

UNIVERSITY OF CALIFORNIA

San Francisco

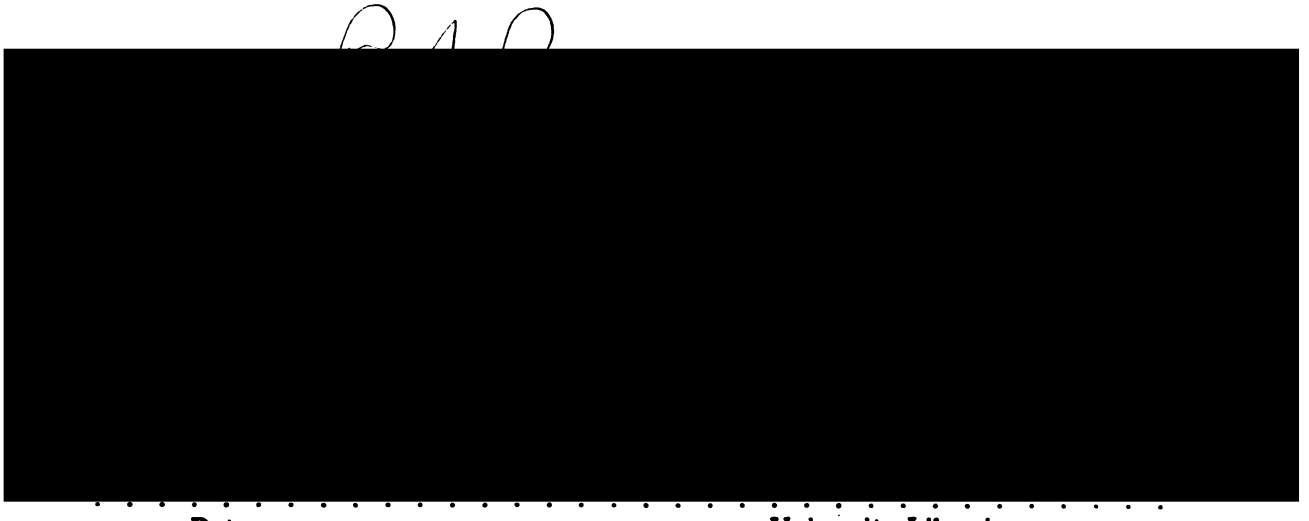

Date . . . . . **University Librarian**

Degree Conferred: JUN 12 1988 . . . . . .

ACKNOWLEDGEMENTS

I thank Dr. Robert Oshima for his gift of anti-Endo B antibody and for his helpful advice throughout the course of these experiments. I am grateful to Dr. Rolf Kemler for his generous gift of the TROMA-1 hybridoma. I am indebted to Ms. Kitty Wu for providing the embryo culture medium, to Mr. Juanito Meneses for technical assistance with the initial microinjection studies, to Dr. Akiko Spindle for her efficient supervision of the laboratory, and to Drs. Caroline Alexander and Fred Carey for their critiques of parts of this dissertation. I appreciate the advice and guidance of Drs. Pat Calarco and Zena Werb, who served on both my orals and thesis committees. Finally, I thank Dr. Roger Pedersen for his support during my graduate studies. The energy required to complete my dissertation research was garnered from days spent with my husband, Matt, at Pt. Reyes National Seashore.

ABSTRACT

The Expression of Cytokeratins in the Preimplantation Mouse Embryo

Julia Andrew Emerson

The distribution of the cytokeratin network in the intact preimplantation mouse embryo and the role of cytokeratin filaments in trophectoderm differentiation were investigated by means of whole-mount indirect immunofluorescence microscopy and microinjection of anti-cytokeratin antibody. Assembled cytokeratin filaments were detected in some blastomeres as early as the compacted 8-cell stage. The incidence and organization of cytokeratin filaments increased during the morula stage, although individual blastomeres varied in their content of assembled filaments. At the blastocyst stage, each trophectoderm cell contained an intricate network of cytokeratin filaments, and examination of sectioned blastocysts confirmed that extensive arrays of cytokeratin filaments were restricted to cells of the trophectoderm. Microinjection of anti-cytokeratin antibody into individual mural trophectoderm cells of expanded blastocysts resulted in a dramatic rearrangement of the cytokeratin network in these cells. Moreover, antibody injection into 2-cell embryos inhibited assembly of the cytokeratin network during the next two days of development. Despite this disruption of cytokeratin assembly, the injected embryos compacted and developed into blastocysts with normal morphology and nuclear numbers. These results suggest that formation of an elaborate cytokeratin network in preimplantation mouse embryos is unnecessary for the initial stages of trophectoderm differentiation resulting in blastocyst formation.

TABLE OF CONTENTS

LIST OF TABLES

LIST OF FIGURES

Introduction

The trophectoderm of the preimplantation mouse embryo is a fluid-transporting epithelium responsible for production of the blastocoel cavity and is the first epithelium to differentiate during embryogenesis (Enders, 1971; Ducibella *et al.* 1975). It is a simple epithelial layer consisting of 20 to 100 cells (Copp, 1978; Handyside, 1978; Chisholm *et al.* 1985), which contain zonular tight junctions, gap junctions, desmosomes, and cytokeratin-type intermediate filaments (Ducibella *et al.* 1975; Magnuson *et al.* 1977; for cytokeratin review, see Lehtonen, 1987). The external location of the trophectoderm facilitates its *in situ* analysis. Furthermore, the mouse embryo is devoid of all other types of intermediate filament proteins during the first several days of development (Jackson *et al.* 1980; Paulin *et al.* 1980). Thus, the preimplantation mouse embryo provides an ideal system in which to examine the role of cytokeratin filaments in the differentiation of a simple, fluid-transporting epithelium.

Intermediate filaments: subunits and structure

Intermediate filaments (IFs) are long, unbranched cytoskeletal elements that are resistant to nonionic detergent extraction in high or low salt conditions and have diameters of 8-10 nm. IFs are assembled from subunit monomers of molecular weight (M_r) 40,000 to 200,000, and they have been subdivided into five distinct classes according to their tissue-specific distributions in mammals: desmin in muscle cells, vimentin in mesenchymal cells, glial fibrillary acidic protein (GFAP) in glial cells, neurofilament proteins in neurons, and cytokeratins in epithelial cells (Table 1). In a limited number of cell types, two different IF proteins are expressed. In these instances of dual IF expression *in vivo*, vimentin is always one of the coexpressed IF polypeptides. Moreover, most cultured cell lines contain vimentin filaments, in addition to their tissue-specific IF (Osborn *et al.* 1980).

Table 1. Expression of intermediate filaments *in vivo*

IF Monomers	Molecular Weight (M_r X 10^{-3})	Cell-Type Distribution
Desmin	53	Muscle cells
Vimentin	57	Mesenchymal cells
GFAP	51	Astrocytes and related cells
Neurofilament proteins	200, 150, 68	Neurons
Cytokeratins	40-68	Epithelial cells, amphibian oocytes*
Vimentin-desmin coexpression		Certain vascular smooth muscle cells†, developing myotubes‡
Vimentin-cytokeratin coexpression		Mesothelial cells§, parietal endoderm cells**

Reviewed in Lazarides, 1980; Franke *et al.* 1982b; Osborn *et al.* 1982; Steinert *et al.* 1984a.
*Gall *et al.* 1983; Franz *et al.* 1983; Godsave *et al.* 1984; Klymkowsky *et al.* 1987.
†Quinlan & Franke, 1982; Schmid *et al.* 1982.
‡Bennett *et al.* 1979; Gard & Lazarides, 1980; Tokuyasu *et al.* 1985.
§Connell & Rheinwald, 1983; Czernobilsky *et al.* 1985; Kim *et al.* 1987.
**Lane *et al.* 1983; Lehtonen *et al.* 1983a.

Cytokeratin is used in this dissertation to refer to the keratin monomers found within living epithelial cells, to distinguish these polypeptides from the related molecules found in specialized epidermal appendages. In contrast to the other classes of IFs, cytokeratin IFs are highly variable in their composition. The cytokeratins comprise a group of at least 20 distinct polypeptides, which are differentially-expressed in various epithelial tissues (Table 2) (Moll *et al.* 1982; Fuchs *et al.* 1984; Sun *et al.* 1984; Quinlan *et al.* 1985). Examinations of their immunoreactivity (Eichner *et al.* 1984; Sun *et al.* 1983, 1985), size and charge (Moll *et al.* 1982; Schiller *et al.* 1982; Quinlan *et al.* 1985), peptide maps (Schiller *et al.* 1982), and nucleic acid hybridization (Fuchs *et al.* 1981) have resulted in the subdivision of cytokeratins into two subfamilies: Type I cytokeratins are generally smaller and acidic (isoelectric pH <5.5), whereas Type II cytokeratins are larger and more basic (isoelectric pH >6.0). Using the 2-D gel pattern as a guide, the human cytokeratins have been numbered in order of decreasing M_r, with the Type II cytokeratins numbered 1 through 8 and the Type I cytokeratins numbered 9 through 19 (Moll *et al.* 1982).

Although anywhere from 2-8 cytokeratins are expressed in any individual epithelial tissue, at least one member of each subfamily is always present (Table 2) (Moll *et al.* 1982; Franke *et al.* 1982b; Kim *et al.* 1983; Sun *et al.* 1983, 1985; O'Guin *et al.* 1987). Moreover, certain combinations of Type I and Type II cytokeratins appear to be characteristic of certain types of epithelia (Tseng *et al.* 1982; Sun *et al.* 1984). For example, cytokeratins 1/2 and 10/11 are characteristic of keratinizing epithelia, cytokeratins 3 and 12 appear only in the cornea, cytokeratins 4 and 13 are present in nonkeratinizing stratified epithelia of internal organs, and cytokeratins 8 and 18 are found primarily in simple epithelia. Sun and co-workers (1985) have termed these typically coexpressed Type I and Type II cytokeratins "keratin pairs," and their characteristic association with different programs of differentiation as the "rules of keratin pair expression." Furthermore, the components of the characteristic

Table 2. Cytokeratin polypeptides in various adult human tissues (adapted from Quinlan *et al.* 1985)

No.	1	2	3	4	5	6	7	8	9	10	11	12	13	14	15	16	17	18	19
M_r (X 10^{-3})	68	65.5	63	59	58	56	54	52.5	64	56.5	56	55	51	50	50	48	46	45	40
Isoelectric pH	7.8	7.8	7.5	7.3	7.4	7.8	6.0	6.1	5.4	5.3	5.3	4.9	5.1	5.3	4.9	5.1	5.1	5.7	5.2
Epidermis	+	(+)			+	+			+	+	+			+	(+)	+			
Vagina	+	(+)		+	+	+					(+)		+	+	(+)	(+)	(+)		
Cornea			+		+							+							
Tongue				+	+	+							+	+	(+)	+	(+)		(+)
Esophagus				+	+	(+)							+	(+)	(+)	(+)	(+)		(+)
Sweat gland					+	+	+	+						+	+		(+)	+	+
Bronchus					+	(+)	(+)	+							+		+	+	+
Urinary bladder				(+)	(+)		+	+					+					+	+
Ureter				(+)	(+)		+	+					+					+	+
Prostate gland					(+)			+										+	(+)
Ductus deferens					+		+	+										+	+
Mesothelium							+	+										+	+
Oviduct							(+)	+										+	+
Endometrium							+	+										+	+
Lung alveoli							+	+										+	+
Gall bladder							+	+										+	+
Small intestine								+										+	+
Colon								+										+	+
Renal tubules								+										+	
Pancreatic acini								+										+	
Hepatocytes								+										+	

\+ Cytokeratin always present in substantial amounts.

(+) Cytokeratin present in minor or variable amounts.

|| Separates Type II from Type I cytokeratins.

cytokeratin pairs have been conserved across various vertebrate species (Moll *et al.* 1982; Schiller *et al.* 1982; O'Guin *et al.* 1987), indicating that evolutionary selection has acted to preserve them. Therefore, the particular structural needs of different epithelia may be fulfilled by cytokeratin networks of defined composition.

When the genomes of several vertebrate species (man, mouse, chicken, and hagfish) were probed for their presence of keratin sequences, each species was found to contain approximately equal numbers of Type I and Type II sequences, with at least one of each (Fuchs *et al.* 1981). Thus, evolutionary pressures have also acted to maintain two types of keratin sequences in vertebrate genomes. As will be discussed in the section on IF assembly, the conservation of two types of keratin gene sequences and the expression of at least one member of each cytokeratin family in all epithelial cells is due to the requirement for both a Type I and a Type II cytokeratin in the assembly of extensive 10-nm cytokeratin filaments.

In recent years, partial or complete amino acid sequence information has been obtained for several IF proteins (Geisler & Weber, 1982; Geisler *et al.* 1982, 1983, 1984, 1985a; Hanukoglu & Fuchs, 1982, 1983; Quax *et al.* 1983, 1985; Quax-Jeuken *et al.* 1983; Steinert *et al.* 1983, 1984b, 1985a; Hoffmann & Franz, 1984; Jorcano *et al.* 1984a, b; Lehnert *et al.* 1984; Lewis *et al.* 1984; Glass *et al.* 1985; Hoffmann *et al.* 1985; Jonas *et al.* 1985; Winkles *et al.* 1985; Bader *et al.* 1986; Franz & Franke, 1986; Knapp *et al.* 1986; Leube *et al.* 1986, 1988; Magin *et al.* 1986; Oshima *et al.* 1986; Singer *et al.* 1986; Alonso *et al.* 1987; Eckert, 1988). Despite their differences in primary amino acid sequences, analyses of secondary structure have revealed that all IF subunits possess a remarkably similar structure (reviewed in Steinert & Parry, 1985; Steinert *et al.* 1985b; Weber & Geisler, 1985; Fuchs *et al.* 1987). In contrast to the globular subunits of microfilaments (actin) and microtubules (tubulin) (Alberts *et al.* 1983), IF monomers are fibrous proteins that contain extensive α-helical regions. The distinguishing features of all IF polypeptides are a central α-helical

domain of approximately 310 amino acid residues flanked by non-α-helical N- and C-terminal domains of variable size and chemical character (Fig. 1). The central α-helical rod of all IF polypeptides is not continuous and is interrupted by three regions of non-α-helical sequences (linkers L_1, L_{12}, and L_2). However the four resulting α-helical subdomains (1A, 1B, 2A, and 2B) are nearly constant in size among all IF subunits, and each half of the α-helical rod has a length of approximately 21-23 nm. The central α-helical regions of IF monomers are able to form interchain coiled-coil elements, due to the arrangement of the amino acid residues into a series of heptad repeats, **a**-b-c-**d**-e-f-g, where **a** and **d** are usually hydrophobic. With 3.6 residues occurring per turn of the α-helix, the hydrophobic residues of the repeating heptads form an inclined stripe around the α-helix. The hydrophobic residues of two α-helical strands can then interface to form a coiled-coil rope structure. Thus, the backbone of the coiled-coil consists of the hydrophobic residues, while residues b, c, e, f, and g, which are usually polar or charged, assume superificial positions. These residues often appear as alternating clusters of charged and uncharged residues with a regular period along the length of the α-helix, suggesting that electrostatic interactions may play a role in the lateral association and stabilization of the two α-helices. Ionic interaction analyses have suggested that the largest number of favorable interactions will occur if the two subunits of the coiled-coil are parallel to each other and in register (Steinert *et al.* 1984b). Sequencing of α-helical-enriched, two-chain particles generated by tryptic digestion and analyses of cross-linked molecules have confirmed the parallel, in-register arrangement of the two chains (Parry *et al.* 1985).

While maintaining the conserved features described above, the exact sequences of the central domains of different IF monomers have diverged, which has formed the basis for their reclassification into sequence types: Type I and Type II IF proteins include the two subfamilies of cytokeratins, as described earlier, and Steinert and co-workers (1984b, 1985a)

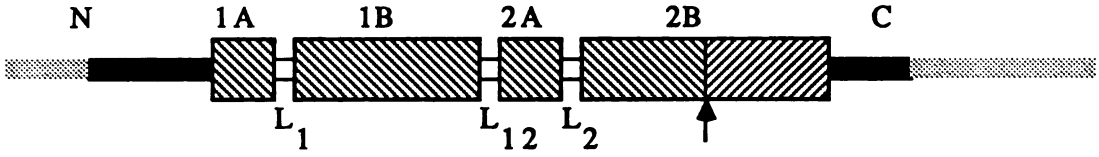

Fig. 1. Predicted secondary structure of IF monomers based on amino acid sequence. The central alpha-helical rod is subdivided into 4 coiled-coil tracts (1A, 1B, 2A, and 2B) by 3 non-alpha-helical spacers (L1, L12, and L2). N and C, respectively, are the non-alpha-helical head and tail end domains, which have variable lengths and sequences depending on the IF type. The arrow indicates an abrupt reversal of the heptad repeats, which is present in coil 2B of all IF monomers.

have attributed the overall charge differences between Type I (acidic) and Type II (neutral-basic) cytokeratins to a greater number of basic residues in the 2B subdomain of Type II cytokeratins; Type III IF proteins include vimentin, desmin, and GFAP; and Type IV includes the neurofilament proteins (Steinert & Parry, 1985; Steinert *et al.* 1985b; Fuchs *et al.* 1987). Recent data have indicated that the amino acid sequences of nuclear lamins A and C are strikingly similar to the cytoplasmic IFs (Fisher *et al* 1986; McKeon *et al.* 1986). Thus, the lamins have been included in the IF gene family (Franke, 1987) and comprise the Type V IF polypeptides (Fuchs *et al.* 1987). Sequence similarities in the rod domain within each type range from 50-100%, whereas similarities across types are less than 30%. The sequence similarities across types are generally restricted to certain subdomains, with the last 30 residues of coil 2B comprising the most highly conserved sequence among the IF proteins. The consensus sequence EIATYR(X)LLEGE demarcates the end of coil 2B in all IF proteins and is the epitope recognized by the anti-IFA antibody (Geisler *et al.* 1983; Magin *et al.* 1987), which readily explains the reactivity of this antibody with all types of IFs (Pruss *et al.* 1981).

The structures of the IF genes that have been characterized to date also support the classification of IF monomers into IF types (Quax *et al.* 1983, 1985; Lehnert *et al.* 1984; Marchuk *et al.* 1984, 1985; Balcarek & Cowan, 1985; Johnson *et al.* 1985; Krieg *et al.* 1985; Rieger *et al.* 1985; Steinert & Parry, 1985; Tyner *et al.* 1985; Lewis & Cowan, 1986; Miyatani *et al.* 1986; RayChaudhury *et al.* 1986; Fuchs *et al.* 1987; Myers *et al.* 1987). As illustrated in Fig. 2, Types I, II, and III have similar intron/exon organizations. The majority of the introns occur within the α-helical rod domain (6/7 in Type I, 7/8 in Type II, and 6/8 in Type III), and the positions of 5 of these are highly conserved among the three types. Interestingly, only one of the conserved introns, which is located at the end of the α-helical domain, demarcates the beginning or end of a major structural subdomain. However, introns that interrupt the α-

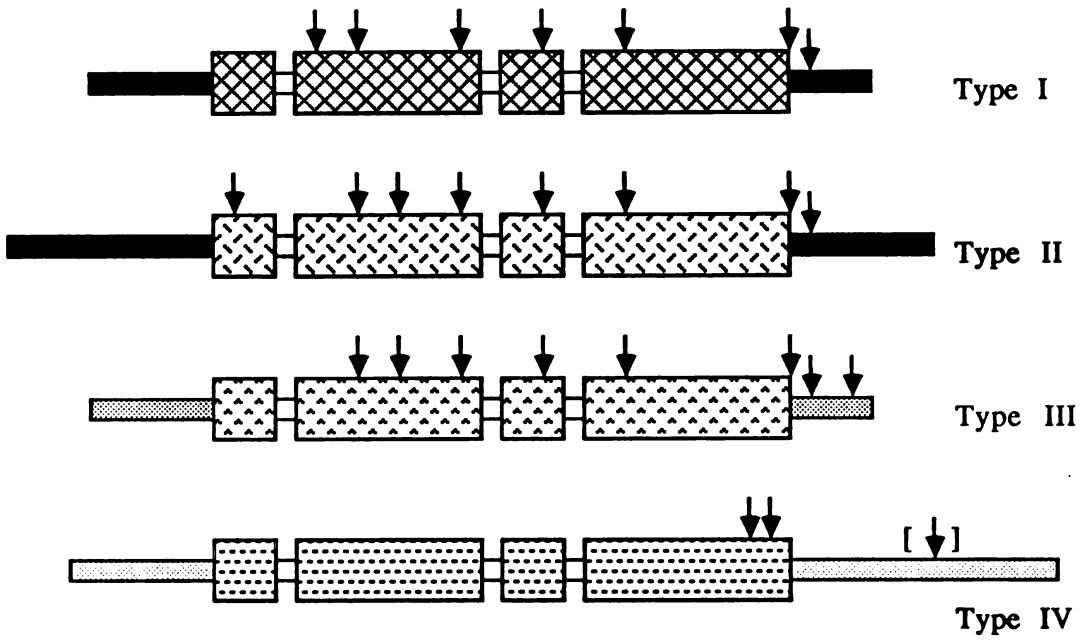

Fig. 2. Organization of IF genes. The positions of the introns as related to the IF subdomain organization (see Fig. 1) are indicated by the arrows. Types as follows: Type I (acidic cytokeratins), Type II (basic cytokeratins), Type III (desmin, GFAP, vimentin), and Type IV (neurofilament proteins). The gene organization of the cytokeratins is a consensus, as some variations in intron location, especially in the C-terminal domain, occur in different members of these families. The brackets around the intron in the terminal domain of the Type IV gene are used to indicate that this intron is absent in the NF-M gene (adapted from Fuchs et al. 1987).

helical domain generally occur at or very near the beginning of heptad repeats. All of these conserved features indicate that the Type I, II, and III IF genes arose from a common ancestral gene. Type I and Type II cytokeratin genes can each be distinguished by one uniquely-positioned intron in their α-helical regions, which differs between types but is highly conserved among all members within a type. The distinguishing feature of Type III IF genes is a second intron in their C-terminal domains, and the location of both C-terminal introns of Type III genes is strictly conserved among all members.

Surprisingly, the organization of neurofilament (NF) genes is very different (Fig. 2). The gene encoding the murine NF polypeptide of M_r 68,000 (NF-L) has only three introns, none of which are in similar positions to any introns of the other three IF types (Lewis & Cowan, 1986). These authors proposed that an mRNA-mediated transposition event of an expressed, intron-less ancestral IF gene created a new sequence that was subsequently duplicated to form the NF gene family; the insertion of introns into the duplicated sequences and the addition of exons to the carboxy termini would have produced the modern NF genes. Because the primary amino acid sequences of NF polypeptides have a higher similarity to the sequences of desmin, vimentin, and GFAP than do those of the cytokeratins, Lewis and Cowan (1986) suggested that this transposition event occurred after the divergence of the cytokeratin genes. However, the gene encoding the human NF protein of M_r 150,000 (NF-M) has only two introns, the positions of which are shared with the first two introns of the NF-L gene (Myers *et al.* 1987). Thus, these authors suggested that the introns shared by the NF-L and NF-M genes must have been acquired by the ancestral NF gene before its duplication to be consistent with the hypothesis of Lewis and Cowan (1986). In addition, Myers and co-workers (1987) proposed an alternative hypothesis to explain the generation of IF gene diversity: NF gene divergence occurred before that of the cytokeratins and the other IFs, from an ancestral IF gene with two (or fewer) introns. Hence, they argued that gene

organization, rather than amino acid similarity, is the major indicator of evolutionary distance. The isolation and characterization of other IF genes, especially the high molecular weight NF gene and the IF genes of early metazoa, may enable investigators to distinguish between these two possibilities.

From the preceeding paragraphs, it is clear that although many amino acid substitutions have been tolerated, the overall structure of the central α-helical rod domain has been highly conserved and is the basis of the structural similarity of IFs composed of different IF monomers (Henderson *et al.* 1982; Milam & Erickson, 1982; Steinert *et al.* 1982a, b). In contrast, the N-terminal head and C-terminal tail domains of IF polypeptides have variable sequences and properties. Consequently, it has been proposed that the variable properties of IFs assembled from different monomers result from the projection of the terminal domains away from the coiled-coil backbone of the filament. Subsequent experiments have confirmed the peripheral location of the terminal domains. When intact IFs were subjected to limited proteolysis, the morphology of the filaments seemed relatively unaffected (Sauk *et al.* 1984; Steinert *et al.* 1984b). However, more detailed analyses of the protease-treated filaments revealed that their relative α-helical content had increased, while the M_r of the subunit monomers had decreased. In addition, Steinert *et al.* (1984b) determined that almost all of the phosphate content (as phosphoserine) and two-thirds of the glycine content of epidermal cytokeratins were removed by this treatment. Because the head and tail domains of epidermal cytokeratins are enriched in glycine and serine residues, all of these results are consistent with the accessibility to and removal of IF end domains by limited proteolytic attack.

Intermediate filament assembly

The major aim of this dissertation was to assess the role of cytokeratin filaments in a developing epithelium. The experimental approach I used to accomplish this aim was the

antibody-mediated inhibition of cytokeratin assembly in the developing mouse embryo. As successful use of this experimental approach requires an understanding of the process of IF assembly, it will be reviewed in this section.

Once the denaturing agents used to solubilize the subunit monomers of IFs are removed, IF polypeptides will reassemble *in vitro* into IFs, without the presence of accessory proteins, metal ions, or energy sources (Henderson *et al.* 1982; Steinert *et al.* 1982a, b). By varying the concentration of certain denaturing agents, soluble intermediates in the assembly of 10-nm filaments have been isolated and characterized. The basic building block of IFs is the protofilament, a tetramer composed of two double-stranded coiled-coils, with a rod-like structure 45-50 nm long and 2-3 nm wide (Geisler *et al.* 1982; Geisler & Weber, 1982; Quinlan *et al.* 1984; Sauk *et al.* 1984). Close examination of protofilaments showed them to be of uniform diameter throughout their length, indicating that the 2 coiled-coils of the protofilament are in exact axial register (Ip *et al.* 1985). The orientation of the two coiled-coil dimers with respect to each other is uncertain, with evidence for both anti-parallel (Geisler *et al.* 1985b; Fraser *et al.* 1985) and parallel (Georgatos & Blobel, 1987a; Ip, 1988) arrangements.

Although the protofilament is the most stable, soluble intermediate in IF assembly, its subunit composition suggests that a single coiled-coil dimer is the first intermediate in IF formation. Quinlan *et al.* (1986) have recently succeeded in stabilizing coiled-coil dimers of Type III and Type IV IF polypeptides in solutions containing 3M guanidinium hydrochloride (Gu•HCl). Direct extraction of IF networks in Gu•HCl followed by chemical cross-linking also revealed complexes consisting of only two subunits, indicating that the dimer is an integral part of native IFs. Furthermore, additional cross-linking experiments of Quinlan and co-workers (1986) have supported the earlier proposals that the coiled-coils of the dimers are parallel and in exact axial register.

The formation of 2-chain and 4-chain complexes appear to be the rate-limiting steps in IF assembly, and after the tetramer is formed, the rest of IF assembly proceeds rapidly (Steinert *et al.* 1985b). However, by varying the ionic strength of the assembly buffer, structures intermediate in size between the protofilament and the 10-nm filament have been detected. One such structure is a 70-nm rod, the diameter of which is 8 nm in the middle, but approximately 5 nm at its ends (Ip *et al.* 1985). In addition, these rods frequently exhibit a longitudinal split into two fibers of equal width. Thus, Ip and colleagues (1985) suggested that these structures represent two laterally-associated protofilaments, each with a half-length (22-24 nm) axial displacement with respect to its neighbor (Fig. 3a). The next largest intermediate observed by Ip *et al.* (1985) were short (66-70 nm), full-width 10-nm filaments. Many of these structures had tapered ends, while other ends were splayed, enabling the number of component fibers to be counted. In no case did the number exceed four. Therefore, Ip and co-workers (1985) proposed that the lateral association of four pairs of staggered protofilaments had occurred, resulting in a minimal-length, full-width 10-nm filament (Fig. 3b). Formation of extended 10-nm filaments would then occur by the end-to-end association of additional protofilaments (Fig. 3c). They concluded that full-width IFs contain eight protofilament strands, and the total number of IF monomers within any cross-sectional unit of an IF is thirty-two. Up to eight protofilament strands per 10-nm filament have been observed in unraveled cytokeratin filaments (Aebi *et al.* 1983), and an 8-protofilament IF correlates well with mass-per-unit-length measurements obtained by scanning transmission electron microscopy (Ip *et al.* 1985 and references therein). Finally, the half-axial stagger of the protofilaments in this model could be responsible for the 21-23 nm axial repeat that is frequently observed in 10-nm filaments by electron microscopy (Henderson *et al.* 1982; Milam & Erickson, 1982; Aebi *et al.* 1983; Ip *et al.* 1985).

A fibrillar, 4.5-nm wide component of 10-nm filaments has been detected in unraveled

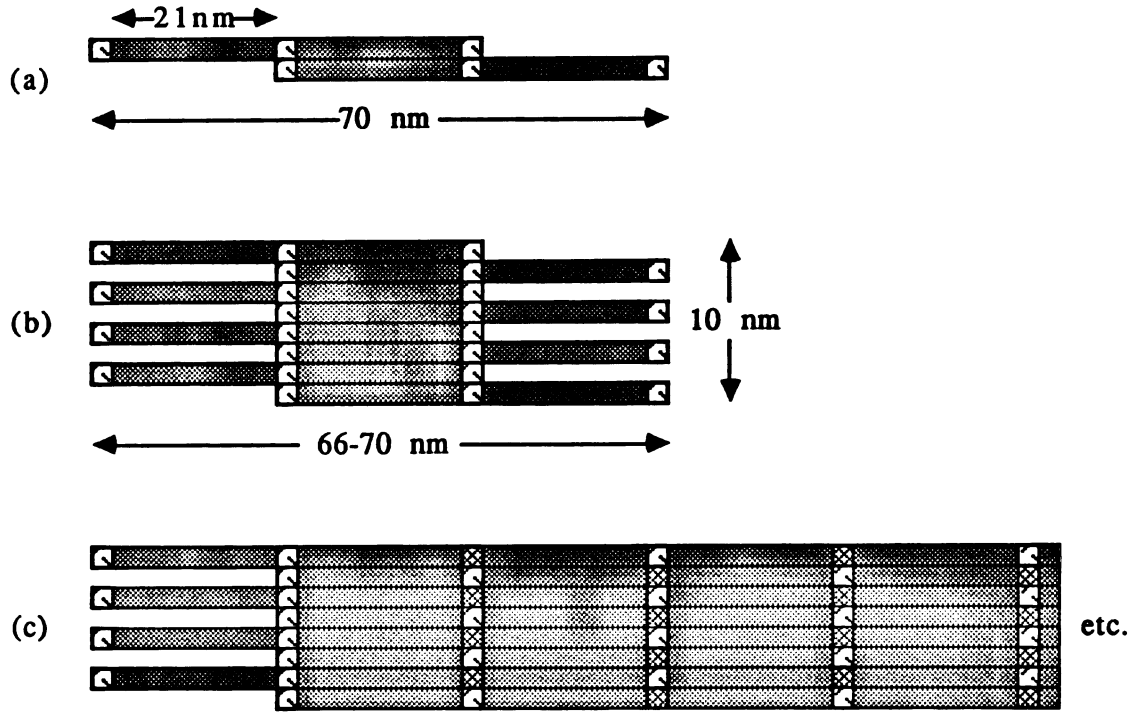

Fig. 3. Hypothetical assembly intermediates of a 10-nm filament. (a) The half-unit staggered arrangement of 2 tetrameric protofilaments. The filled bars represent the two major alpha-helical coils of the central rod domain, which are separated by spacer L12 and bordered by the non-alpha-helical N- and C-terminal domains (open boxes). (b) The minimal-length, full-width IF, composed of 8 protofilaments, each staggered by 21 nm with respect to its neighbors. (c) The end-to-end addition of protofilaments to form an extended, 10-nm filament. Notice only 4 protofilaments are predicted to protrude from either end of the IF (adapted from Ip et al. 1985).

segments of IFs (Aebi *et al.* 1983; Quinlan *et al.* 1984; Sauk *et al.* 1984; Ip, 1988). Aebi and co-workers suggested that this component represents a dimer of protofilament strands, is a distinct level of organization of 10-nm filaments, and named it a protofibril. As no more than four protofibrils have been detected per 10-nm filament, this intermediate is not inconsistent with the model of Ip *et al.* (1985). A schematic drawing that includes all of the proposed structural elements of an IF is shown in Fig. 4.

The ability of IF polypeptides to self-assemble *in vitro* indicates that all information necessary for IF assembly is contained within the monomers themselves. As discussed earlier, the central α-helical rods of the IF polypeptides form the structural backbone of IFs, and the ability to form coiled-coil dimers is inherent in the amino acid arrangement of this domain. However, the possible roles of the non-α-helical end domains in IF assembly is not obvious from analyses of their amino acid sequences. Therefore, several experiments have been performed to investigate the importance of the N- and C-terminal domains in IF assembly. If intact IFs are subjected to limited proteolysis (of slightly longer duration than discussed earlier), the filaments dissociate into protofilaments, which cannot reassemble into 10-nm filaments (Geisler & Weber, 1982; Sauk *et al.* 1984; Steinert *et al.* 1984b). Because the non-α-helical terminal domains are selectively digested by this treatment, they were deemed necessary for the assembly of both full-width (lateral associations) and full-length (end-to-end associations) 10-nm filaments.

Subsequently, more precise analyses were performed to determine whether both of the non-α-helical termini are necessary for *in vitro* IF assembly. Removal of N-terminal peptides with a proteinase specific for the head domain of vimentin and desmin completely inhibited their assembly into IFs (Nelson & Traub, 1983). Moreover, addition of N-terminal peptides to intact vimentin polypeptides also inhibited their assembly into 10-nm filaments (Traub & Vorgias, 1983). When Kaufmann and co-workers (1985) removed as few as 67 N-terminal

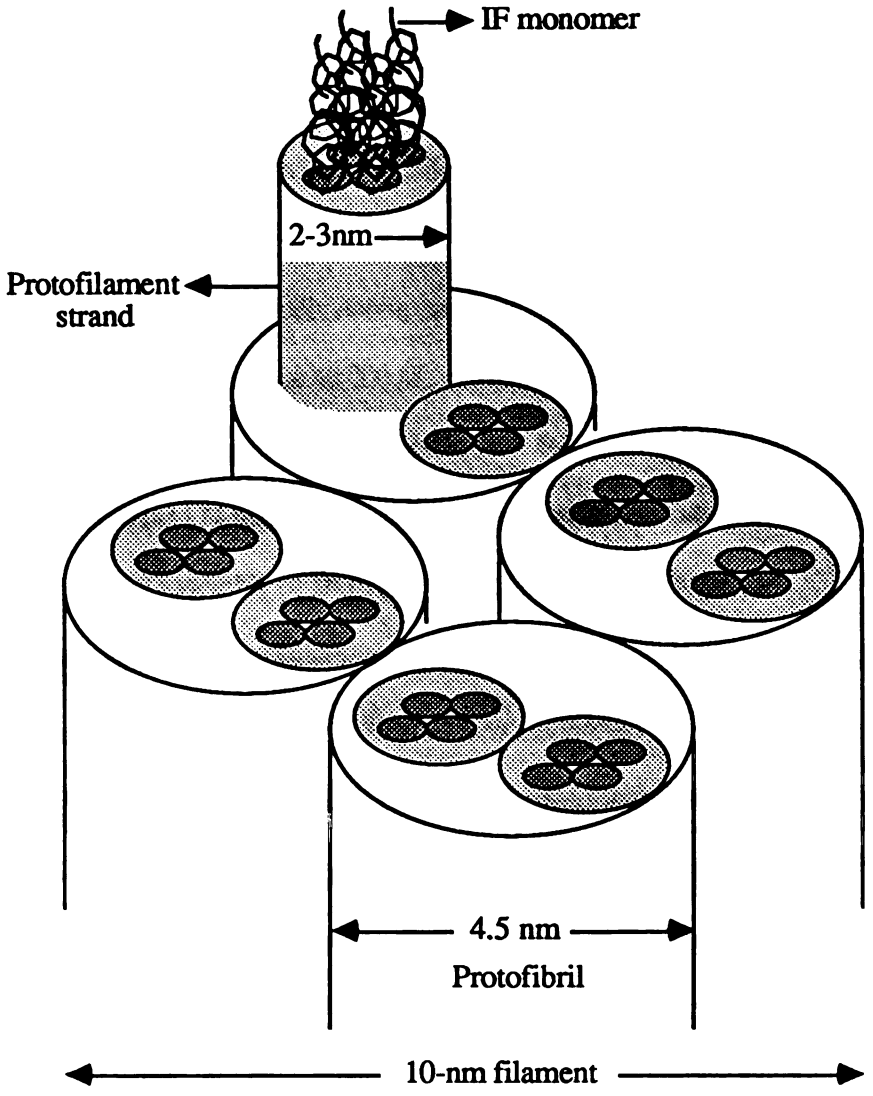

Fig. 4. An exploded, schematic diagram of an intermediate filament, consisting of three levels of fibrillar organization: the protofilament, the structural basis of which is a tetramer of coiled-coil IF monomers; the protofibril, made up of two protofilament strands helically-twisted around each other; the 10-nm filament, consisting of 4 protofibrils, also in a helical arrangement (adapted from Fuchs et al. 1987).

residues from desmin, IF assembly was completely inhibited. In contrast, removal of the last half of the C-terminal domain (27 residues) had no effect on the assembly of desmin polypeptides into IFs of normal morphology. This apparent non-requirement of the C-terminal domain for IF assembly is indicated simply by the existence of the 40,000 M_r cytokeratin (K19). This protein is the smallest IF monomer, primarily due to the absence of a non-α-helical carboxy tail: a 13-amino acid extension of the heptad repeats follows the consensus sequence that normally demarcates the end of the α-helix (Bader *et al.* 1986; Eckert, 1988). Nevertheless, the 40,000 M_r cytokeratin is an integral component of cytokeratin filaments in many different epithelia (Moll *et al.* 1982; Quinlan *et al.* 1985). Thus, whereas the nonhelical N-terminal domain is required, a non-α-helical tail appears to be unnecessary for the assembly of IF polypeptides into 10-nm filaments.

If IF monomers with N-terminal deletions are mixed with intact IF monomers, the shortened polypeptides will be incorporated into assembled IFs (Sauk *et al.* 1984; Kaufmann *et al.* 1985). However, if this mixing is done at the protofilament stage, the protofilaments composed of the N-terminal-deleted polypeptides are excluded from the assembled IFs (Kaufmann *et al.* 1985). Therefore, the presence of some N-terminal sequences in the tetrameric protofilament is able to compensate for the absence of others in assembling IFs beyond the protofilament stage. Hence, a major role of the N-terminal domains in IF assembly may be to align and stabilize the staggered arrangement of the protofilaments (Fig. 3) (Ip *et al.* 1985; Kaufmann *et al.* 1985).

The putative binding activity of the N-terminal heads of IF monomers may be mediated by their arginine-rich, basic nature (Geisler *et al.* 1982, 1983; Quax-Jeuken *et al.* 1983; Jorcano *et al.* 1984b; Steinert *et al.* 1984b; Glass *et al.* 1985; Bader *et al.* 1986; Franz & Franke, 1986; Oshima *et al.* 1986; Singer *et al.* 1986; Alonso *et al.* 1987; Eckert, 1988). Synthesis of vimentin in the presence of canavanine, an amino acid analogue of arginine, will

inhibit the incorporation of newly-synthesized vimentin monomers into the Triton-X-100-insoluble cytoskeletal fraction of chicken erythroid cells (Moon & Lazarides, 1983). Moreover, all 10 arginine residues in the head domain of desmin are contained in the 67 amino acids removed to produce the assembly-incompetent derivative of Kaufmann and co-workers (1985). Furthermore, Traub and Vorgias (1983) observed that the addition of free arginine, but not free lysine, to the assembly buffer will inhibit vimentin filament assembly *in vitro*. Finally, Traub and Vorgias (1983) also demonstrated the retention by an arginine-affinity matrix of α-helical core particles derived from desmin and vimentin. Because the NF-L polypeptide, GFAP, and cytokeratin monomers also exhibited strong affinities for the arginine matrix, these authors suggested that the arginine-rich, N-terminal domains of IF monomers interact with central nonhelical domains of neighboring polypeptides during IF assembly. Thus, the 21-nm axial repeat of IFs may be due to the staggered arrangement of the central α-helical rods, each half of which is approximately 21 nm in length, produced by the N-terminal association of IF monomers in one protofilament with the central, non-α-helical spacer (L_{12}) of IFs in neighboring protofilaments.

Since the basic N-terminal domains of IF monomers seem to be essential for their assembly into 10-nm filaments, antibodies directed against N-terminal epitopes are predicted to have a pronounced inhibitory effect on IF assembly. In a related set of experiments, Ip (1988) showed that a monoclonal antibody, which recognizes an epitope near the N-terminal end of the central α-helical rod of desmin, will inhibit the *in vitro* assembly of desmin protofilaments into 10-nm filaments, but has no effect on the assembly state of preformed desmin filaments. Because this antibody does not decorate intact filaments, it is likely that its epitope becomes buried (hence inaccessible to the disrupting influence of the antibody) upon assembly into IFs. Nevertheless, these results indicate that even antibodies whose epitopes are close to the N-terminal domain may be effective in the inhibition of *de novo* intracellular

assembly of IFs. Interestingly, another monoclonal antibody, which binds to a more central epitope of the α-helix, had no effect on either assembly or disassembly of desmin filaments (Ip, 1988). Thus, antibody-mediated inhibition of IF assembly cannot be accounted for simply by steric hindrance of an antibody molecule bound to any region of the IF molecule. Rather, it appears to be site-specific, with the proposed location of active epitopes in the N-terminal domain, or very close to it. Mapping the epitopes of known IF-disrupting monoclonal antibodies (Klymkowsky, 1982; Lane & Klymkowsky, 1982; Klymkowsky *et al.* 1983; Tölle *et al.* 1985; Tölle *et al.* 1986; Results, this dissertation) should address this hypothesis.

As mentioned previously, although the various classes of IF monomers have different sizes and chemical properties, they all assemble into structurally-similar filaments (Steinert *et al.* 1982a, b). However, a major difference in assembly properties exists between the cytokeratins and the other classes of IFs. Whereas purified Type III monomers and the 68,000 M_r neurofilament protein readily self-assemble into homopolymers, cytokeratin IFs are obligate heteropolymers. Cytokeratin filament assembly will occur only if both a Type I and a Type II cytokeratin are present (Hatzeld & Franke, 1985; Eichner *et al.* 1986). Moreover, the different classes of Type III monomers readily copolymerize with each other, both *in vitro* (Steinert *et al.* 1981; Steinert *et al.* 1982a, b) and intracellularly (Quinlan & Franke, 1982; Quinlan & Franke, 1983; Sharp *et al.* 1982; Tokuyasu *et al.* 1985; Tölle *et al.* 1986). Although Steinert *et al.* (1982a) achieved limited copolymerization *in vitro* of cytokeratin and Type III monomers, other investigators (Franke *et al.* 1983; Hatzfeld *et al.* 1987) have not detected any cytokeratin/Type III complexes. Furthermore, the intracellular networks of cytokeratin and Type III IFs are always separate (Osborn *et al.* 1980; Franke *et al.* 1982; Kreis *et al.* 1983). Therefore, the requirement of a Type I and a Type II cytokeratin for cytokeratin filament formation appears to be rigid and the only biologically-relevant

association of the cytokeratin monomers.

More detailed examinations of cytokeratin assembly intermediates have revealed that the cytokeratin protofilament is a heterotypic tetramer, containing equimolar amounts of a Type I and a Type II cytokeratin (Franke *et al.* 1983; Quinlan *et al.* 1984; Hatzfeld & Franke, 1985; Parry *et al.* 1985). Although cytokeratin dimers consisting of a single cytokeratin type have been obtained by the *in vitro* reconstitution of purified monomers in GuHCl (Quinlan *et al.* 1986), these complexes were not especially stable and have not been isolated from native cytokeratin filaments by chemical cross-linking (Quinlan *et al.* 1984). In contrast, two-chain particles consisting of equimolar amounts of Type I and Type II molecules have been isolated from native cytokeratin filaments (Parry *et al.* 1985). Thus, the biologically-relevant composition of the coiled-coil is most likely a heterodimer.

An additional peculiarity of cytokeratin expression is the presence of characteristic cytokeratin pairs in certain kinds of epithelial tissues (Sun *et al.* 1985). Recent experiments have investigated whether there is a structural basis for the "rules of keratin pair expression." For example, structural incompatabilities do not appear to be the basis for cytokeratin pair association, as Hatzfeld and Franke (1985) have demonstrated that pairs of cytokeratins that are never coexpressed *in vivo* will nevertheless associate into complexes *in vitro*. However, the stabilities of the foreign pair complexes were not as great as the stabilities of the normal pairs, and structural differences may lead to the preferential association of cytokeratins that normally copolymerize *in vivo*. In this respect, Eichner *et al.* (1986) have detected the preferential association of specific cytokeratin pairs in a mixture of epidermal cytokeratins, which resulted in the formation of cytokeratin filaments with different physical properties. Therefore, although all combinations of Type I and Type II cytokeratins can complex with each other *in vitro*, the *in vivo* expression and association of certain subsets of cytokeratin pairs predominates and probably results in filaments of distinct physical properties and

functions. One regulatory mechanism which could easily account for the rules of cytokeratin pair expression is the coordinate regulation of cytokeratin gene expression via similar *cis*-acting DNA sequences. Continuing analyses of cytokeratin genes and their expression will undoubtedly address this possibility (for example, see RayChaudhury *et al.* 1986).

A novel assay has been recently developed to study the structural basis of Type I and Type II cytokeratin association (Hatzfeld *et al.* 1987; Magin *et al.* 1987). The specificity of the blot-association assay was affirmed by the binding of labeled cytokeratins to blotted cytokeratins of the complementary type, but not to cytokeratins of the same subfamily, desmin, or vimentin (Hatzfeld *et al.* 1987). In addition, the isolated α-helical core of each cytokeratin tested was sufficient for its association with complementary cytokeratins. Moreover, each coil (1 and 2) of the rod domain of a Type II cytokeratin was able to individually associate with the intact rod domain of Type I cytokeratins. Therefore, Magin *et al.* (1987) investigated the ability of a Type II cytokeratin, which possessed N- or C-terminal deletions of varying size, to bind to a blotted Type I cytokeratin. Their results suggest that there are at least two independent sites in the α-helical rod that can mediate heterotypic association of cytokeratins: a 37 amino acid stretch in the middle of coil 2 and an as yet undefined region in coil 1. As will be discussed later in this dissertation, experimental results of this nature are important when designing experiments to interfere with the intracellular assembly of cytokeratin filaments.

The intracellular assembly of intermediate filaments

The factors controlling the intracellular assembly of IFs are less well understood, due to the increased difficulty in performing experiments to address this issue. However, a few interesting studies have been performed and are reviewed in this section.

Unlike the other major cytoskeletal elements, there does not appear to be a large,

soluble pool of IF subunits within cells, and newly-synthesized IF polypeptides are rapidly incorporated into the cytoskeletal fraction (Blikstad & Lazarides, 1983). Moreover, IF subunits in the soluble fraction exist primarily as tetrameric protofilaments (Soellner *et al.* 1985), indicating the increased stability of IF monomers in the tetrameric state. Using isolated nuclear envelope and plasma membrane fractions from avian erythrocytes, Georgatos and Blobel (1987a, b) have proposed that the intracellular assembly of vimentin is vectorial, initiating with the association of the C-terminal tails of vimentin monomers with lamin B in the nuclear envelope, followed by filament assembly and extension, and terminating by binding of the N-terminal head of the filaments to ankyrin (Georgatos & Marchesi, 1985). However, the intracellular *de novo* assembly of cytokeratins may occur in a different fashion. Kreis and co-workers (1983) microinjected an mRNA fraction enriched for epidermal cytokeratins into nonepithelial cells, which do not normally express cytokeratin. The assembly of cytokeratin IFs occurred in the injected cells after a lag of a few hours, but the appearance of an extensive cytokeratin network was preceeded by the formation of short rods and fibrils scattered throughout the cytoplasm. Thus, cytokeratin filament assembly appeared to initiate in many areas of the cell and was not restricted to the plane of the nuclear envelope.

Slightly different results were obtained if the mRNA fraction enriched in epidermal cytokeratins was injected into simple epithlial cells, which do not normally express epidermal cytokeratins, but do express an IF network composed of other cytokeratins (Franke *et al.* 1984). In these cells, the epidermal cytokeratins rapidly (within half an hour) assembled into filaments that extended throughout the cell. Moreover, the epidermal cytokeratins were colocalized with the endogenous cytokeratins in the same filaments. Thus, in the presence of an intact cytokeratin network, even if it is composed of foreign cytokeratins, cytokeratin monomers are rapidly integrated into filaments. The integration of epidermal cytokeratins

into the cytokeratin filaments of simple epithelial cells was also observed by Giudice and Fuchs (1987), who transfected plasmids containing SV40 enhancer-driven epidermal cytokeratin genes (K14 or K6b) into PtK_2 cells. Whether the expression of epidermal cytokeratins in cells of a simple epithelium has any long-term effect on the function or differentiative state of those cells has not yet been reported.

When the chimeric, K14 construct of Giudice and Fuchs (1987) was transfected into fibroblasts, the K14 gene was expressed and translated, but the cytokeratin accumulated into aggregates. Thus, the nonepithelial environment of the fibroblast appears to be permissive for the synthesis and accumulation of a Type I cytokeratin, but the cytokeratin cannot assemble into filaments in the absence of a complementary Type II cytokeratin. Moreover, as shown in the *in vitro* assembly experiments, vimentin cannot substitute for the complementary cytokeratin in IF assembly, as no colocalization of K14 with the endogenous vimentin filament network of the fibroblasts was observed. In a related study, Kulesh and Oshima (1988) investigated the expression of a transfected, simple cytokeratin gene (K18) in both epithelial and nonepithelial murine cell lines. Because indirect immunofluorescence analyses were not performed as part of this study, the assembly of K18 into filaments was not revealed by the results. However, an intriguing observation was made on the relative levels of K18 protein in fibroblasts as compared to epithelial cells: whereas the K18 gene was expressed efficiently and equally well in both cell types, the K18 protein was stable only in the epithelial cells. Therefore, in the absence of a complementary Type II cytokeratin with which it can complex, the K18 protein is turned over relatively quickly. However, some K18 does accumulate in the transfected fibroblasts and may form aggregates similar to those seen by Giudice and Fuchs (1987).

When the desmin gene was transfected into nonmuscle cells, a small percentage of transfected cells expressed desmin, which was colocalized with the endogenous vimentin in

extensive IF arrays (Quax *et al.* 1985). Thus, it appears that a muscle-specific environment is not essential for desmin synthesis. However, because the desmin molecules in the transfected cells colocalized with the vimentin filaments endogenous to the cell, the integration of desmin monomers into filaments may simply be due to their ability to readily coassemble with vimentin (Steinert *et al.* 1982a, b). Thus, the ability of a nonmuscle cell to *assemble* desmin IFs may be better addressed using a cell type that lacks vimentin. As most cultured cell lines possess vimentin, alternative strategies, such as the production of transgenic mice containing hybrid IF genes (for example, see Krimpenfort *et al.* 1988), may have to be employed to address this problem.

Although the experimental results of Kreis and co-workers (1983) demonstrate that fibroblasts will synthesize and assemble epithelial-specific cytokeratin filaments if provided with abundant cytokeratin mRNAs, the expression of cytokeratins normally does not occur in nonepithelial cells. The nature of epigenetic factors that may influence cytokeratin expression has been explored by analyses of cultured cells. The mesothelium is a simple squamous epithelium that lines the body cavities and coats the viscera contained within them, and its cells express cytokeratins 7, 8, 18, and 19 and variable amounts of vimentin (Connell & Rheinwald, 1983; Czernobilsky *et al.* 1985; Kim *et al.* 1987). When present, the vimentin content of mesothelial cells *in vivo* is low relative to their content of cytokeratins. However, when placed in culture and exposed to different culture conditions, mesothelial cells will alter their synthesis of the two IF classes (Connell & Rheinwald, 1983; Kim *et al.* 1987). The results of both studies strongly suggest that high levels of cytokeratin synthesis are dependent upon extensive intercellular contacts. A similar conclusion was reached by Ben-Ze'ev (1984), who cultured Madin-Darby bovine kidney cells at different densities. Futhermore, changes in the levels of synthesis of the cytokeratin polypeptides were correlated with changes in cytokeratin mRNA levels (Ben-Ze'ev, 1984; Kim *et al.* 1987). Thus, formation of extensive

intercellular contacts appears to result in an up-regulation of cytokeratin gene expression, although differences in mRNA stability have yet to be ruled out. However, extensive cell-cell contacts do not appear to be sufficient for high levels of cytokeratin expression *in vitro*, as Kim *et al.* (1987) demonstrated an additional requirement for retinoids in this process. Hence, the control of cytokeratin synthesis *in vivo* is likely regulated by many components.

Intermediate filaments: structures in search of a function

The identification of cells lacking IFs has indicated that IFs are not essential for basic cellular functions, such as cell proliferation or cell growth (Jackson *et al.* 1980; Traub *et al.* 1983; Venetianer *et al.* 1983; Hedberg & Chen, 1986). However, the cell-type specific expression of IFs composed of different polypeptides argues inherently for a tissue-specific functional role of these structures. Unfortunately, while abundant descriptive data have been accumulated correlating specific IFs with certain pathways of differentiation, few experimental studies that directly assess the role of IFs in this process have been performed.

The availability of drugs such as colchicine and colcemid or the cytochalasins has resulted in a detailed understanding of many functions of microtubules and microfilaments, respectively (Alberts *et al.* 1983). In contrast, functional analysis of IFs has been hampered by the lack of a drug, which, when added to cells, will specifically disrupt IFs. Although many chemicals will perturb the IF network of cultured cells (Durham *et al.* 1983; Eckert, 1985; Zimmerman *et al.* 1986; Klymkowsky, 1988), all of these substances are metabolic inhibitors, which affect other cellular processes as well (Klymkowsky, 1988). Therefore, the functional consequences of IF perturbation are difficult to distinguish from the other inhibitory effects of these chemicals. An alternative approach that has been used to effect the *selective* disruption of IF networks is the intracellular microinjection of anti-IF antibodies (Gawlitta *et al.* 1981; Klymkowsky, 1981; Lin & Feramisco, 1981; Eckert *et al.* 1982; Klymkowsky, 1982; Lane & Klymkowsky, 1982; Klymkowsky *et al.* 1983; Tölle *et al.* 1985; Tölle *et al.* 1986; Murti

et al. 1988). However, with one exception (discussed below), antibody-mediated IF disruption had no obvious effects on the behavior of cells in culture. In sum, there is to date no precise, experimentally-defined function for IFs. Nonetheless, it is instructive to consider some of the possibilities of IF function, which have been derived from descriptive studies, with the hope of identifying possible functions of IFs suitable for experimental examination.

IFs are some of the most insoluble structures in cells. In addition, IF monomers appear to have relatively long half-lives (Denk *et al.* 1987), and they exist almost exclusively in a polymerized state. Consequently, it has been suggested that IFs perform a relatively nondynamic, structural role in cells, acting as "mechanical integrators of cellular space" (Lazarides, 1980). An examination of the organization of certain IF types makes this conclusion self-evident. For example, neurofilaments are one of the most abundant neuron-specific molecules, especially in the axons of peripheral neurons, and the correlation of the number of NFs with the cross-sectional area of axons has resulted in the hypothesis that NFs are major determinants of axonal caliber (Lasek *et al.* 1983; Hoffman *et al.* 1987). Due to their ability to self-assemble and the unique properties of their extended C-terminal tails (Geisler *et al.* 1983; 1984; 1985a), NFs are able to form an extensive, space-filling 3-D meshwork at relatively little metabolic cost to the neuron (Shaw, 1986). As axonal caliber is the major determinant of conduction velocity in myelinated nerves, NF expression may directly affect an important physiological attribute of neurons, as well as providing support for processes that may be over a meter in length (Hoffman *et al.* 1987).

The organization of desmin filaments in muscle suggests that they create a mechanically-continuous network throughout each muscle cell. Desmin filaments are wrapped around the myofibrils at the level of the Z disks (Bennett *et al.* 1979; Granger & Lazarides, 1979; Gard & Lazarides, 1980; Tokuyasu *et al.* 1985), and as a result, they may function to maintain the lateral registration of individual myofibrils and to integrate their

contractile actions (Lazarides, 1980). However, the desmin filaments are probably not responsible for bringing the Z disks of the myofibrils into lateral register, as this occurs prior to the localization of the desmin filaments to the Z disks (Bennett *et al.* 1979; Tokuyasu *et al.* 1985).

Through their insertion into desmosomes, cytokeratin filaments of epithelial cells provide a mechanically-continuous network throughout the entire epithelial tissue. Thus, this integrated network of filaments may function to provide tensile strength to epithelial layers such as the epidermis or the esophageal lining, which are subjected to many stresses. The dense packing of cytokeratin filaments into tonofilaments supports a mechanical role for these structures. Furthermore, extensive, dense filament meshworks are formed *in vitro* by filaments composed of epidermal cytokeratins (Eichner *et al.* 1986), and similar arrangements *in vivo* obviously enhance the protective abilities of the outer epidermal cells.

Rather than integrating cellular space, vimentin filaments may function in some cells to mechanically compartmentalize intracellular space. For example, vimentin filaments are rearranged from their extended, fibrillar state during two cellular processes to encircle a cellular subdomain. In one instance, the subdomain is occupied by the nascent lipid globule formed during adipogenesis (Franke *et al.* 1987). In the other situation, the subdomains are cleared of most major cytoplasmic structures to provide a high-efficiency assembly site for the DNA virus, frog virus 3 (Murti *et al.* 1988). In the latter instance, vimentin rearrangement has been shown to be essential for the formation of normal viral assembly sites, as anti-vimentin antibody injection inhibits both the rearrangement of the vimentin network and the efficient formation of viral particles.

IFs also may function to compartmentalize the cytoplasm of eggs and early embryos. Jeffery and Wilson (1983) have shown that more than 90% of the egg mRNA is present in the cortical domain of *Chaetopterus* eggs and codistributes with the cortical domain during

ooplasmic segregation and cleavage. Because part of the cortical domain is differentially-partitioned into daughter blastomeres at the first and second cleavages, the association of mRNA with the cortical domain may result in a differential localization of specific mRNA molecules. The continued colocalization of mRNA molecules with the cortical domain in eggs following stratification has indicated a strong association of the mRNA molecules to structural elements within this region (Jeffery, 1985). When eggs were treated with cytochalasin, colchicine, or nocadozole or extracted with nonionic detergent in the presence of high salt, the localization of mRNA to the cortical domain was unaltered, suggesting that IFs, and not microfilaments or microtubules, are the structural elements to which the mRNA binds (Venuti *et al.* 1987). Proteins with IF-like characteristics have been isolated from *Chaetopterus* eggs (Venuti *et al.* 1987). Thus, the localization of mRNA in *Chaetopterus* eggs by IF-binding is consistent with data obtained until now. If *Chaetopterus* eggs prove amenable to microinjection, it should be possible to test this hypothesis directly by the antibody-mediated disruption of IFs.

In sum, descriptive analyses have provided many insights into the possible functions of some IFs. However, with the exception of the role of vimentin filaments in the organization of viral assembly sites, direct experimental evidence in support of these functions does not yet exist. From the preceeding discussion, it is apparent that certain IF monomers are tailored to suit the structural needs of the cells which contain them. Thus, the requirement for a space-filling, open-meshed 3-D matrix to provide support for the axon of a peripheral nerve can be contrasted to the need for a dense, protective layer of cytokeratin filaments in the outer cells of the epidermis. However, possible functions of other IFs are not readily apparent from descriptive examinations of their distribution, and many questions remain. Perhaps the greatest source of questions about IF function arises from the complexity of the cytokeratins. For instance, why are there so many cytokeratins expressed in epithelia, when

other tissue-types function quite well with IFs composed of just one to three monomers? Secondly, why are certain cytokeratin pairs preferentially expressed in certain epithelia? A discussion of the evolutionary significance of previously-obtained data may provide some answers to these questions. The cytokeratins characteristic of specific routes of differentiation have been highly conserved among mammals (Moll *et al.* 1982; Schiller *et al.* 1982; Fuchs *et al.* 1987), which suggests that these cytokeratins provide different functions, if one assumes that what is functionally important is what is conserved during evolution. Moreover, IFs with characteristics of NFs, cytokeratins, and possibly desmin have been detected in invertebrates (Bartnik *et al.* 1985, 1986, and references therein), indicating an early, functional need for IFs of different types. Sun and co-workers (1984) have proposed that the evolution of cytokeratin heterogeneity may be recapitulated by the embryological development of epidermis. Thus, if the function of cytokeratin filaments is simply to maintain an integrated, intact, protective epithelium, then the development of more complicated, stratified epithelia may have required the generation of larger and more complicated cytokeratins. In this scenario, the cytokeratins typical of simple epithelia provide a basal amount of mechanical support, which is increased by the expression of more complex cytokeratins in epithelial tissues subjected to increasing amounts of stress. However, this hypothesis addresses only the protective function of some epithelia, which is not the primary function of many other epithelia. Thus, while a mechanical and protective role of cytokeratins is consistent with the functions of the epidermis and stratified epithelia such as found in the esophagus, the role of cytokeratins in simple epithelia, such as the absorptive epithelium of the intestine or the glandular epithelium of the pancreas, may be quite different. The aim of this dissertation was to examine the role of cytokeratin filaments in the differentiation and functioning of a simple epithelium.

Cytokeratins 8 and 18

As illustrated in Table 2, cytokeratins 8 and 18 are the cytokeratin expression pair characteristic of human simple epithelia. Not only are these cytokeratins expressed in all simple epithelia, but they are the sole cytokeratins of hepatocytes, pancreatic acinar cells, and renal tubule cells (Moll *et al.* 1982). Moreover, the intestinal epithelia contain only one additional cytokeratin (#19). Cytokeratins equivalent to 8 and 18 have been identified and purified from rodent cells (cytokeratin A and cytokeratin D, Franke *et al.* 1981a; Endo A and Endo B, Oshima 1981, 1982). K8/K18 and Endo A/Endo B are used to indicate the species of origin (human or mouse) in the following discussion of the characteristics of these cytokeratins.

With the exception of cytokeratin 19, K8 (Endo A) and K18 (Endo B) are the smallest members of their respective cytokeratin subfamilies (Table 2). Recent cDNA sequencing data have confirmed that these cytokeratins contain typical α-helical rods of approximately 310 amino acids, and their smaller size is due to their relatively short nonhelical N- and C-terminal domains (Leube *et al.* 1986; Magin *et al.* 1986; Oshima *et al.* 1986; Romano *et al.* 1986; Singer *et al.* 1986; Alonso *et al.* 1987). Thus, for example, the C-terminal domain of Endo B contains only 39 amino acid residues, whereas the same domain can be as long as 112 residues in Type I epidermal cytokeratins (Steinert *et al.* 1983; Krieg *et al.* 1985). Likewise, the head domain of Endo B (73 residues) is relatively short in comparison to the head domains of Type I epidermal cytokeratins (as long as 142 residues). Similar size differences occur between the C-terminal domains of K8 and Type II epidermal cytokeratins (Johnson *et al.* 1985; Steinert *et al.* 1985a).

The variations in the non-α-helical end domains of the epidermal and simple cytokeratins are not restricted to their size, as the amino acid sequences of these domains also differ. The major difference between the end domain sequences of the epidermal and

simple cytokeratins is the absence in simple cytokeratins of G-G-G-(X) repeats interspersed with stretches of serine residues, which are typical of the terminal domains of epidermal cytokeratins (Steinert *et al.* 1985a, b). It has been suggested that the lack of these sequences may be responsible for the decreased strength of association between K8 and K18, when compared to complexes of epidermal cytokeratins (Franke *et al.* 1983; Romano *et al.* 1986). Moreover, these sequences may be the sites of association for filaggrin, a histidine-rich protein expressed in large quantities in the upper layers of the epidermis, which aggregates cytokeratin filaments into macrofibrils *in vitro* and presumably *in vivo* (Dale *et al.* 1985; Steinert *et al.* 1985a, b). Thus, the absence of the G-rich repeats may impart a more dynamic, nonprotective function of K8 and K18 in simple epithelia.

The non-α-helical N-terminal sequences of Endo B are only 16% identical to the corresponding sequences of Type I epidermal cytokeratins (Singer *et al.* 1986). The C-terminal domains of Endo B/K18 and K8 are also relatively unique, with the exception of the heptapeptide DGRVVSE (DGKVVSE in K18, DGKLVSE in K8) (Leube *et al.* 1986; Oshima *et al.* 1986; Singer *et al.* 1986; Alonso *et al.* 1987). This heptapeptide has been highly conserved, as it is found in all species examined from amphibian to man (Jonas *et al.* 1985; Winkles *et al.* 1985; Franz & Franke, 1986). The heptapeptide is located at the end of the C-terminal domain in most nonepidermal cytokeratins, and it is found in a slightly modified form in Type III IFs. The relatively strict conservation of the heptapeptide and its absence from the tails of complex, epidermal cytokeratins suggests that this conserved sequence may be important in the functioning of IFs in nonepidermal cells.

Although the most striking variations in amino acid sequence occur in the non-α-helical end domains of keratin 18, its central rod domain also is unusual in its low degree of sequence similarity (47%) to other members of the Type I subfamily (Bader *et al.* 1986; Leube *et al.* 1986; Oshima *et al.* 1986). Interestingly, the conserved sequence that demarcates

the end of the α-helical rod of the K18 polypeptide contains an insertion of an aspartic acid residue (EIATYR(X)LLEDGE). These unique characteristics of the K18 polypeptide have been highly conserved across mammals, as Endo B is 85% identical to K18 in its entirety and also contains the aspartic acid insertion (Singer *et al.* 1986; Alonso *et al.* 1987). K8 has also been highly conserved among mammals, as its bovine equivalent is 91% identical in the rod domain and 88% identical in the tail (Leube *et al.* 1986; Magin *et al.* 1986). Moreover, a K8-equivalent from Xenopus has been cloned and is 90% similar in its rod domain with the bovine K8-equivalent (Franz & Franke, 1986). Unlike its coexpressed partner, however, the rod domain of K8 is also highly similar (83%) to the rod domain of other members of the Type II cytokeratin family. Consequently, the unique properties of the K8/K18 expression pair may be determined not only by the unique characteristics of their terminal domains, but also by the relatively unique sequence of the α-helical rod of the K18 (Endo B) polypeptide.

The recent isolation and characterization of the Endo A, K18, and Endo B genes has revealed an additional difference between the epidermal and simple cytokeratins: each gene contains one less intron than the other members of their respective subfamilies (see Fig. 2). Thus, the Endo A gene has only 7 introns, while the Endo B (K18) gene contains only 6 introns (Vasseur *et al.* 1985; Kulesh & Oshima, 1988; Oshima *et al.* 1988). To date, only the first two introns of the K18 gene have been mapped in relation to the subdomains of the K18 polypeptide (Kulesh & Oshima, 1988). The position of these introns is typical of the first two introns of other Type I cytokeratin genes. Thus, it is likely that the final, C-terminal intron is missing in the K18 gene. The same situation may exist for the Endo A gene, as the lengths of the introns and the first 6 exons correlates with typical patterns of other Type II genes (Vasseur *et al.* 1985). It is interesting to speculate about the evolutionary implications of these data. For instance, the lower number of introns in these genes may be indicative of the more primitive nature of these sequences. Furthermore, the relatively unique amino acid

sequence of the Endo B polypeptide may be suggestive of an early appearance of this gene. Subsequent gene duplication events, combined with intron and exon additions, may have then generated the more complex cytokeratins associated with the evolution of stratified epithelia (Sun *et al.* 1984).

The C-terminal sequence of the K8-equivalent cytokeratin from *Xenopus* presents an interesting evolutionary conundrum. This cytokeratin is expressed in simple epithelia of the tadpole and adult frog, similar to the K8 gene of mammals, and contains the conserved sequence (DGRLVSE) at the end of the tail, which is typical of nonepidermal cytokeratins. However, the tail of the *Xenopus* K8 polypeptide is 20 residues longer than its bovine counterpart, primarily due to the presence of four G-G-G-(X) repeats (Franz & Franke, 1986). Thus, this cytokeratin possesses characteristics of both epidermal and nonepidermal cytokeratins. The presence of this sequence in *Xenopus* may argue that it represents a more primitive K8 gene than its mammalian equivalent. If so, one would have to argue that the mammalian K8 gene was generated by the selective *loss* of the G-rich subdomain. The loss of this domain may reflect its unneccesary and/or possibly detrimental role in the functioning of this molecule in the simple epithelia of mammals. Alternatively, the C-terminal domains of the amphibian and mammalian K8 polypeptides may have evolved separately after the divergence of amphibians and terrestial vertebrates. Thus, the complexity of the K8 tail in *Xenopus* may be a reflection of a dual function of this molecule: the G-rich repeats may be necessary for the functions of this molecule peculiar to its expression in the large, yolky egg and early embryo of *Xenopus*, while its functional role in simple epithelia of the tadpole and adult may be mediated in part by the conserved heptapeptide.

In summary, cytokeratins 8 and 18 are different from the epidermal cytokeratins in their sequence and gene organization, as well as in their differential expression. The

increased length of the terminal domains of the epidermal cytokeratins is associated with the appearance of G-G-G-(X) repeats and the formation of cytokeratin networks of greatly increased density. These structural modifications can be readily correlated with the increased protective functions of stratified epithelia in terrestial vertebrates. However, the function of the simple cytokeratins remains an enigma. The coexpression of K8 and K18 with more complex cytokeratins in several epithelial tissues (Table 2; Bosch *et al.* 1988) argues that these polypeptides play a role separate from the putative protective functions of the filament networks composed of more complex cytokeratins. Moreover, the divergence of the sequence of the K18 gene, coupled with its conservation among mammals, suggests that this cytokeratin provides an essential function that cannot be substituted for by other cytokeratins. Thus, these analyses of K8/K18 gene and protein stucture have confirmed the importance of assessing the functional role of cytokeratins in simple epithelia.

In selecting the best system to use in an examination of the functional role of cytokeratins 8 and 18, several items should be considered. First, one should choose an epithelial tissue where analyses are not complicated by the presence of additional IF polypeptides. Thus, the best candidates from adult mammalian tissues are the liver, pancreas, and kidney (Table 2). Secondly, the context in which these tissues are studied should be carefully evaluated. For example, the cytokeratin profile of hepatocyte-derived cell cultures often varies from the endogenous pattern (Franke *et al.* 1981b). Moreover, a major problem associated with the culture of epithelial tissues or cell lines on a solid substratum is the induction of vimentin synthesis under these conditions. The resulting redundancy of IF expression may complicate analyses of cytokeratin function. Consequently, *in situ* analyses of cytokeratin function may be preferable to the use of isolated, cultured material. Finally, the method used to examine IF function has to be appropriate for the selected system. In the absence of identified mutants with defects in cytokeratin gene sequences, cytokeratin

function can be directly examined only by analyzing the phenotypic effects of the disruption of cytokeratin synthesis and/or assembly. In this dissertation, the disruption of cytokeratin assembly by the intracellular injection of anti-cytokeratin antibody was the method chosen to examine cytokeratin function. *In vivo* analyses of cytokeratin function in tissues that comprise large numbers of cells located in the interior of the animal is not practical using this approach. However, one simple epithelium, which consists of relatively few cells and occupies an external location, does exist: the trophectoderm of the mouse blastocyst. Therefore, I selected the preimplantation mouse embryo as the system to use to examine the possible functions of Endo A and Endo B.

At the blastocyst stage, the expression of cytokeratins is enriched in the cells of the trophectoderm (Brûlet *et al.* 1980; Jackson *et al.* 1980; Paulin *et al.* 1980; Lehtonen *et al.* 1983b; Oshima *et al.* 1983; Duprey *et al.* 1985; Lehtonen, 1985, 1987). Chisholm & Houliston (1987) recently described the assembly of cytokeratin filaments at several earlier stages of preimplantation development. Their results indicate that cytokeratins are assembled into filaments in some blastomeres of the embryo as early as the 8-cell stage; during subsequent development, there is a progressive increase in their incidence, density, and organization. Most of Chisholm & Houliston's results were obtained by culture of isolated blastomeres or by disaggregation of embryos just before fixation. However, these methods do not provide information on the pattern of filament assembly in neighboring cells or the content of assembled cytokeratin filaments in intact, individual embryos. This information is essential to an analysis of the effects of anti-cytokeratin antibody injection into the early embryo. Therefore, I used whole-mount indirect immunofluorescence microscopy to examine the appearance and distribution of cytokeratin filament bundles in intact, individual preimplantation embryos, both before and after antibody injection.

Materials and Methods

Embryos

Six- to ten-week-old female CF_1 mice (Charles River Lab) were induced to superovulate, as described previously (Cruz & Pedersen, 1985). The females were placed singly with males overnight and examined for vaginal plugs the following morning (day 1 of embryogenesis). Cumulus masses were recovered on day 1 from the oviductal ampullae, and the follicle cells were dispersed by a brief incubation in an excess of 0.1% hyaluronidase (type IV, Sigma). The zygotes were retrieved with a finely drawn glass pipet and washed several times with modified Hanks' balanced salt solution (flushing medium I; Spindle, 1980). Cleavage-stage embryos were recovered by flushing entire oviducts approximately 45 h (2-cell stage) or 67 h (8-cell stage) after injection of human chorionic gonadotropin. Morulae were obtained by culture of 8-cell embryos for 10-24 h, depending on the desired cell number. Blastocysts were recovered by flushing uteri on day 3.5 with modified Hanks' balanced salt solution supplemented with amino acids and fetal calf serum (FCS) (flushing medium II; Spindle, 1980). If not used immediately, embryos were maintained in organ culture dishes (Falcon) at 37°C in an atmosphere of 5% (v/v) CO_2 in air. Zygotes and cleavage-stage embryos were cultured in standard egg culture medium, while blastocysts were cultured in supplemented Eagle's medium (BME + AA; Spindle, 1980).

Cytokeratin antibodies

A monospecific rabbit antibody (IgG fraction) to the type I cytokeratin Endo B (Oshima, 1981) and a rat monoclonal antibody (TROMA-1) to the type II cytokeratin Endo A (Brûlet *et al.* 1980) were provided by Dr. Robert Oshima, La Jolla, and Dr. Rolf Kemler, Tübingen, respectively. These antibodies recognize cytokeratins of M_r 50,000 and M_r 55,000, respectively, in the preimplantation mouse embryo (Oshima *et al.* 1983). For microinjection,

milligram quantities of TROMA-1 antibody were produced by a 2-week culture of hybridoma cells in a closed tissue culture roller bottle (Corning) containing 300 ml Dulbecco's modified Eagle's medium and 10% FCS (Bodeus *et al.* 1985). TROMA-1 IgG was purified from the roller bottle supernate by absorption to a matrix of affinity-purified goat anti-rat IgG-conjugated agarose (Zymed Lab). The purity of the eluted IgG was confirmed by sodium dodecyl sulfate polyacrylamide gel electrophoresis (SDS-PAGE) and silver staining. The purified IgG was dialyzed exhaustively against injection buffer (10 mM KH_2PO_4, 0.12 M KCl, pH 7.4) and concentrated to 10-20 mg/ml with Centricon 30 microconcentrators (Amicon). A small amount of anti-Endo B antibody was affinity-purified for use in microinjection studies (if necessary). This was accomplished by absorption of the anti-Endo B IgG to strips of nitrocellulose paper containing gel-purified Endo B (Fig. 5) (Nigg *et al.* 1985; Olmsted, 1986). All antibody preparations were tested for activity by indirect immunofluorescence screening of PFHR9 cells, the parietal endoderm cell line from which Endo B and Endo A were first isolated (Fig. 6) (Oshima, 1981, 1982).

Immunoblotting of preimplantation mouse embryos

Approximately 100 to 1000 embryos of various stages were lysed in 20-30 μl of SDS-sample buffer (10% [w/v] glycerol, 5% [v/v] β-mercaptoethanol, 2.3% [w/v] SDS, and 0.0625 M Tris-HCl, pH 6.8), and the embryo lysates were separated on a 10% SDS-polyacrylamide gel (Laemmli, 1970; Thomas & Kornberg, 1975). The gel was equilibrated in 25 mM sodium phosphate, pH 6.5, and the separated proteins were transferred to nitrocellulose paper for detection of Endo A and Endo B by immunoblotting (Burnette, 1981). After blocking the unbound sites with 3% Carnation non-fat dry milk in phosphate-buffered saline (PBS) (Johnson *et al.* 1984), the nitrocellulose paper was incubated in 10-20 ml of primary antibody solution. The primary antibody solution was either a 1:500 dilution of anti-Endo B IgG in PBS/milk or undiluted culture supernate of the TROMA-1 hybridoma. After 5 washes of 6

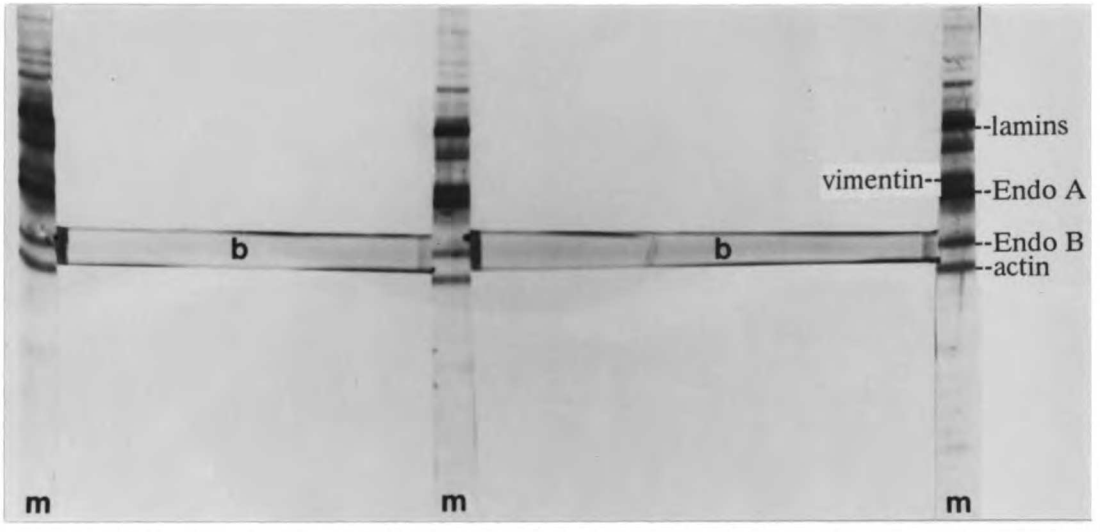

Fig. 5. Blot purification of anti-Endo B IgG. A cytoskeletal fraction enriched in IFs was isolated from confluent cultures of PFHR9 cells and separated on a 10% preparative SDS-polyacrylamide gel. The proteins were transferred to nitrocellulose, and three narrow strips (m) were cut out of the nitrocellulose sheet. The marker strips (m) were stained with India ink (Hancock & Tsang, 1983) to visualize the cytoskeletal proteins. The marker strips were then realigned with the unstained nitrocellulose sheets, and narrow strips containing Endo B (b) were cut out. These strips were used for affinity-purification of the anti-Endo B IgG.

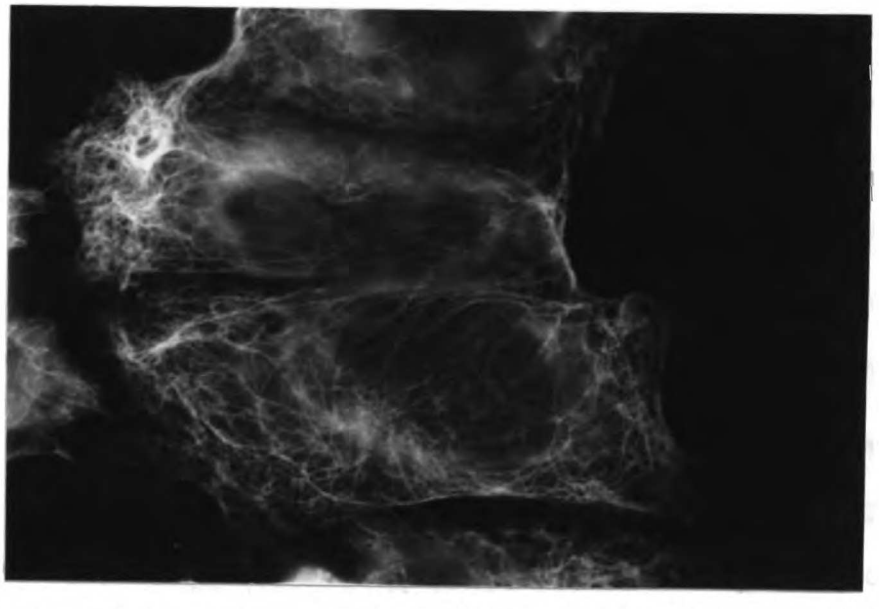

Fig. 6. Cytokeratin filament organization in PFHR9 cells, visualized with purified TROMA-1 IgG (final concentration approx. 25 μg/ml) and FITC-conjugated goat anti-rat IgG. Similar patterns were obtained with anti-Endo B IgG.

min each with PBS, the nitrocellulose was re-blocked with PBS/milk, then incubated for 1 hr with a 1:750 dilution of secondary antibody (affinity-purified, biotin-conjugated goat anti-rabbit or anti-rat IgG, respectively). The nitrocellulose was washed as above and incubated 45-60 min in a 1:500 dilution of peroxidase-conjugated avidin (Cappel) in PBS/milk. After 5 washes with PBS, the peroxidase reaction was developed using a solution of diaminobenzidine, heavy metal salts, and H_2O_2 (DeBlas & Cherwinski, 1983).

Whole-mount indirect immunofluorescence

Twenty-five or more embryos of each of the following stages were recovered from three or more mice: zygote, early 8 cell, compacted 8 cell, mid morula, late morula, and blastocyst. The embryos were fixed for 30 min with 2% paraformaldehyde in Dulbecco's PBS and washed through two changes of PBS containing 0.1 M glycine to quench the free aldehydes of the fixative (Geiger & Singer, 1979). The embryos were made permeable by incubation in 0.25% Triton X-100 in PBS for 4 min (Maro *et al.* 1984) and washed 3X in PBS containing 3 mg/ml polyvinyl pyrrolidone (PVP) (Calbiochem). The embryos were preincubated for 30 min in PBS + 1 mg/ml ovalbumin, followed by incubation in 20-50 μl of primary antibody solution for 60 min at 37°C in a humid chamber. Primary antibodies were either TROMA-1 culture supernate, the anti-Endo B IgG fraction at 50 μg/ml in PBS + 3% bovine serum albumin (BSA) + 0.1% Tween 20, or the corresponding nonimmune IgGs at 5-10 μg/ml (rat or rabbit, respectively; Cappel). Secondary antibodies were affinity-purified, fluorescein-conjugated goat anti-rat IgG or anti-rabbit IgG, respectively (Cappel), diluted 1:40 in PBS/BSA/Tween. Washing steps were for a total of 50 min in 2 changes of PBS + 0.1% Tween and 3 changes of PBS/PVP. After a quick rinse through a drop of water, the embryos were placed on a microscope slide in a small drop of mounting medium (70% glycerol, 30% 0.1 M Tris, pH 9.0) containing 2% n-propyl gallate to reduce photobleaching (Giloh & Sedat, 1982). An 18-mm round coverslip was gently lowered over the drop and

sealed with nail polish. The nuclear numbers of compacted 8-cell embryos and morulae were verified by a 5-min incubation in 5 μg/ml Hoechst 33258 dye followed by four 2-min washes in PBS/PVP just before mounting. Mid morulae were defined as having an average of 16 nuclei, while late morulae contained an average of 28 nuclei.

Microscopy was performed with a Zeiss compound microscope equipped with phase and epifluorescence optics, using 16X plan-phase, 40X neofluor, and 63X plan-neofluor objectives. Filter sets 48-77-09 and 48-77-01 were used for fluorescein and Hoechst fluorescence, respectively. Photographs were taken with Kodak Tri-X film (400 ASA).

Isolation of [^{35}S]methionine-labeled blastocyst cytoskeletons

Fifty to 100 blastocysts were washed with methionine-free flushing medium I and placed under paraffin oil in a 25-μl drop of modified Eagle's medium (with methionine omitted), containing 1% dialyzed FCS and 1 mCi/ml of [^{35}S]methionine (specific activity, 1116 Ci/mmol, New England Nuclear). After a 4-h incubation at 37°C and 5% CO_2, the embryos were washed four times and extracted as described by Oshima *et al.* (1983). Briefly, the embryos were first lysed in a Tris-buffered saline solution containing 1% Triton X-100 and the protease inhibitor PMSF. The embryo residue was then digested with 50 μg/ml of micrococcal nuclease and re-extracted with 0.5% Triton X-100 in the presence of 1.5 M KCl. The cytoskeletal material was recovered by centrifugation and dissolved in 25 μl of SDS-sample buffer. A 2 μl aliquot was removed from the sample for determination of the radioactivity incorporated into trichloroacetic acid-precipitable material. The remainder of the sample was analyzed by SDS-PAGE and autoradiography at -80°C using Kodak X-Omat AR film (Bonner, 1984).

Immunoprecipitation of blastocysts and inner cell masses (ICMs)

Sixty to 140 blastocysts or ICMs were washed with methionine-free flushing medium I and placed under paraffin oil in a 25-μl drop of modified Eagle's medium (with methionine omitted), containing 1% dialyzed FCS and 1 mCi/ml of [^{35}S]methionine (specific activity, 1116 Ci/mmol, New England Nuclear). After a 3-h incubation at 37°C and 5% CO_2, the embryos were washed four times and embryo lysates were prepared by incubation in a 10 mM Tris-HCl, pH 7.4 solution containing SDS and protease inhibitors, as described previously (Oshima *et al.* 1983). A 10-μl aliquot was removed from each sample for determination of the radioactivity incorporated into trichloroacetic acid-precipitable material. The remainder of the lysate was placed in microfuge tubes and stored at -80°C until further use.

Each blastocyst sample was thawed and divided into two equal volumes, both of which were preabsorbed for 15 min on ice with 15 μl of normal rabbit serum and 150 μl of 10% Staph A (Zysorbin, Zymed). The mixture was centrifuged for 2.5 min at 8,000 X *g*; the supernate was saved, and the pellet was discarded. One duplicate of each sample received 12 μl of Endo B antiserum (final concentration, 25 μg/ml), while the other duplicate received 12 μl of normal rabbit serum. All samples were incubated for 4 h on ice. Next, 150 μl of 10% Staph A was added and the samples were incubated an additional 15-20 min on ice. The remainder of the procedure followed the protocol of Oshima *et al.* (1983). The immunoprecipitated protein was eluted into 40 μl of SDS-sample buffer and analyzed by SDS-PAGE and autoradiography.

ICMs were isolated from 3.5-day blastocysts by the process of immunosurgery (Solter & Knowles, 1975). ICM lysates were processed as described above, with one difference: ICM lysates from three separate days were pooled and then divided into two aliquots.

Indirect immunofluorescence of sectioned blastocysts

Blastocyst sections were obtained by a histological procedure involving embedding in polyethylene glycol (PEG) (Wolosewick & De Mey, 1982), which was modified for use with preimplantation mouse embryos (Watson & Kidder, 1988). Groups of 30 to 50 3.5-day blastocysts were fixed and washed as for whole-mount analysis, and embedding was performed in micromolds (Polysciences) using an 82% PEG 3350:18% PEG 1450 solution (Sigma). One-micrometer sections were cut on a dry glass knife with a Sorvall JB-4A microtome, and ribbons of sections were stuck to glass coverslips coated with poly-L-lysine (150,000-300,000 MW; Sigma) by briefly heating to 55°C before rehydration. Immunostaining was performed as described for whole-mount immunofluorescence, except that biotin and streptavidin conjugates were used to enhance the specific staining. The primary antibody was either TROMA-1 culture supernate or nonimmune rat IgG at 10 μg/ml in culture medium. The secondary antibody was affinity-purified, biotin-conjugated goat anti-rat IgG (Zymed Lab) diluted 1:200 in PBS + 1% BSA, and the tertiary incubation was in Texas Red-conjugated streptavidin (Zymed Lab) diluted 1:200 in PBS/BSA. The coverslips were inverted onto 1 μl of mounting medium on a microscope slide and sealed with nail polish. Observations were with 40X planapo-phase, 40X neofluor, and 63X plan-neofluor objectives, and Zeiss filter set 48-77-15 was used for Texas Red fluorescence. Photographs were taken with Kodak T-Max or Ektachrome film (ASA 400) developed to give an effective film speed of 800 ASA.

Microinjection of mural trophectoderm cells

Individual cells of the mural trophectoderm of 3.5-day blastocysts were injected with cytokeratin antibody using a modification of the technique of Cruz and Pedersen (1985). A Zeiss compound microscope equipped with epifluorescence optics and Leitz micromanipulators fitted with microelectrode holders (W-P Instruments, Inc.) was used for

iontophoretic coinjection of 8 mg/ml TROMA-1 IgG (rat anti-Endo A) and 0.8% rhodamine-conjugated dextran (RDX; Gimlich & Braun, 1985). After back-filling the tip of the injection needle with the TROMA-1/RDX solution, the shaft of the needle was filled with 50 mM KCl. Blastocysts were placed in injection chambers made by pipetting flushing medium II under a 5 x 50 mm sterilized coverslip strip placed lengthwise across the gasket of a 1-chamber tissue culture slide (Lab-Tek), with the remainder of the chamber flooded with mineral oil (Sigma) to prevent evaporation. Injections into the perinuclear region of the cytoplasm of individual mural trophectoderm cells were monitored at 200X. An electrometer and bridge (Winston Electronics) were used to perform constant-[+]-current (9×10^{-9} A) iontophoresis for 15-20 sec. Successful injections were confirmed by briefly viewing the rhodamine fluorescence image through a silicon-intensified target video camera (Dage-MTI, Inc.) with a 50% neutral density filter.

The antibodies to Endo A and Endo B were derived from different species (Brûlet *et al.* 1980; Oshima, 1981), which allowed for an examination of both the fate of the injected antibody and the status of the cytokeratin network in single embryos using whole-mount double-label immunofluorescence. Blastocysts were processed within 1-2 h of injection (Fig. 7). The primary incubation was with rabbit anti-Endo B IgG at 75 μg/ml, followed by a secondary incubation with affinity-purified, fluorescein-conjugated goat anti-rabbit IgG and Texas Red-conjugated goat anti-rat IgG, each diluted 1:20.

Microinjection of 2-cell embryos

TROMA-1 IgG (10-20 mg/ml) mixed with RDX (0.8% final concentration) was pressure-injected into either one or both blastomeres at the 2-cell stage. Thirty to 40 embryos were placed in a small drop of flushing medium I in the center of one chamber of a 2-chamber tissue culture slide with the chamber removed (Lab-Tek). A 1.5-μl drop of the TROMA-1/RDX solution was placed beside the embryo drop, and the chamber was flooded

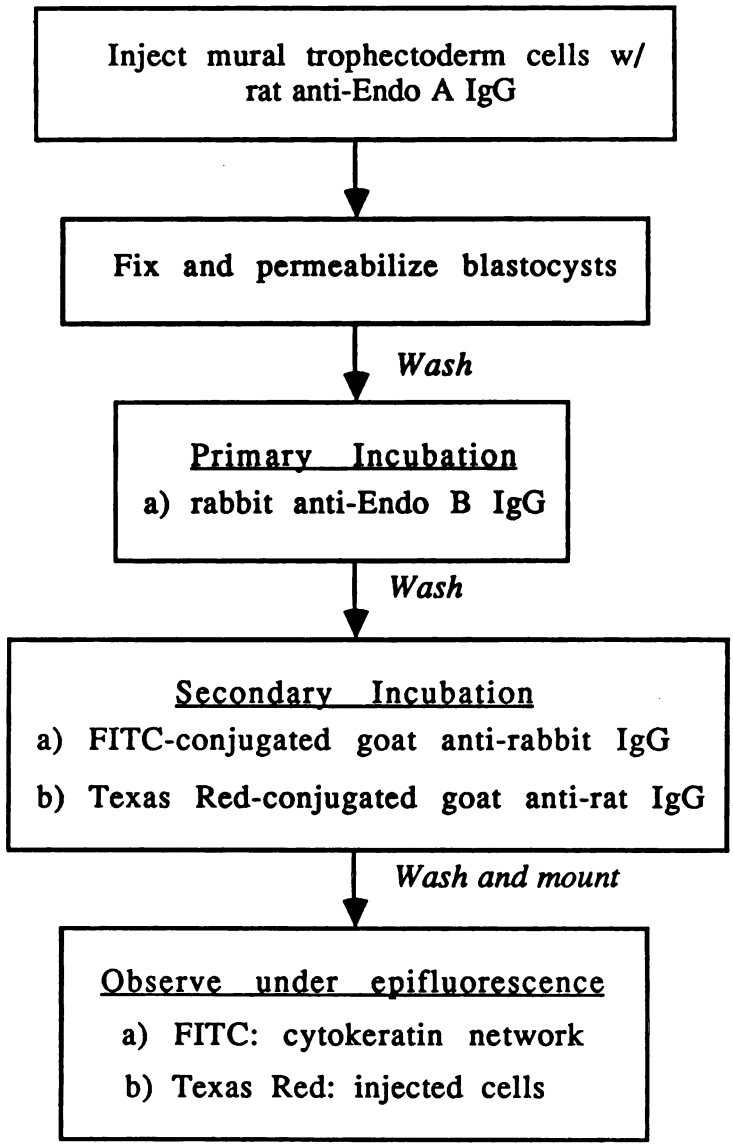

Fig. 7. Processing of blastocysts after injection of TROMA-1 IgG into individual mural trophectoderm cells.

with mineral oil. Injection needles were placed in the antibody drop and filled by drawing the antibody solution into the tip. Antibody was injected at 200X into the cytoplasm of one or both blastomeres. The success and extent of injection were assessed by briefly viewing the rhodamine fluorescence image.

The amount of antibody injected into 2-cell blastomeres was determined by immunoblot analysis (Hawkes, 1986). Lysates of 10-30 injected embryos and serial dilutions of rat IgG were slot-blotted (Hybriblot; BRL) onto nitrocellulose paper. The nitrocellulose was blocked for 30 min with PBS + 3% Carnation nonfat dry milk and incubated for 2 h in a 1:750 dilution of affinity-purified biotin-conjugated goat anti-rat IgG in PBS/milk. After 5 washes of 6 min each with PBS, the nitrocellulose was incubated for 45 min with a 1:200 dilution of the DETEK I-*alk* signal-generating complex (Enzo Biochem, Inc.). Alkaline phosphatase activity was visualized using the method of Ey and Ashman (1986). The blots were scanned with a Bio-Rad densitometer in reflectance mode, and the area of the peaks was quantified with a Hewlett-Packard integrator. The amount of TROMA-1 IgG injected into 2-cell blastomeres was determined by extrapolation to the standard curve.

Injected and control embryos were placed in separate microdrops of egg culture medium under oil and incubated at 37°C and 5% CO_2. Embryos obviously damaged by microinjection were not cultured, and embryos that arrested at the 2- and 3-cell stages were removed from the culture drops. After 2-2.5 days, the remaining embryos were processed for triple-label fluorescence (Fig. 8). The primary incubation was for 1 h at 37°C with a mixture of a 1:100 dilution of affinity-purified biotin-conjugated goat anti-rat IgG and a 1:40 dilution of rabbit anti-Endo B IgG in PBS/BSA/Tween. The secondary incubation was with a mixture of a 1:100 dilution of Texas Red-conjugated streptavidin and a 1:40 dilution of affinity-purified fluorescein-conjugated goat anti-rabbit IgG for 45-60 min at 37°C. The tertiary incubation was for 5 min with 5 μg/ml Hoechst 33258 in PBS.

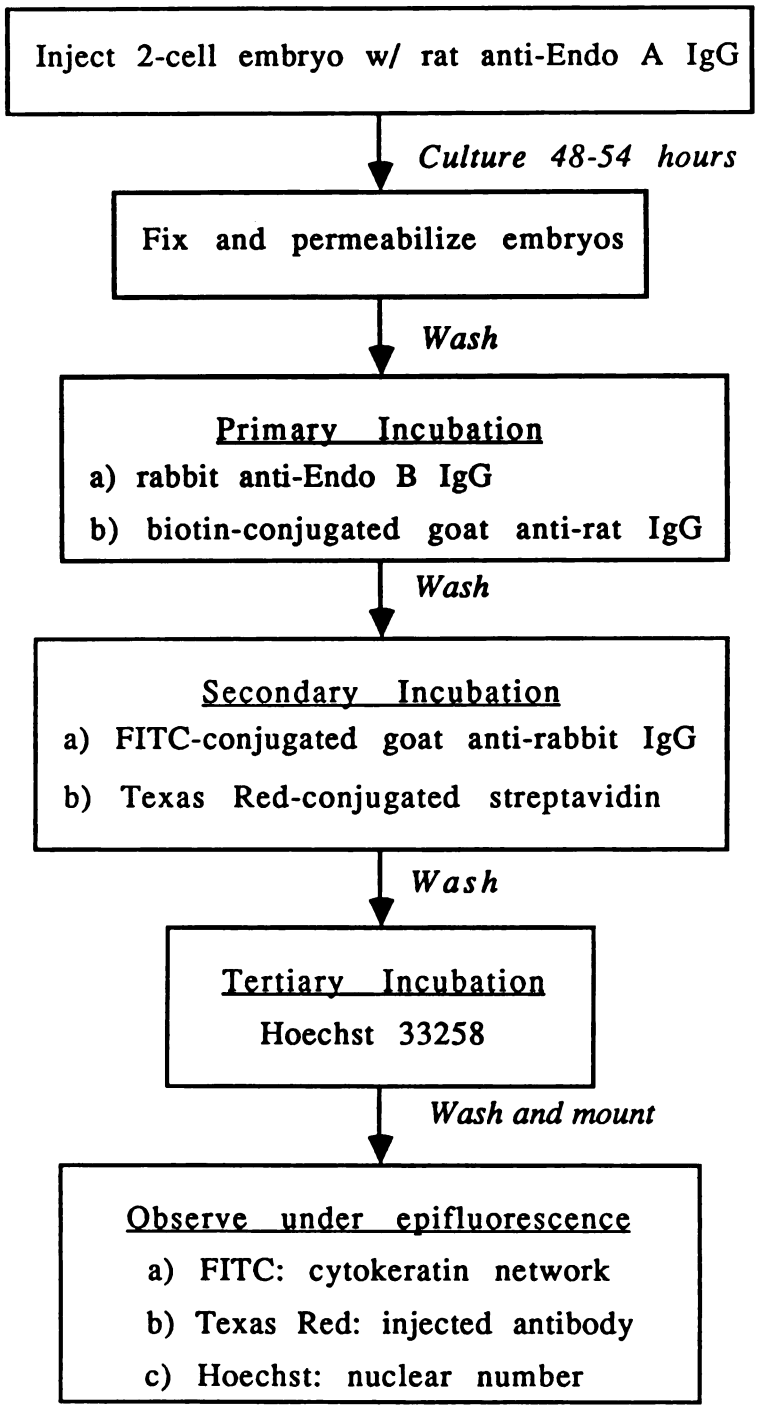

Fig. 8. Processing of 2-cell embryos after injection of TROMA-1 IgG.

Results

Accumulation of cytokeratins in the preimplantation mouse embryo

Endo A and Endo B are synthesized as early as the 8-cell stage of embryogenesis (Oshima *et al.* 1983; Duprey *et al.* 1985). However, analyses of the total cytokeratin content of mouse eggs and cleavage-stage embryos have been conflicting and inconclusive (for discussion, see Lehtonen, 1987). Therefore, several different stages of embryos were surveyed for their levels of Endo A and/or Endo B by the protein immunoblot technique. Endo A and Endo B were easily detected in as few as 80 day-3.5 blastocysts (Fig. 9). Unfortunately, Endo B was undetectable using this approach in as many as 1000 cleavage-stage embryos (4- or 8-cell stages) and 700 mid-to-late morulae (not shown). Although Chisholm and Houliston (1987) achieved a slightly higher sensitivity by use of [^{35}S]StreptAvidin, they did not observe a consistent, strong signal for Endo A before the mid-morula stage. Consequently, the abundance of cytokeratin monomers at early stages of development is still unclear. However, as will be discussed in the following section, cytokeratin filaments are clearly detectable by whole-mount indirect immunofluorescence in single embryos as early as the 8-cell stage of embryogenesis.

One explanation for the low sensitivity of the immunoblot analysis may be that the antigenic epitopes of the anti-Endo B and TROMA-1 antibodies are altered, and hence less recognizable, when the cytokeratin monomers are complexed with SDS. Before transfer to nitrocellulose, Achtstaetter *et al.* (1986) routinely incubate SDS gels in solutions containing 4M urea to allow the cytokeratin polypeptides to reconstitute some of their native conformation. In the future, this methodological adaptation may allow for a higher detectability of Endo A and Endo B in early mouse embryos on immunoblots. However, due to the great cost and time involved in accumulating thousands of cleavage-stage embryos, combined with the success in detecting cytokeratins in single embryos by indirect

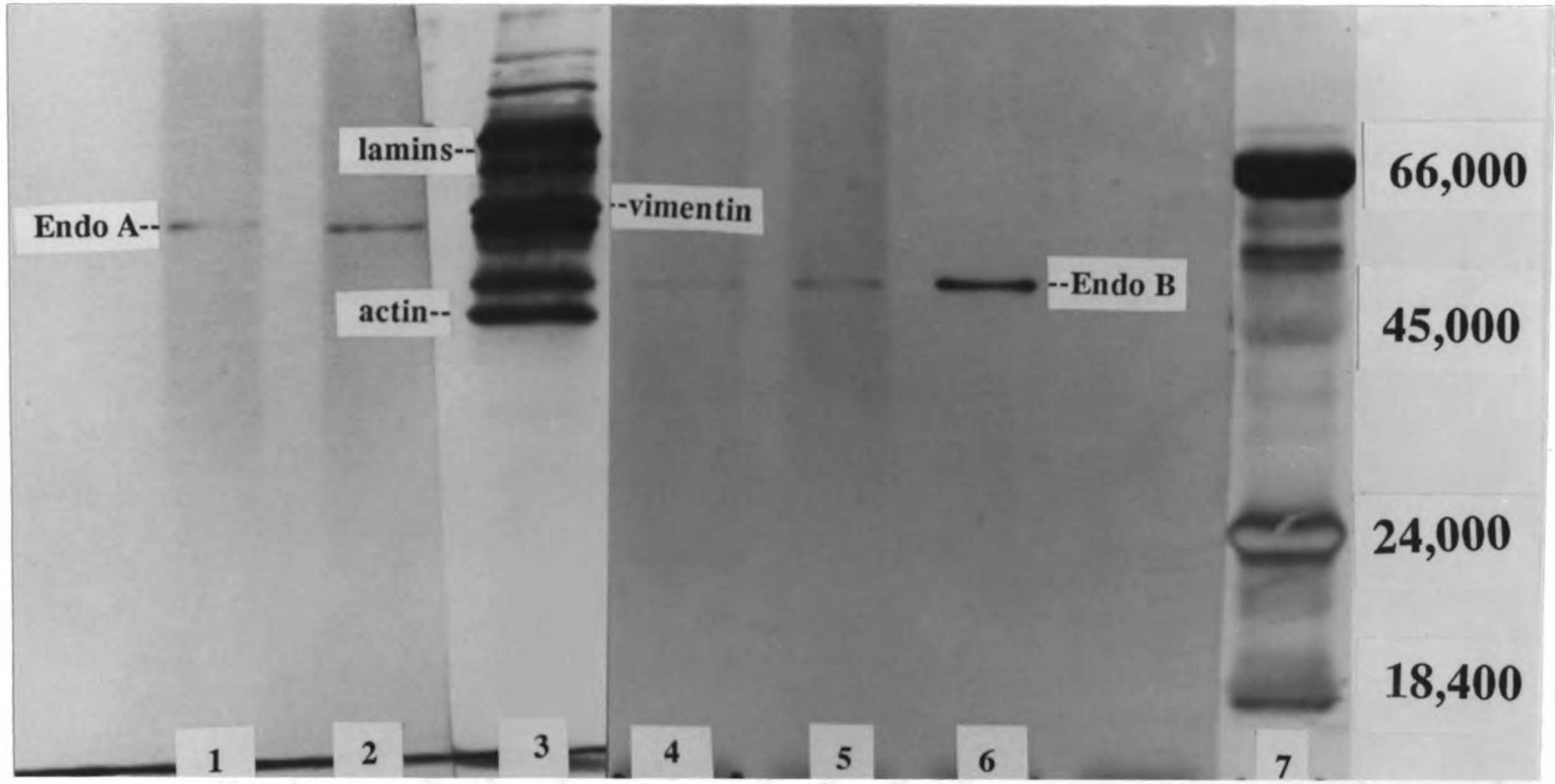

Fig. 9. Immunoblot analysis of mouse blastocysts with anti-cytokeratin antibodies.
Lane 1: 80 3.5-day blastocysts (treated with TROMA-1 supernate)
Lane 2: 100 3.5-day blastocysts (treated with TROMA-1 supernate)
Lane 3: 3 μg PFHR9 cytoskeletal fraction (India ink stained)
Lane 4: 185 3.5-day blastocysts (treated with anti-Endo B IgG)
Lane 5: 185 4.5-day blastocysts (treated with anti-Endo B IgG)
Lane 6: PFHR9 cytoskeletal fraction (treated with anti-Endo B IgG)
Lane 7: MW markers (stained with India ink)

immunofluorescence (next section), these experiments were not repeated. Nevertheless, one important conclusion can be drawn from the immunoblot analysis: there is apparently at least a 10-fold increase in the total amount of cytokeratins in blastocysts as compared to mid-to-late morulae. Because the protein content of these stages differs by only 10-20% (Brinster, 1967), this difference must be due to a selective increase in the accumulation of cytokeratins, rather than a general increase in the amount of all proteins with blastocyst formation.

Cytokeratin filament distribution in the preimplantation mouse embryo

The organization of the cytokeratin network in preimplantation mouse embryos at various stages of development was visualized by whole-mount indirect immunofluorescence with anti-Endo A or anti-Endo B antibody. The appearance of the cytokeratin network was the same regardless of which antibody was used. The first filamentous staining for Endo A and Endo B was detected in compacted 8-cell embryos, 60% of which contained light filament patches in 1 to 4 of the blastomeres (Fig. 10A, B). As in the study of Chisholm & Houliston (1987), no staining above background levels was observed before compaction. When morulae and blastocysts were analyzed by whole-mount indirect immunofluorescence, only the outer blastomeres could be definitively assayed for their content of assembled cytokeratin filaments. This analysis revealed an interesting pattern of filament organization in the outer blastomeres of morulae. Although 100% of the embryos had assembled filaments by the 16-cell stage, most morulae were mosaics, with outer blastomeres containing differing amounts of cytokeratin filaments (Fig. 10C, D). In general, outer blastomeres of late morulae contained a more uniform, organized, and dense network (Fig. 10E, F) than outer blastomeres of mid morulae, although the correlation was not strict. The mosaic distribution of cytokeratin filaments in morulae is in contrast to the uniform distribution of other cytoskeletal elements in the preimplantation embryo. For example, actin

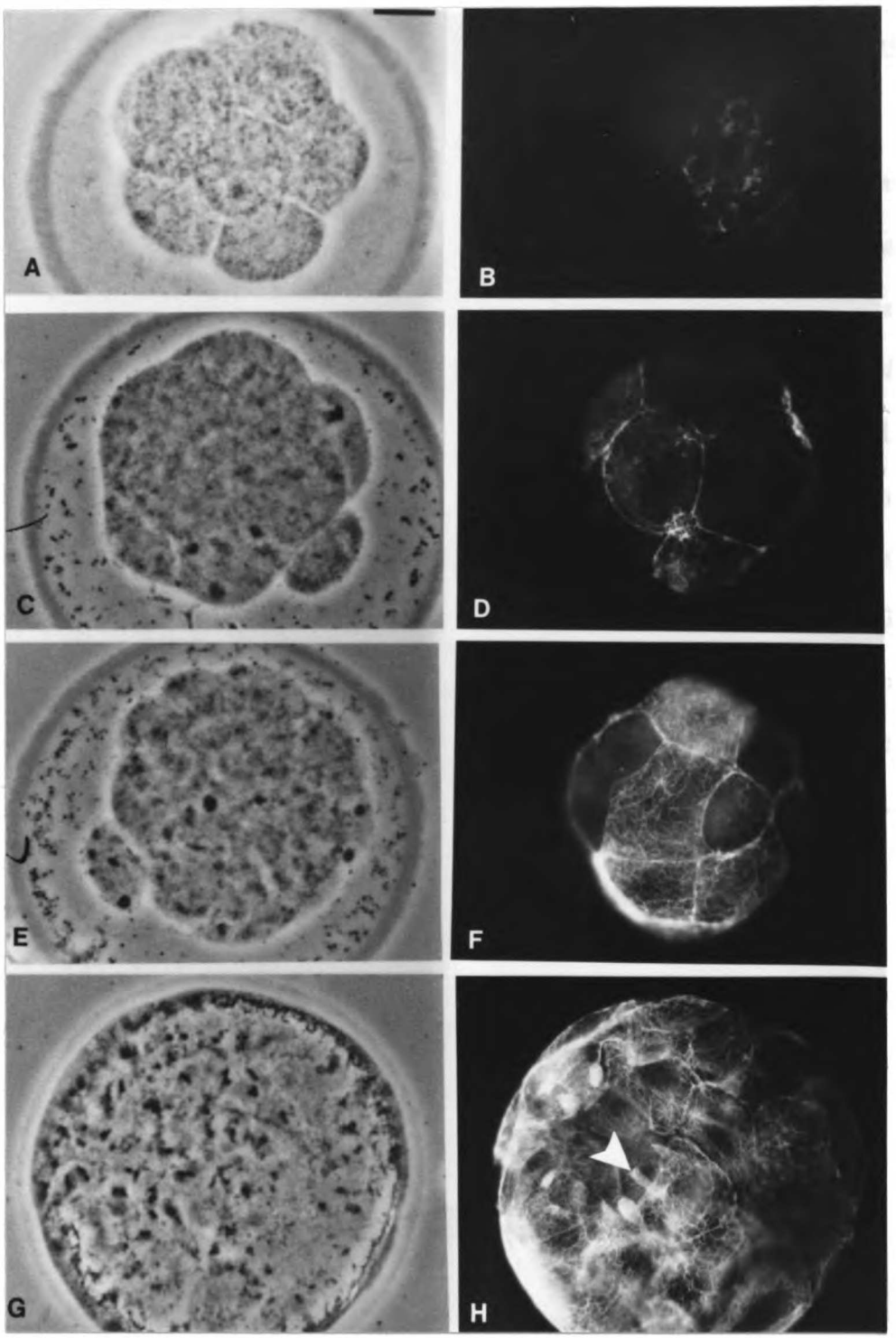

Fig. 10. Cytokeratin filament organization in the preimplantation mouse embryo, visualized by whole-mount indirect immunofluorescence. (A, C, E, G) Phase-contrast microscopy. (B, D, F, H) Fluorescence microscopy. (A, B) Compacting 8-cell embryo. (C, D) Mid morula. (E, F) Late morula. (G, H) Expanded blastocyst. (Arrowhead) Projection of a trophectoderm cell that underlies the ICM. Bar, 20 μm.

staining of similar intensity is observed in the cortical layer of all blastomeres throughout cleavage and blastocyst formation (Lehtonen & Badley, 1980; Reima & Lehtonen, 1985; [also, data not shown]).

As the cytokeratin network became more organized, it appeared to occupy primarily a cortical or slightly subcortical position. This would be consistent with attachment of the cytokeratin filaments to desmosomes (Cowin *et al.* 1985; Steinberg *et al.* 1987), which are assembled as part of the junctional complexes of the outer blastomeres (Ducibella *et al.* 1975; Magnuson *et al.* 1977; Jackson *et al.* 1980). Mitotic cells of morulae often stained diffusely, suggesting a substantial modification of the cytokeratin polypeptides during mitosis (Franke *et al.* 1982a; Lane *et al.* 1982; Chisholm & Houliston, 1987). At the blastocyst stage, each trophectoderm cell contained an intricate array of cytokeratin filaments (Fig. 10G, H). Trophectoderm cell projections, which underlie the ICM (Ducibella *et al.* 1975; Fleming *et al.* 1984), were often highlighted by their dense cytokeratin network (Fig. 10H). At no time did embryos of any stage that were incubated with nonimmune IgG exhibit staining above background levels.

Cytokeratin synthesis and assembly in blastocysts and ICMs

Examination of the high-salt, Triton X-100-insoluble fraction of mouse blastocysts that had been metabolically-labeled with [^{35}S]methionine revealed abundant amounts of newly-synthesized Endo A and Endo B in the cytoskeletal fraction (Fig. 11A). However, neither this approach nor the examination of blastocysts by whole-mount indirect immunofluorescence allowed for the characterization of the cytokeratin content of the ICM. Therefore, this problem was addressed in two ways. First, ICMs were isolated by immunosurgery (Solter & Knowles, 1975), and their synthesis of Endo B was examined. Immunoprecipitation of ICM lysates revealed that isolated ICMs do synthesize Endo B (Fig. 11B), but only at about 10% of the level of synthesis of intact blastocysts. It was important to

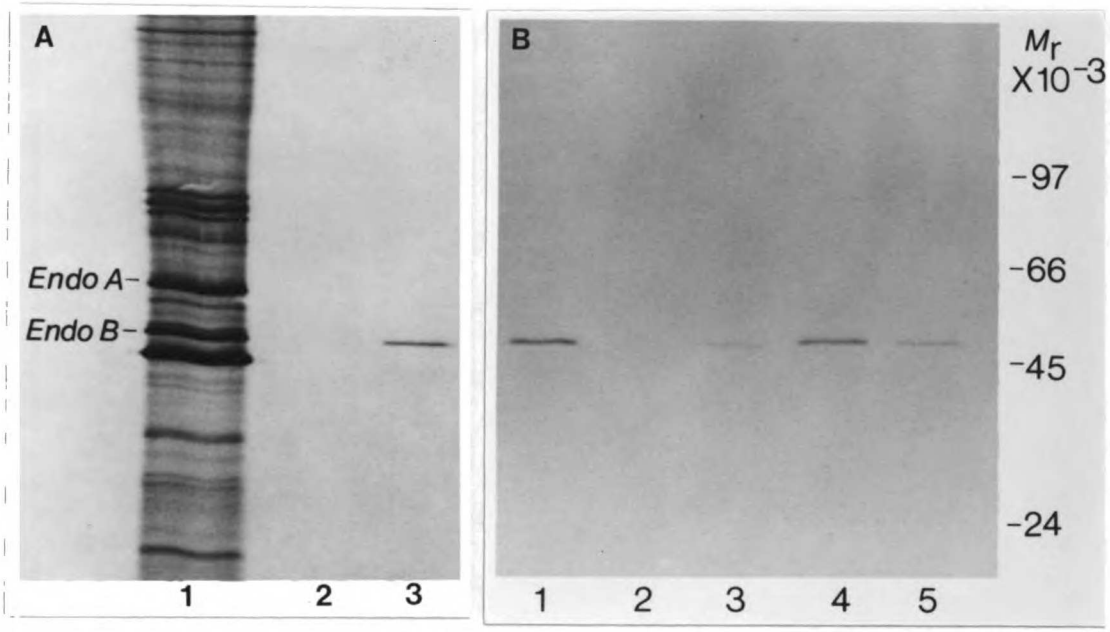

Fig. 11. Cytokeratin synthesis in blastocysts and isolated ICMs.
(A) Analysis of proteins present in the cytoskeletal fraction of blastocysts or recovered from blastocyst lysates by immunoprecipitation with anti-Endo B antibody.

Lane 1: cytoskeletal fraction from 115 blastocysts metabolically-labeled with [^{35}S]methionine, 5800 cpm of acid-insoluble material.

Lane 2: nonimmune immunoprecipitate of blastocysts, 65,000 cpm of acid-insoluble, pre-immunoprecipitation lysate.

Lane 3: anti-Endo B immunoprecipitate of blastocysts, 65,000 starting cpm.

(B) Immunoprecipitation of [^{35}S]methionine-labeled blastocysts and isolated ICMs.

Lane 1: anti-Endo B immunoprecipitate of blastocysts, 62,000 starting cpm.

Lane 2: nonimmune IgG immunoprecipitate of isolated ICMs, 73,000 starting cpm.

Lane 3: anti-Endo B immunoprecipitate of isolated ICMs, 55,000 starting cpm.

Lane 4: anti-Endo B immunoprecipitate of intact blastocysts, 50,000 starting cpm.

Lane 5: anti-Endo B immunoprecipitate of isolated ICMs, 100,000 starting cpm.

Molecular weight markers (X 10^{-3}) are indicated at the right.

distinguish whether this low level of synthesis reflects real synthesis carried out by ICM cells of intact blastocysts or is simply part of the initial response to the altered cell contacts of the outer cells of isolated ICMs (Handyside, 1978; Hogan & Tilly, 1978; Spindle, 1978; Johnson, 1979; Fleming *et al.* 1984). Therefore, the distribution of cytokeratin filaments was examined by indirect immunofluorescence of fixed and sectioned blastocysts. Although unassembled cytokeratin proteins cannot be detected with this approach, its major advantage over other methodologies is that the distribution of cytokeratin filaments can be assayed simultaneously in both trophectoderm and ICM. Similar to the results of whole-mount indirect immunofluorescence, distinct cytokeratin filament bundles were observed in the trophectoderm of all blastocyst sections (Fig. 12). In contrast, no organized cytokeratin filaments were detected in the ICM of most of the sectioned blastocysts (Fig. 12B). Sections incubated with nonimmune antibody exhibited dim, nonfilamentous staining of equal intensity throughout the section (not shown). Occasionally, small patches of brightly stained material were observed in some cells of the ICM (Fig. 12D). These patches, which may correspond to the occasional small cluster of cytokeratin filaments seen in the ICM of extracted blastocysts examined by immunoelectron microscopy (Chisholm & Houliston, 1987), may be the result of new cytokeratin synthesis by ICM cells of intact blastocysts.

Disruption of the cytokeratin filament network in mural trophectoderm cells

Because large quantities of anti-Endo A antibody were readily obtained by culture of the TROMA-1 hybridoma, all microinjection studies were done with purified TROMA-1 IgG. The intracellular activity of TROMA-1 IgG was assessed initially by iontophoretic microinjection of limited amounts of antibody into individual mural trophectoderm cells of 3.5-day blastocysts. Double-label immunofluorescence revealed that the cytokeratin network was visibly disorganized in two thirds of the TROMA-1-injected cells (Table 3; Fig. 13A-D). In contrast, injections of nonimmune IgG had no disruptive effect on the organization of the

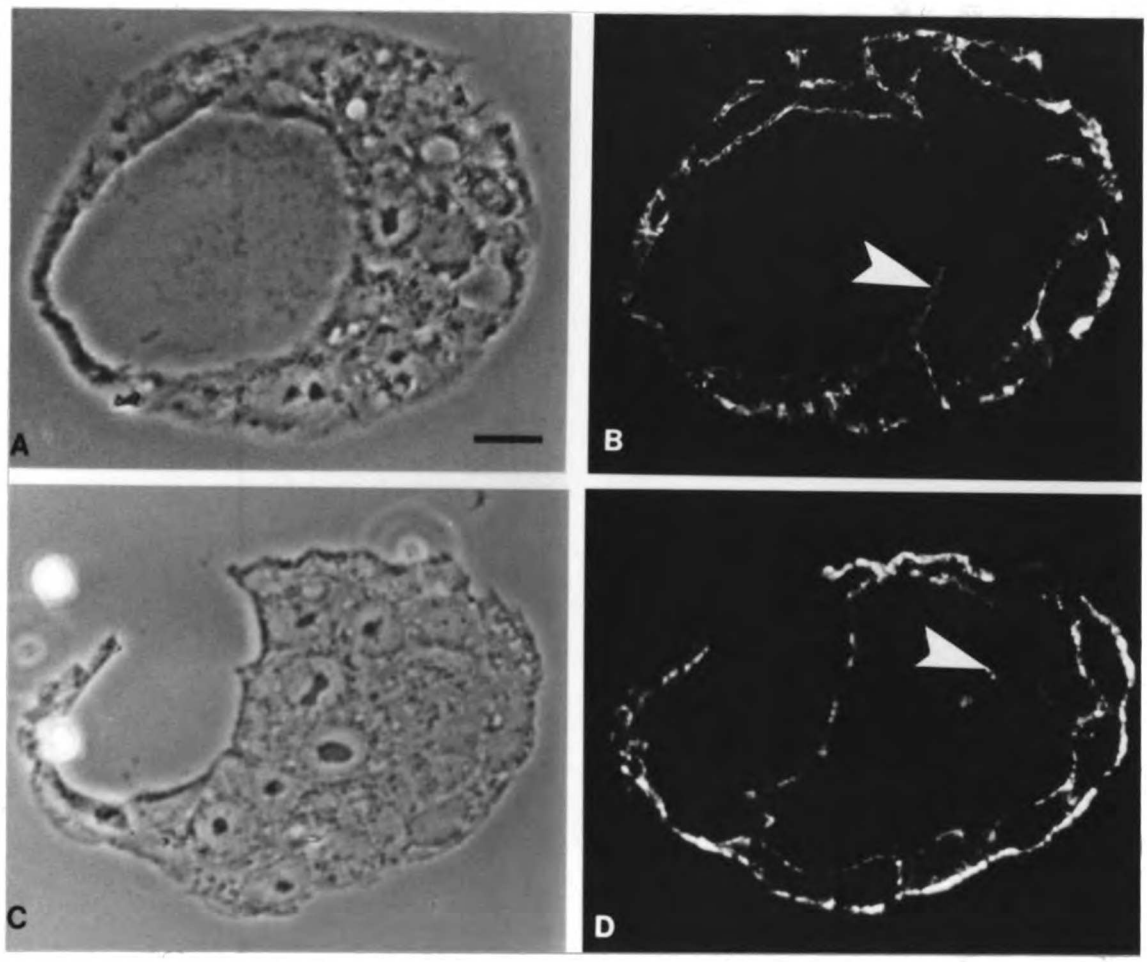

Fig. 12. Distribution of cytokeratin filaments in sectioned blastocysts. (A, C) Phase-contrast microscopy. (B, D) Fluorescence microscopy. Note the distinct staining of the outer, trophectoderm cells in both sections and the primarily cortical location of the assembled cytokeratin filaments. (A, B) The ICM of this representative blastocyst contains no organized cytokeratin filaments. Note the trophectoderm process on the blastocoel surface of the ICM (arrowhead, B). (C, D) Small patches of stained material are present in some cells of the ICM of this blastocyst (arrowhead, D). Bar, 10 μm.

Table 3. *Disruption of the cytokeratin filament network after microinjection of TROMA-1 IgG into preimplantation mouse embryos*

Stage injected	No. embryos cultured	No. developed to 4- to 8-cell stage	No. developed to morulae/blastocysts[†]	No. embryos processed*	No. blastocysts with disrupted filaments
Blastocyst (mural trophectoderm)	N.A.	N.A.	N.A.	30	20 (67)[‡]
2-cell stage					
Uninjected	198	191 (96)	182 (95)	>100	0
1 cell (immune IgG)	36	30 (83)	29 (97)	23	23 (100)
2 cells (immune IgG)	131	108 (82)	94 (87)	47[§]	40 (total) (85) 5 (partial) (11)
2 cells (nonimmune IgG)	28	19 (68)	11 (58)	9	0

[†]The percentage of embryos that developed to these stages was based on the number that had progressed to the 4- to 8-cell stage by 18-24 h after injection.
*Because morulae are normally mosaics for filament expression (see Fig. 1), only the blastocysts were scored for filament disruption.
[‡]Numbers in parentheses indicate percentages.
[§]Not all of the blastocysts in this series were processed for immunofluorescence.
N.A. Not applicable.

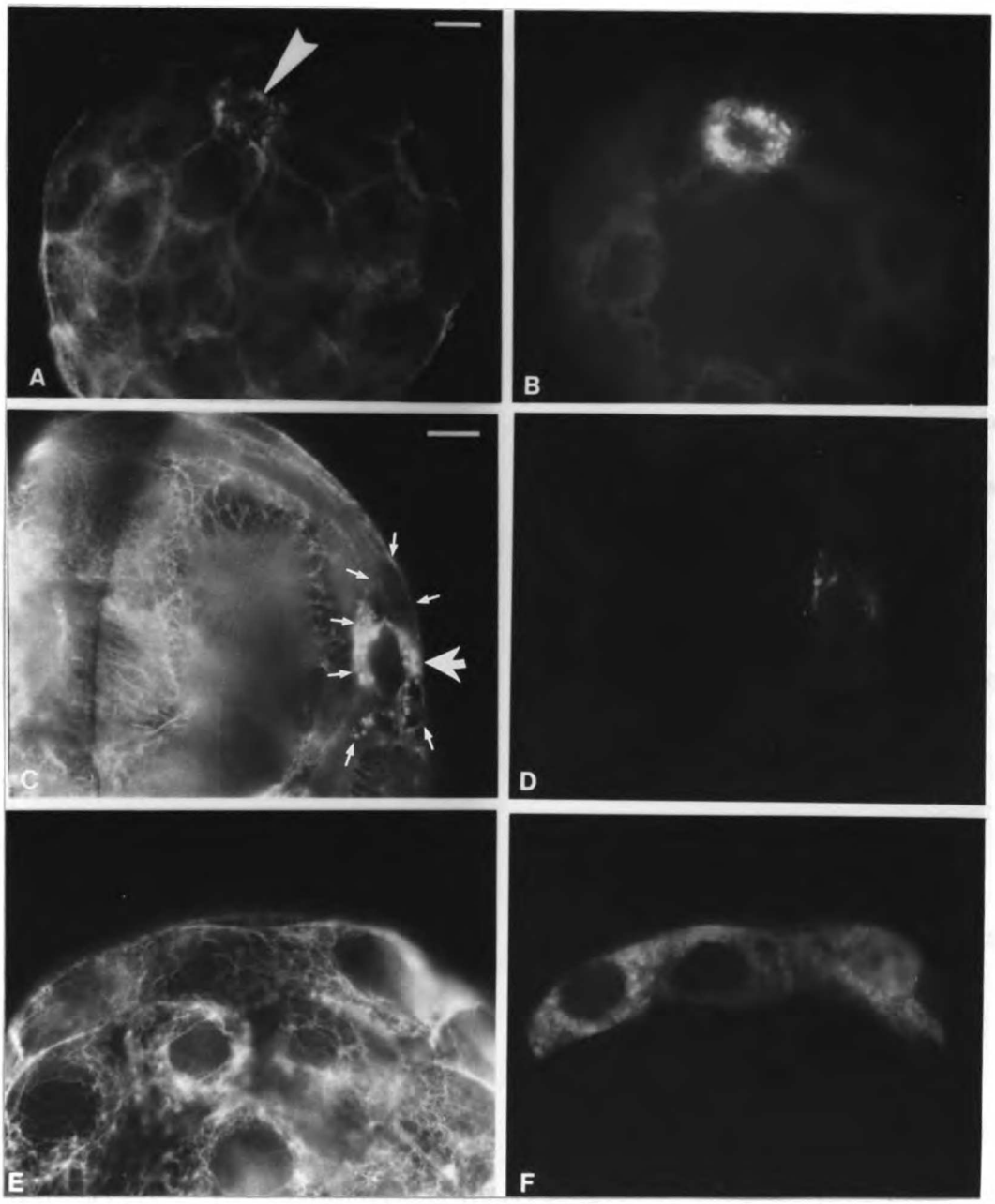

Fig. 13. Injection of IgG into mural trophectoderm cells. (A, C, E) Organization of cytokeratin filaments in the entire blastocyst, visualized by staining with anti-Endo B IgG and fluorescein-conjugated anti-rabbit IgG. (B, D, F) Identification of the injected cells with Texas Red-conjugated anti-rat IgG. (A-D) The trophectoderm cells with the disorganized networks (arrowheads) are the cells that were injected with TROMA-1 IgG. In (C), the boundaries of the injected cell are marked. Although a few residual extended filaments remain (lower right corner of cell), most of the network has collapsed around the nucleus. (E, F) Three mural trophectoderm cells injected with nonimmune IgG. The cytokeratin network is unperturbed in these cells. Areas of brighter staining in (E) represent bundles of superimposed filaments, and serial focusing through cells injected with nonimmune IgG never revealed filament aggregates and clearing, such as illustrated in B & D. Bar, 10 μm.

filaments (Fig. 13E, F). Thus, these results indicate that TROMA-1 IgG can function intracellularly to disrupt the organization of a pre-assembled cytokeratin network.

Microinjection of TROMA-1 IgG into 2-cell embryos

The ability of TROMA-1 IgG to inhibit *de novo* cytokeratin filament assembly was assessed by its injection into 2-cell embryos, which have not yet assembled cytokeratin filaments. Initially, TROMA-1 IgG was injected into one of the two blastomeres, with the uninjected blastomere serving as an internal control for cytokeratin assembly. The injected embryos were cultured in microdrops of egg culture medium, and their development was scored on both the first and second days after injection. Most embryos developed to the late morula or blastocyst stages (Table 3). Of the 7 embryos that did not develop, 6 arrested at the 2- or 3-cell stage, and most of this arrest was attributed to damage during the injection process. When the rate of development was adjusted by excluding the early-arrested embryos, it was found to be equivalent to the development of uninjected controls (Table 3). In all of the blastocysts that developed from the injected 2-cell embryos, cytokeratin filaments were greatly reduced in number or absent in up to half of the trophectoderm cells (Fig. 14). These affected cells contained TROMA-1 IgG, as indicated by Texas Red fluorescence, and, therefore, were the descendants of the injected 2-cell blastomere. Uninjected embryos or embryos injected with nonimmune IgG never showed patches of filament-negative or filament-aggregated trophectoderm cells at the blastocyst stage. Interestingly, despite the inhibition of filament assembly in up to half of the trophectoderm cells, the TROMA-1-injected embryos formed blastocysts, and the descendants of the injected blastomeres were integral members of the trophectoderm layer.

The results of the preceding experiment suggested that formation of an extensive cytokeratin network may not be necessary for trophectoderm differentiation. To rule out the possibility that the nonperturbed cells were somehow compensating for the affected ones,

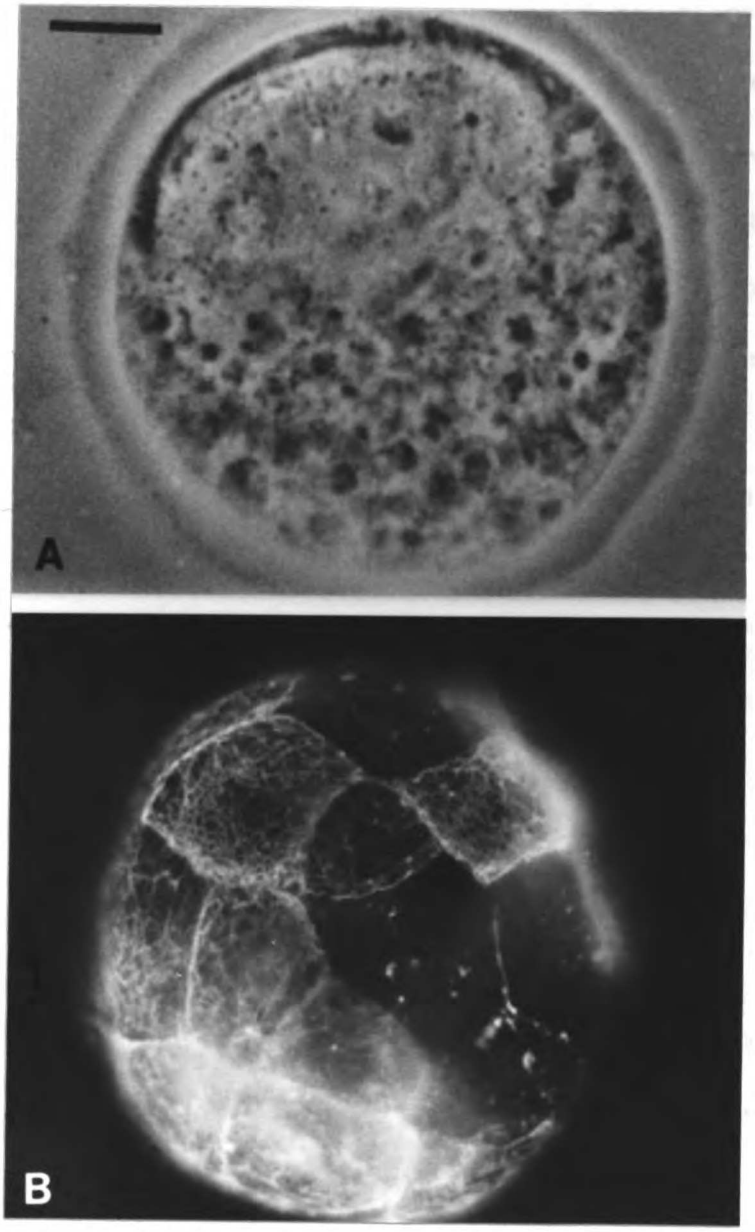

Fig. 14. Injection of TROMA-1 IgG into one of the 2-cell blastomeres. (A) Phase-contrast microscopy. An injected embryo that developed into a blastocyst. (B) The distribution of the cytokeratin network, revealed with anti-Endo B IgG and fluorescein-conjugated anti-rabbit IgG. Note the absent or disrupted network in many of the trophectoderm cells, which are descendants of the injected 2-cell blastomere. Bar, 20 μm.

both blastomeres at the 2-cell stage were injected with TROMA-1 IgG (Fig. 15). The quantity of TROMA-1 IgG injected into 2-cell embryos was determined by immunoblot analysis. A standard curve was generated with serial, doubling dilutions of nonimmune rat IgG blotted onto nitrocellulose paper (Fig. 16). Collections of TROMA-1-injected 2-cell embryos were lysed and blotted in the adjoining row of the slot-blot apparatus, and the IgG was visualized using standard immunoblot methods. When a starting concentration of 16 mg/ml of TROMA-1 IgG was used for injection, an average of 500 pg of antibody was introduced into each 2-cell embryo (Fig. 16). The amount of Endo A in the preimplantation mouse embryo was estimated as follows: the total protein content of a 3.5-day blastocyst is approximately 22 ng (Brinster, 1967), of which 5-9% is estimated to be β-actin (Abreu & Brinster, 1978; Brinster *et al.* 1979). The level of synthesis of Endo A in intact blastocysts is approximately 25% the level of β-actin (Van Blerkom *et al.* 1976; Brûlet *et al.* 1980; Jackson *et al.* 1980; personal observation). Assuming relatively similar rates of degradation for β-actin and Endo A in the embryo (see Fig. 3, Brinster *et al.* 1979), the amount of Endo A in a mouse blastocyst was calculated to be in the range of 300-500 pg. An antibody concentration of 0.625 IgG molecules per intermediate filament monomer was sufficient to inhibit the *in vitro* assembly of desmin into extended 10-nm filaments (Ip, 1988). Moreover, Gawlitta *et al.* (1981) achieved disruption of the vimentin filament network in fibroblasts with an intracellular anti-vimentin antibody concentration estimated to be 10-fold lower than the intracellular concentration of vimentin. Therefore, 500 pg of TROMA-1 IgG was deemed sufficient for the inhibition of cytokeratin filament assembly in the preimplantation mouse embryo.

After culture for 48-54 h, the embryos were scored for their morphological development. Most of the injected embryos developed into late morulae or blastocysts (Table 3; Fig. 17). Although their rate of development was slightly reduced as compared to

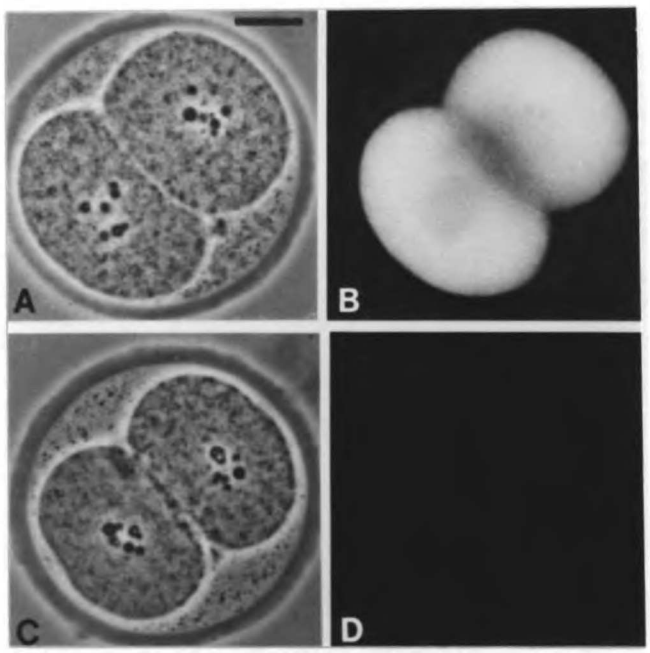

Fig. 15. Two-cell embryos stained with Texas Red-conjugated anti-rat IgG. (A, C) Phase-contrast microscopy. (B, D) Fluorescence microscopy. (A, B) An embryo fixed and stained immediately after injection of both blastomeres with TROMA-1 IgG. (C, D) An uninjected embryo identically fixed and stained. Bar, 25 μm.

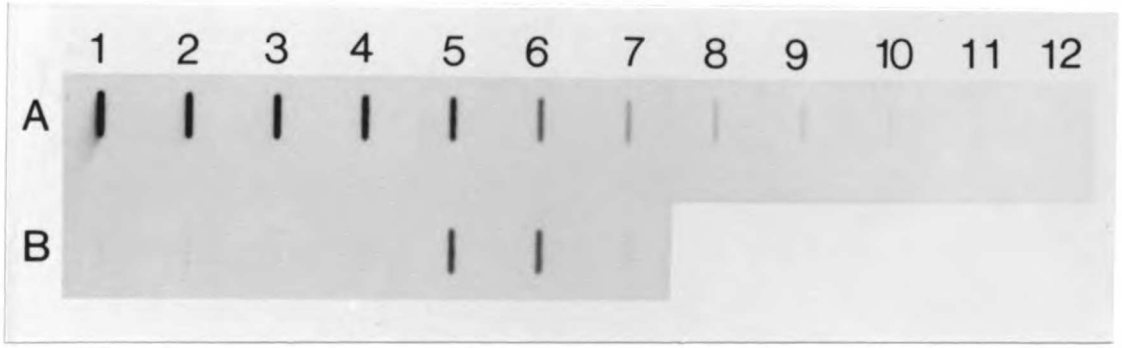

Fig. 16. Quantification of TROMA-1 IgG injected into 2-cell embryos. (Row A) Serial doubling dilutions of rat IgG mixed *in vitro* with 2-cell embryo extract: Slot 1, 100 ng; Slot 11, 0.098 ng; Slot 12, no IgG. (Row B) Slots 1-4, PBS; Slots 5 + 6 (each), lysate from duplicate samples of 9.5 injected 2-cell embryos; Slot 7, lysate from 10 uninjected 2-cell embryos. By extrapolation to the standard curve generated by Row A, lanes 5 and 6 contain 4.2 ng and 3.4 ng, respectively, of TROMA-1 IgG. These results were combined with the results from a second slot blot to yield an average of 500 pg of IgG injected per embryo.

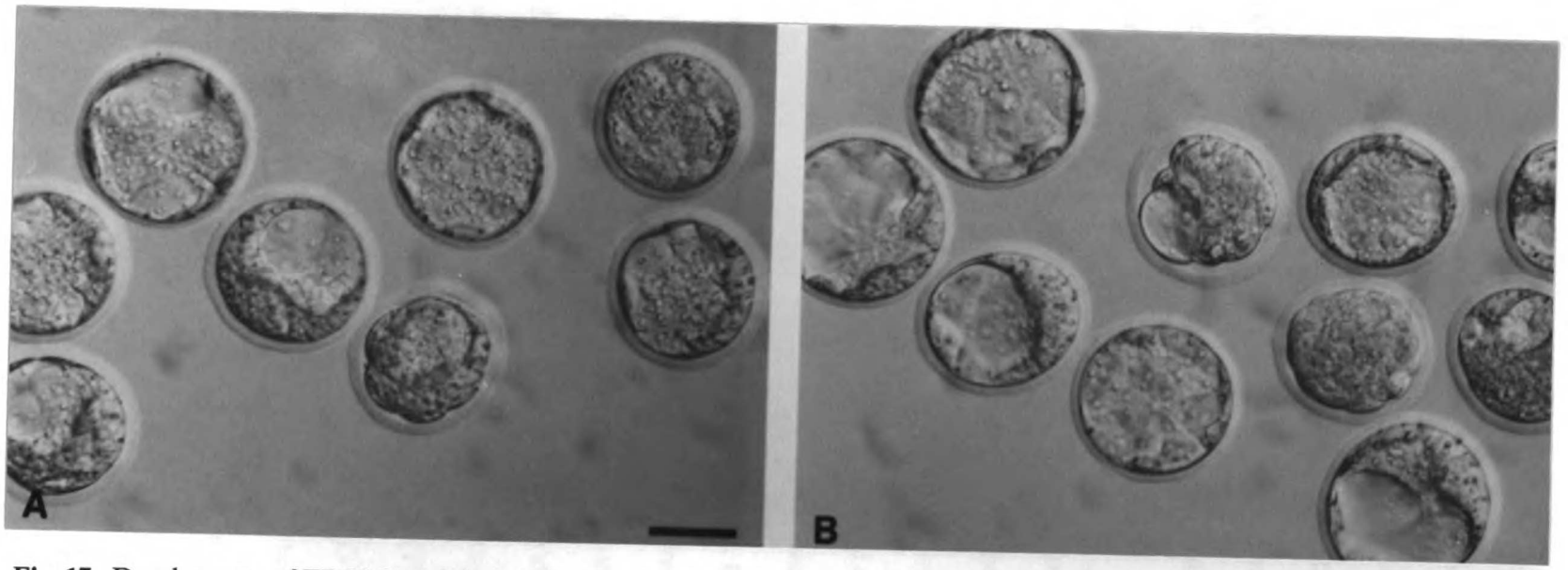

Fig. 17. Development of TROMA-1-injected 2-cell embryos into blastocysts. The morphology of the injected embryos (A) is indistinguishable from that of uninjected controls (B) by Nomarski optics. Bar, 60 μm.

uninjected controls or 2-cell embryos injected in only one blastomere, this was most likely due to the increased trauma caused by a second injection of the same embryo. A control series with nonimmune rat IgG injected into both blastomeres supports this assumption (Table 3). Most of the embryos injected with TROMA-1 IgG that did not develop into late morulae or blastocysts were arrested at the same (early) stages as embryos injected with nonimmune IgG. Therefore, the slightly lower rate of development of the TROMA-1-injected embryos, as compared to uninjected controls, was not attributed to any specific effects of the anti-cytokeratin antibody.

Fluorescent staining of blastocysts derived from 2-cell embryos that were injected with nonimmune rat IgG showed that they contained normal numbers of nuclei and an extensive cytokeratin network (Fig. 18A-C). Staining of blastocysts derived from the TROMA-1-injected embryos revealed that the antibody was present in all cells of the embryo (Fig. 18D). The diffuse nature of the Texas Red fluorescence suggested that the injected antibody was still in excess of the endogenous levels of Endo A. In general, these blastocysts also contained normal numbers of nuclei (Fig. 18E). When examined for their cytokeratin distribution, 85% of the blastocysts derived from TROMA-1-injected 2-cell embryos contained a significantly disorganized cytokeratin network (Table 3; Fig. 18F). Examination of the cytokeratin network at higher magnification revealed that only traces of filamentous material were present in most TROMA-1-injected embryos (Fig. 19B), whereas the cytokeratin network of embryos injected with nonimmune IgG was extensive and unperturbed (Fig. 19A). Many of the trophectoderm cells of blastocysts developed from TROMA-1-injected embryos were devoid of both injected antibody and cytokeratin filaments, suggesting that the cytokeratin and antibody concentrations were at equivalence and that all precipitates were cleared away. Examination of trophectoderm cells in later-stage blastocysts revealed the emergence of an extensive cytokeratin network that was lightly

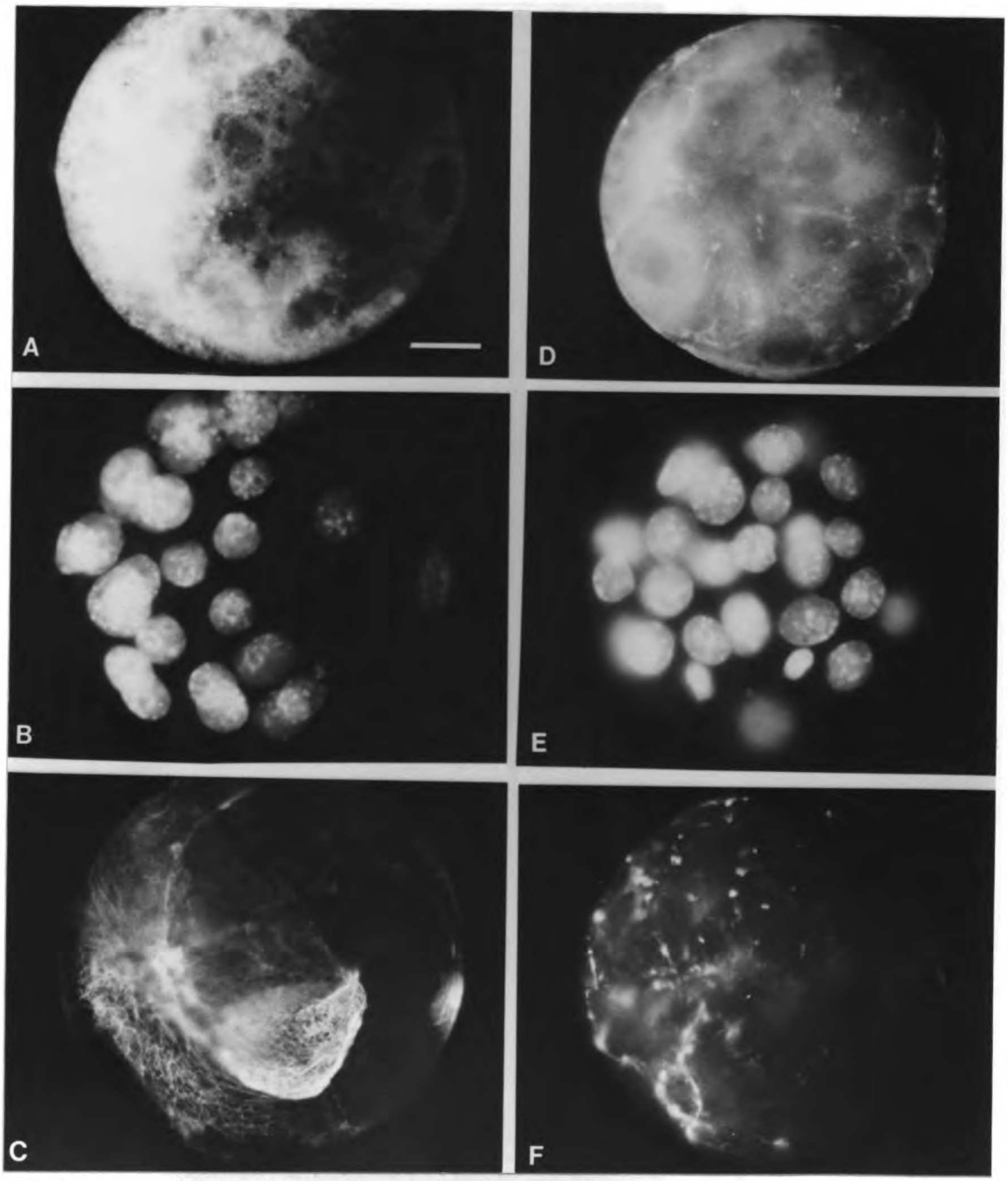

Fig. 18. Triple-label fluorescence of 2-cell embryos injected in both blastomeres and grown to the blastocyst stage. (A-C) Nonimmune rat IgG-injected embryo. (D-F) TROMA-1 IgG-injected embryo. (A, D) Texas Red fluorescence. The injected antibodies were present in all cells of the blastocysts. (B, E) Hoechst fluorescence. Both blastocysts had normal numbers of nuclei (32 and >35, respectively). (C, F) Fluorescein fluorescence. The cytokeratin network of the nonimmune rat IgG-injected embryo (C) was unaffected. Note the absence of an extensive cytokeratin network in the TROMA-1-injected embryo (F). Bar, 20 μm.

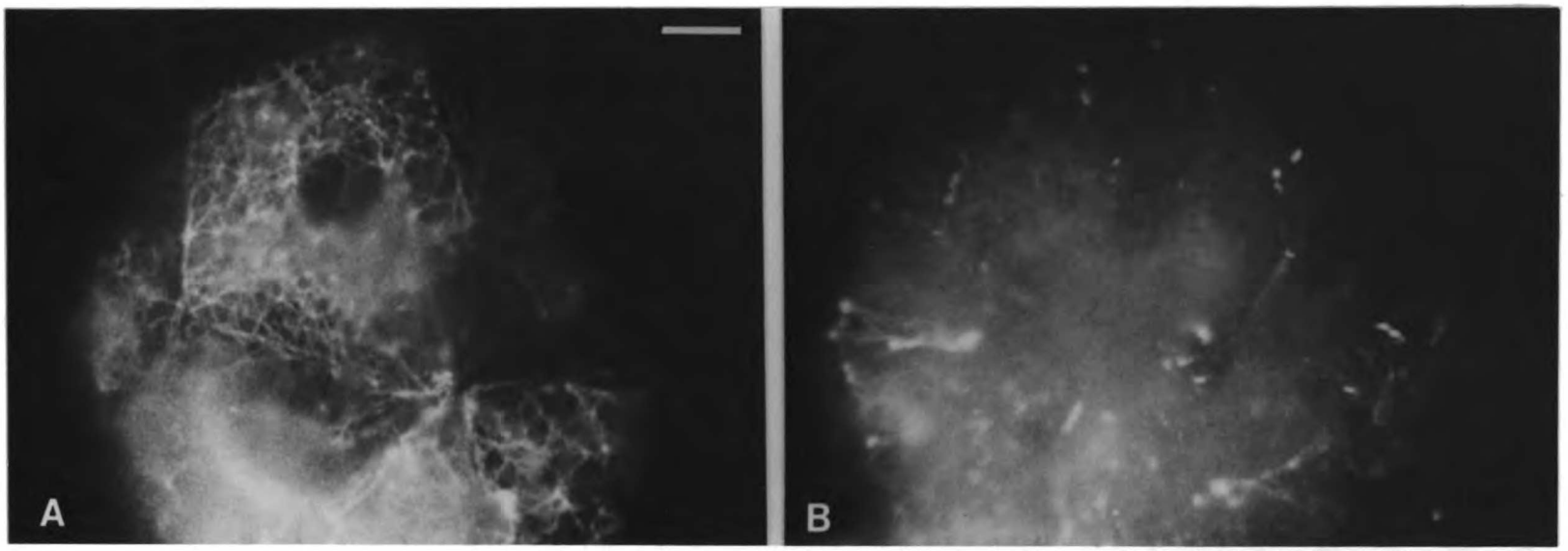

Fig. 19. Organization of the cytokeratin network in 2-cell embryos injected in both blastomeres and grown to the blastocyst stage (fluorescein fluorescence). (A) The cytokeratin network is intact and extensive in trophectoderm cells of embryos injected with nonimmune rat IgG. (B) Only traces of filamentous material appear in embryos injected with TROMA-1 IgG. Bar, 10 μm.

decorated with the injected TROMA-1 IgG. At this time, the cytokeratin polypeptides most likely were in excess of the injected antibody, and filament assembly was not inhibited. Some 2-cell embryos inadvertently received reduced amounts of TROMA-1 IgG in one of the blastomeres (as determined by the RDX fluorescence intensity immediately after injection) but nevertheless were included in the study sample. The 11% of embryos that contained cytokeratin filaments in up to one half of their trophectoderm cells (Table 3) probably were the descendants of these embryos.

Discussion

The assembly of cytokeratin filaments in the preimplantation mouse embryo

The first detectable synthesis of Endo A and Endo B in the mouse embryo is at the 4- to 8-cell stage (Oshima *et al.* 1983). Results of the whole-mount immunofluorescence analysis presented here have confirmed the recent observations of Chisholm and Houliston (1987) that assembly of cytokeratin filaments is a gradual process and occurs at least two cell cycles before overt epithelial formation. Thus, there appears to be relatively little lag time between the synthesis of Endo A and Endo B and their assembly into filaments. Because individual IF monomers are unstable in physiological solutions, Endo A and Endo B most likely associate and assemble into filament intermediates as soon as a critical concentration of both is reached in the embryo.

The assembly of cytokeratin filaments at the 8- and 16-cell stages of embryogenesis is reminiscent of the assembly of cytokeratin filaments in fibroblasts after microinjection of mRNA enriched in sequences for epidermal cytokeratins (Kreis *et al.* 1983). In both instances, the formation of an extensive cytokeratin network is preceded by the appearance of short rods and fibrils scattered throughout the cytoplasm of the cells. These data support the hypothesis of Ip and co-workers (1985) that assembly of short, full-width IF intermediates occurs prior to the elongation of extended filaments. Moreover, the *de novo* assembly of cytokeratin filaments in both the injected fibroblasts and in blastomeres of the preimplantation mouse embryo appears to be a relatively slow process, occurring over a period of several hours to days. In contrast, the incorporation of newly-synthesized IF monomers into filaments in cells that contain a pre-existing IF network occurs within minutes (Blikstad & Lazarides, 1983; Franke *et al.* 1984). Thus, once an extensive IF network is assembled within cells, the incorporation of newly-synthesized IF monomers into the cytoskeletal fraction may occur by a relatively rapid exchange process, rather than by the

assembly of IFs consisting entirely of new IF monomers. Finally, the detection of short rods of cytokeratin material scattered throughout the cytoplasm of the cleavage-stage blastomeres suggests that assembly of cytokeratin filaments does not initiate at the nuclear envelope in the blastomeres of the early mouse embryo, as has been suggested for vimentin assembly in erythroid cells (Georgatos & Blobel, 1987a, b).

One of the most striking observations of the present study is that assembly is not uniform and synchronous throughout the embryo, but rather results in a mosaic distribution of cytokeratin filaments in the outer blastomeres at the morula stage. The data of Chisholm and Houliston (1987, Fig. 7) on disaggregated embryos also indicate a mosaic assembly of cytokeratin filaments at the morula stage, as only 30% of the outer cells of mid morulae and 65% of the outer cells of late morulae contained filamentous material. This mosaicism is perhaps trivially explained by assembly occurring first in the older (i.e., earlier-dividing) blastomeres because the division of individual blastomeres is asynchronous starting at the 2-cell stage of mouse embryogenesis (Kelly *et al.* 1978). Alternatively, these differences may be significant and may affect subsequent lineage decisions involved in the allocation of cells to either the trophectoderm or ICM of the blastocyst. For example, blastomeres that contain a less dense cytokeratin network may be those that will allocate a daughter cell to the ICM, while blastomeres with a more dense network may be those that contribute exclusively to the trophectoderm. In this scenario, the younger (i.e., later-dividing) blastomeres may be the ones that assemble a more extensive cytokeratin network, since the older blastomeres contribute disproportionately more inner cells (Kelly *et al.* 1978; Surani & Barton, 1984; Garbutt *et al.* 1987). These possibilities could be distinguished in the following way: at the 3-cell stage, a fixable lineage tracer (i.e., lysinated RDX, Gimlich & Braun, 1985) could be injected into the later-dividing blastomere; after development to the morula stage, the cytokeratin content of the descendant cells of the injected blastomere would be assessed by

whole-mount indirect immunofluorescence, using a fluorescein-conjugated secondary antibody. If cytokeratin assembly is merely a reflection of the age of the blastomere, RDX-positive cells would be predicted to contain fewer filaments. In contrast, if descendants of the later-dividing blastomere are preferentially segregated to the trophectoderm, then RDX-positive cells would be expected to have a higher filament content than RDX-negative cells. Once an embryo is fixed and processed for indirect immunofluorescence, lineage analysis of subsequent stages is impossible. Thus, the fate of outer blastomeres at the mid-morula stage that contain varying levels of cytokeratin filaments cannot be assessed in a similar way.

The results of this study demonstrate that although cells of the ICM synthesize a low level of cytokeratin, there is little, if any, assembly of cytokeratin filaments in the ICM of 3.5-day blastocysts. This pattern of cytokeratin assembly may be generated in two ways: (1) the expression and assembly of cytokeratins is reduced or absent in inner cells of 16-cell morulae, reflecting the eventual allocation of their descendant cells to the ICM (Fleming, 1987); or (2) the expression of cytokeratins is not restricted to the outer blastomeres of mid-morulae, but is selectively down-regulated in inner cells with blastocyst formation. Some evidence for the latter possibility has been presented by Chisholm and Houliston (1987). These data were obtained by either the culture of isolated blastomeres or the disaggregation of embryos just prior to fixation. However, the interpretation of these experimental results is complicated by two factors. First, if the pattern of cytokeratin filament expression is modulated by cell-cell interactions, then the abnormal cell contacts produced by culture of isolated 1/4 or 1/8 blastomeres may alter the subsequent assembly and distribution of the cytokeratin filaments. Secondly, the treatment used to disaggregate morulae (trypsin + EDTA + Ca^{2+}-free medium) is known to greatly affect the distribution and integrity of cytokeratin filaments in cultured epithelial cells (Jones *et al.* 1982; Bologna *et al.* 1986) and may have this same effect in cells of the embryo. Therefore, an *in situ* analysis may be a

more appropriate approach to this problem. The assembly state of cytokeratins in the inner blastomeres of morulae has been unresolved in this study by use of the whole-mount immunofluorescence method. Preliminary attempts to assay the distribution of cytokeratin filaments in PEG sections of morulae were unsuccessful, most likely due to the low abundance of cytokeratins at pre-blastocyst stages. An alternative approach that could be tried in the future to resolve this question is potentially quite simple: to do optical sectioning of morulae processed for whole-mount indirect immunofluorescence by scanning confocal fluorescence microscopy.

The high-level synthesis and assembly of cytokeratin filaments in cultured epithelial cells appears to be dependent on the formation of desmosomal junctions. As discussed earlier, the expression of abundant levels of cytokeratin in cultured epithelial cells is dependent upon extensive cell-cell interactions (Connell & Rheinwald, 1983; Ben-Ze'ev, 1984; Kim *et al.* 1987). A major consequence of culturing epithelial cells at high densities is the ability of adjoining cells to form desmosomal junctions. In the absence of intimate cell-cell contacts, desmosomal proteins are synthesized at steady-state levels, but they are unstable and rapidly degraded (Penn *et al.* 1987; Pasdar & Nelson, 1988a). Induction of cell-cell interactions results in the assembly at the cell periphery of desmosomal junctions, the proteins of which have greatly increased half-lives (Pasdar & Nelson, 1988a, b). In the absence of desmosomes at the cell periphery, cytokeratin filaments are either undetectable or localized in a juxtanuclear region, whereas desmosome formation is accompanied by the appearance of cytokeratin filaments extending throughout the cytoplasm (Jones & Goldman, 1985; Bologna *et al.* 1986; Pasdar & Nelson, 1988b).

In the preimplantation mouse embryo, the outer blastomeres that will become integral members of the trophectoderm increase their synthesis and assembly of cytokeratins, whereas the inner blastomeres that will form the ICM do not. The gradual organization of

an extensive cytokeratin network in the outer blastomeres of the embryo is paralleled by a gradual appearance and maturation of desmosomal junctions. "Nascent" desmosomes have been detected in outer blastomeres of late morulae (Jackson *et al.* 1980), whereas fully formed, typical desmosomal junctions are first present in the trophectoderm cells of mid-to-late blastocysts (Ducibella *et al.* 1975; Jackson *et al.* 1980; Soltyñska 1985). As the first appearance of cytokeratin filaments (compacted 8-cell stage) precedes the first appearance of desmosomal structures (late morula), the assembly of cytokeratin filaments can apparently occur in the absence of desmosomes. However, the stability and density of cytokeratin filaments in the embryo may be regulated by the formation of desmosomes, which serve as anchors for bundles of cytokeratin filaments. Thus, the differential expression of cytokeratins during blastocyst development is likely modulated by differences in cell-cell contacts, which result in the formation of desmosomes in the trophectoderm but not in the ICM. Furthermore, the maturation of desmosomal junctions is accompanied by at least a 10-fold increase in the cytokeratin content of the embryo (Chisholm & Houliston, 1987; Results), and the subsequent differentiation of trophectoderm into trophoblast during blastocyst outgrowth is accompanied by an increase in both the number of desmosomes and the number of cytokeratin filaments (Jackson *et al.* 1980).

As suggested by Chisholm and Houliston (1987), the presence of cytokeratin material in some cells of the ICM may be a result of its residual retention in cells that are descendants of outside cells of the 16-cell morula (Pedersen *et al.* 1986; Fleming, 1987). However, this material could also be an indicator of initial steps in primitive endoderm formation. The synthesis of cytokeratin protein by ICMs detected in the present study may argue for the latter situation. Moreover, Chisholm and Houliston (1987) observed a 3- to 4-fold increase in the percentage of inner cells positive for cytokeratin material during blastocyst expansion. Because there is very little, if any, additional allocation to the ICM

from outside cells during the blastocyst stage (Pedersen *et al.* 1986; Dyce *et al.* 1987), this increase must be accounted for by new assembly and not simply by previous inheritance from an outer cell. Therefore, like trophectoderm differentiation, primitive endoderm formation may be a gradual process carried out over two cell cycles, in which synthesis and assembly of cytokeratin filaments in some cells precede overt epithelial formation. In this way, final commitment of cells to the trophectoderm or primitive endoderm lineages may simply be the result of their acquiring enough epithelial-specific traits to ensure their membership in the epithelial layers.

Disruption of the cytokeratin network in the mouse embryo

The microinjection of anti-cytokeratin antibodies is an effective means of specifically disrupting the cytokeratin network of cultured epithelial cells (Eckert *et al.* 1982; Klymkowsky, 1982; Lane & Klymkowsky, 1982; Klymkowsky *et al.* 1983; Tölle *et al.* 1985). Results of the present study indicate that microinjection of anti-Endo A antibody does perturb the cytokeratin network of mouse embryos and is a valid approach for studying the developmental consequences of inhibiting cytokeratin filament assembly in the preimplantation embryo. The amount of anti-Endo A antibody injected into 2-cell blastomeres was quantified by slot-blot analysis and was estimated to be sufficient to titrate mid-blastocyst levels of Endo A. The disruptive effects of injected TROMA-1 IgG on cytokeratin filament assembly in the embryo was confirmed by double-label indirect immunofluorescence. Surprisingly, dramatic disruption of the cytokeratin network had no obvious effects on the morphological development of the embryos into blastocysts. Therefore, it appears that an extensive cytokeratin filament network is not essential for compaction of preimplantation mouse embryos and their subsequent development into blastocysts. Furthermore, these results suggest that the inability of mouse embryos homozygous for the t^{12} lethal mutation to form blastocysts is not due solely to their reduced

levels of cytokeratin proteins, as postulated by Nozaki and co-workers (1986). In a similar set of experiments, disruption of the cytokeratin network of cleavage-stage *Xenopus* embryos had no morphological effect on their development to the mid-blastula stage (Maynell & Klymkowsky, personal communication).

It is difficult to explain the diversification of intermediate filaments during evolution and their assembly into intricate intracellular arrays without arguing for critical roles in the functioning of cells that contain them (Sun *et al.* 1984; Steinert *et al.* 1985b; Fuchs *et al.* 1987). Thus, the results of the experiments described here may be somewhat perplexing. It has been proposed that cytokeratin filaments may provide tensile strength to maintain the structural integrity of epithelial cells when stressed (Lazarides, 1980; Steinert *et al.* 1984a). However, the cytokeratin filaments are most likely assisted in this job by desmosomes, zonulae adherens, zonular tight junctions, microfilaments, and microtubules. The trophectoderm of the mouse blastocyst contains all of these structural elements (Ducibella *et al.* 1975; Magnuson *et al.* 1977; Jackson *et al.* 1980; Lehtonen & Badley, 1980; Paulin *et al.* 1980), as well as cortical concentrations of spectrin (Reima & Lehtonen, 1985; Sobel & Alliegro, 1985; Damjanov *et al.* 1986) and myosin (Sobel, 1983). Therefore, in the present experiments only a single component was removed from a set of structures that most likely function coordinately to maintain the structural integrity of epithelial layers. Moreover, mid-stage blastocysts are still enclosed in the zona pellucida, which may provide additional support for the trophectoderm cells of the expanding blastocyst. Thus, perhaps it is not surprising that disruption of the cytokeratin network had no effect on the structural integrity of the trophectoderm layer. Furthermore, these results suggest that cytokeratin filaments are not required for the differentiation of a simple, polarized, fluid-transporting epithelium, as blastocoel cavities of normal size were formed in embryos lacking extensive cytokeratin arrays. Therefore, cytokeratin filaments are probably not involved in the localization of

Na^+/K^+-ATPase molecules to the basolateral margins of the trophectoderm cells (Watson & Kidder, 1988).

While the results presented in this dissertation clearly show that cytokeratin filaments are not necessary for the initial stages of trophectoderm differentiation and blastocoel formation, they do not rule out the possibility that cytokeratin filaments play an active role in the subsequent functioning of the trophectoderm. Therefore, it would be informative to study the effects of cytokeratin filament disruption beyond the mid-blastocyst stage, when trophectoderm differentiates into trophoblast and there is a great increase in the number of cytokeratin filaments (Jackson *et al.* 1980; unpublished observations). In addition, differentiation of the ICM into primitive endoderm and embryonic ectoderm is accompanied by desmosome formation and expression of cytokeratin filaments consisting of Endo A and Endo B (Kemler *et al.* 1981; Jackson *et al.* 1981). Because all tissues of the fetus are derived from the embryonic ectoderm, examination of the function of Endo A and Endo B during postimplantation development should be especially interesting.

Unfortunately, analyses of cytokeratin filament disruption by antibody microinjection into cleavage-stage embryos cannot be carried beyond the mid-blastocyst stage, owing to the degradation and dilution of the injected antibody that takes place during the two days that elapse between the 2-cell stage and the formation of the blastocyst at the 32-cell stage. Furthermore, the synthesis and accumulation of cytokeratins increase continually from the 4- to 8-cell stage to the blastocyst stage and beyond (Oshima *et al.* 1983; Chisholm & Houliston, 1987). Moreover, any possible effects of cytokeratin filament disruption in the preimplantation embryo at the biochemical level are difficult to examine because of the large numbers of injected embryos needed to do these studies. Therefore, alternative strategies must be designed to further address the role of cytokeratins in mammalian development. One approach that was tried in this study to examine the effects of filament disruption in

later-stage blastocysts was to introduce large quantities of antibody into all cells of morulae or blastocysts made permeable with various chemicals. Embryos were incubated in solutions containing lysolecithin (Miller *et al.* 1979), polyethylene glycol (Yarosh & Setlow, 1981), high salt (Castellot, Jr. *et al.* 1978), and dimethyl sulfoxide (DMSO) (Fraser *et al.* 1987). Horseradish peroxidase (HRP)-conjugated IgG was used as a tracer molecule for protein uptake by the cells of the embryo. However, none of these procedures worked consistently well. At most, only a few cells of individual embryos took up the antibody (as assessed by staining for HRP), and many embryos contained no positive cells. Moreover, the viability of many cells was suspect after many of these treatments. The only success obtained with any of these methods was the introduction of large quantities of protein into the blastocoel *cavity* of mid-to-late blastocysts using DMSO. Thus, DMSO apparently loosened the intercellular junctions in the trophectoderm, such that IgG molecules passed between the cells of the epithelial layer, but very infrequently into them.

Because the mouse embryo grows considerably during postimplantation development, a bulk-loading approach would have been of limited use, even if one had worked. The need for a self-perpetuating inhibition of filament assembly to study IF function at later stages of embryogenesis is obvious. One promising approach to this problem is the production of "dominant negative mutations," whereby the overproduction of a defective monomer inhibits the subsequent association and assembly of the wild-type monomers into multimeric form (Herskowitz, 1987). Experiments performed by Albers and Fuchs (1987) indicate that this approach can be used to disrupt the cytokeratin network of simple epithelial cells in culture. In these experiments, SV40-enhancer-driven K14 cDNA constructs that contained C-terminal deletions of varying size were transfected into PtK_2 cells. As shown in an earlier study (Giudice & Fuchs, 1987), the K14 protein is readily incorporated into the endogenous network of the PtK_2 cells. Moreover, deletion of the entire non-α-helical C-terminus had no

effect on the ability of the K14 protein to coassemble into filaments, confirming the previous observations that the C-terminus of IF monomers is unnecessary for IF assembly. However, removal of only 10 amino acid residues from the end of coil 2B (see Fig. 1) resulted in a collapse of the endogenous cytokeratin network of the transfected cells, and deletions of larger regions of coil 2B resulted in a dramatic disruption of the cytokeratin network. In these latter instances, no filaments were detected and the mutant and endogenous cytokeratins were co-localized into aggregates scattered throughout the cytoplasm. Thus, even in the presence of an endogenous cytokeratin of the same type, expression in cells of a mutant cytokeratin can result in a dramatic disruption of the cytokeratin network. Albers and Fuchs (1987) suggested that these results are most easily explained if a dynamic equilibrium exists within cells, such that newly-synthesized cytokeratin monomers are exchanged with monomers along the length of pre-existing filaments; the presence of mutant monomers throughout the filament network of the cell creates an instability in the filaments, resulting in their collapse and/or fragmentation. The experiments of Franke and co-workers (1984) are supportive of a dynamic equilibrium between new and old cytokeratin monomers because the entire, endogenous cytokeratin network of epithelial cells was stained with antibodies to the epidermal cytokeratins within minutes of microinjection of mRNA enriched in epidermal cytokeratin sequences.

It is informative to evaluate the results of Albers and Fuchs (1987) with reference to those of Magin and co-workers (1987). Thus, one of the domains that can mediate the heterotypic association of cytokeratin pairs (i.e., the middle of coil 2) (see Fig. 1) was removed in the mutants that have a disruptive effect on filament organization. The presence in these mutants of a second domain that can mediate cytokeratin pair association (i.e., coil 1) may explain the ability of mutant monomers to initially integrate into the native cytokeratin network. Thus, data compiled from several sources suggest that removal of

sequences in one coil of the α-helical rod of a cytokeratin monomer with the retention of the other coil may be the best constructs to use in these types of experiments. Removal of only the non-α-helical N- or C-terminal sequences is not predicted to have a disruptive effect on cytokeratin organization (p. 17 and Albers & Fuchs, 1987).

The data of Albers and Fuchs (1987) were obtained with transient transfectants. Therefore, the establishment of permanent cell lines that continue to exhibit the mutant phenotype should be accomplished before this approach is attempted in transgenic mice. An encouraging observation comes from the experiments of Kulesh and Oshima (1988), who produced stable transfectants of PFHR9 cells expressing high levels of the human K18 protein. Thus, a high level of expression from a transfected cytokeratin gene can occur in cells that express abundant amounts of the equivalent cytokeratin protein. Moreover, the greater the level of expression from the transfected gene, the lower the amount of endogenous cytokeratin produced (Kulesh & Oshima, 1988). These results imply that transfection of a mutant gene into cells that express the equivalent cytokeratin may have a two-pronged inhibitory effect: one at the level of synthesis of the endogenous cytokeratin and another at the level of filament assembly.

Transfection of the mutant K14 cDNA into epidermal cells had a much less frequent and dramatic effect on filament organization (Albers & Fuchs, 1987). This decreased disruptive effect may be due to the increased stability of cytokeratin networks composed of epidermal cytokeratins. Alternatively, it may simply be due to the greater number of cytokeratins in these cells (7) as compared to the PtK_2 cells (2). Thus, fewer mutant monomers per filament segment are likely to be incorporated into the filaments of the epidermal cells, resulting in a decreased destabilizing effect on the filaments in these cells as compared to the PtK_2 transfectants. These results once again emphasize the advisability of exploring the function of simple cytokeratins in epithelial tissues of low cytokeratin

complexity. Because the cDNAs (Brûlet & Jacob, 1982; Leube *et al.* 1986; Oshima *et al.* 1986; Romano *et al.* 1986; Singer *et al.* 1986) and genes (Vasseur *et al.* 1985; Kulesh & Oshima, 1988; Oshima *et al.* 1988) for both the mouse and human K8 and K18 cytokeratins have been cloned, the successful adaptation of this approach using these cloned sequences should allow for a further definition of the roles of cytokeratin filaments in the developing mouse embryo.

References

Abreu, S. L. & Brinster, R. L. (1978). Actin and tubulin synthesis in murine blastocyst outgrowths. *Expl Cell Res.* **115**, 89-94.

Achtstaetter, T., Hatzfeld, M., Quinlan, R. A., Parmelee, D. C. & Franke, W. W. (1986). Separation of cytokeratin polypeptides by gel electrophoretic and chromatographic techniques and their identification by immunoblotting. *Meth. Enzymol.* **134**, 355-371.

Aebi, U., Fowler, W. E., Rew, P. & Sun, T.-T. (1983). The fibrillar substructure of keratin filaments unraveled. *J. Cell Biol.* **97**, 1131-1143.

Albers, K. & Fuchs, E. (1987). The expression of mutant epidermal keratin cDNAs transfected in simple epithelial and squamous cell carcinoma lines. *J. Cell Biol.* **105**, 791-806.

Alberts, B., Bray, D., Lewis, J., Raff, M., Roberts, K. & Watson, J. D. (1983). *Molecular Biology of the Cell.* New York: Garland Publishing, Inc.

Alonso, A., Weber, T. & Jorcano, J. L. (1987). Cloning and characterization of keratin D, a murine endodermal cytoskeletal protein induced during in vitro differentiation of F9 teratocarcinoma cells. *Roux's Arch. devl Biol.* **196**, 16-21.

Bader, B. L., Magin, T. M., Hatzfeld, M. & Franke, W. W. (1986). Amino acid sequence and gene organization of cytokeratin no. 19, an exceptional tail-less intermediate filament protein. *EMBO J.* **5**, 1865-1875.

Balcarek, J. M. & Cowan, N. J. (1985). Structure of the mouse glial fibrillary acidic protein gene: implications for the evolution of the intermediate filament multigene family. *Nucl. Acids Res.* **13**, 5527-5543.

Bartnik, E., Osborn, M. & Weber, K. (1985). Intermediate filaments in non-neuronal cells of invertebrates: isolation and biochemical characterization of intermediate filaments from the esophageal epithelium of the mollusc *Helix pomatia*. *J. Cell Biol.* **101**, 427-440.

Bartnik, E., Osborn, M. & Weber, K. (1986). Intermediate filaments in muscle and epithelial cells of nematodes. *J. Cell Biol.* **102**, 2033-2041.

Bennett, G. S., Fellini, S. A., Toyama, Y. & Holtzer, H. (1979). Redistribution of intermediate filament subunits during skeletal myogenesis and maturation in vitro. *J. Cell Biol.* **82**, 577-584.

Ben-Ze'ev, A. (1984). Differential control of cytokeratins and vimentin synthesis by cell-cell contact and cell spreading in cultured epithelial cells. *J. Cell Biol.* **99**, 1424-1433.

Blikstad, I. & Lazarides, E. (1983). Vimentin filaments are assembled from a soluble precursor in avian erythroid cells. *J. Cell Biol.* **96**, 1803-1808.

Bodeus, M., Burtonboy, G. & Bazin, H. (1985). Rat monoclonal antibodies. IV. Easy method for in vitro production. *J. immunol. Meth.* **79**, 1-6.

Bologna, M., Allen, R. & Dulbecco, R. (1986). Organization of cytokeratin bundles by desmosomes in rat mammary cells. *J. Cell Biol.* **102**, 560-567.

Bonner, W. M. (1984). Fluorography for the detection of radioactivity in gels. *Meth. Enzymol.* **104**, 460-465.

Bosch, F. X., Leube, R. E., Achtstätter, T., Moll, R. & Franke, W. W. (1988). Expression of simple epithelial type cytokeratins in stratified epithelia as detected by immunolocalization and hybridization in situ. *J. Cell Biol.* **106**, 1635-1648.

Brinster, R. L. (1967). Protein content of the mouse embryo during the first five days of development. *J. Reprod. Fert.* **13**, 413-420.

Brinster, R. L., Brunner, S., Joseph, X. & Levey, I. L. (1979). Protein degradation in the mouse blastocyst. *J. biol. Chem.* **254**, 1927-1931.

Brûlet, P., Babinet, C., Kemler, R. & Jacob, F. (1980). Monoclonal antibodies against trophectoderm-specific markers during mouse blastocyst formation. *Proc. natn. Acad. Sci. U.S.A.* **77**, 4113-4117.

Brûlet, P. & Jacob, F. (1982). Molecular cloning of a cDNA sequence encoding a trophectoderm-specific marker during mouse blastocyst formation. *Proc. natn. Acad. Sci. U.S.A.* **79**, 2328-2332.

Burnette, W. N. (1981). "Western blotting": electrophoretic transfer of proteins from sodium dodecyl sulfate-polyacrylamide gels to unmodified nitrocellulose and radiographic detection with antibody and radioiodinated Protein A. *Anal. Biochem.* **112**, 195-203.

Castellot, Jr., J. J., Miller, M. R. & Pardee, A. B. (1978). Animal cells reversibly permeable to small molecules. *Proc. natn. Acad. Sci. U.S.A.* **75**, 351-355.

Chisholm, J. C. & Houliston, E. (1987). Cytokeratin filament assembly in the preimplantation mouse embryo. *Development* **101**, 565-582.

Chisholm, J. C., Johnson, M. H., Warren, P. D., Fleming, T. P. & Pickering, S. J. (1985). Developmental variability within and between mouse expanding blastocysts and their ICMs. *J. Embryol. exp. Morph.* **86**, 311-336.

Connell, N. D. & Rheinwald, J. G. (1983). Regulation of the cytoskeleton in mesothelial cells: reversible loss of keratin and increase in vimentin during rapid growth in culture. *Cell* **34**, 245-253.

Copp, A. J. (1978). Interaction between inner cell mass and trophectoderm of the mouse blastocyst. I. A study of cellular proliferation. *J. Embryol. exp. Morph.* **48**, 109-125.

Cowin, P., Franke, W. W., Grund., C., Kapprell, H.-P. & Kartenbeck, J. (1985). The desmosome-intermediate filament complex. In *The Cell in Contact: Adhesions and Junctions as Morphogenetic Determinants*. (eds. G. M. Edelman & J.-P. Thiery), pp. 427-460. New York: John Wiley & Sons.

Cruz, Y. P. & Pedersen, R. A. (1985). Cell fate in the polar trophectoderm of mouse blastocysts as studied by microinjection of cell lineage tracers. *Devl Biol.* **112**, 73-83.

Czernobilsky, B., Moll, R., Levy, R. & Franke, W. W. (1985). Co-expression of cytokeratin and vimentin filaments in mesothelial, granulosa and rete ovarii cells of the human ovary. *Eur. J. Cell Biol.* **37**, 175-190.

Dale, B. A., Resing, K. A. & Lonsdale-Eccles, J. D. (1985). Filaggrin: a keratin filament associated protein. In *Intermediate Filaments, Ann. N. Y. Acad. Sci.* **455**, 330-342.

Damjanov, I., Damjanov, A., Lehto, V.-P. & Virtanen, I. (1986). Spectrin in mouse gametogenesis and embryogenesis. *Devl Biol.* **114**, 132-140.

DeBlas, A. L. & Cherwinski, H. M. (1983). Detection of antigens on nitrocellulose paper immunoblots with monoclonal antibodies. *Anal. Biochem.* **133**, 214-219.

Denk, H., Lackinger, E., Zatloukal, K. & Franke, W. W. (1987). Turnover of cytokeratin polypeptides in mouse hepatocytes. *Expl Cell Res.* **173**, 137-143.

Ducibella, T., Albertini, D. F., Anderson, E. & Biggers, J. D. (1975). The preimplantation mammalian embryo: characterization of intercellular junctions and their appearance during development. *Devl Biol.* **45**, 231-250.

Duprey, P., Morello, D., Vasseur, M., Babinet, C., Condamine, H., Brûlet, P. & Jacob, F. (1985). Expression of the cytokeratin endo A gene during early mouse embryogenesis. *Proc. natn. Acad. Sci. U.S.A.* **82**, 8535-8539.

Durham, H. D., Pena, S. D. J. & Carpenter, S. (1983). The neurotoxins 2,5-hexanedione and acrylamide promote aggregation of intermediate filaments in cultured fibroblasts. *Muscle & Nerve* **6**, 631-637.

Dyce, J., George, M., Goodall, H. & Fleming, T. P. (1987). Do trophectoderm and inner cell mass cells in the mouse blastocyst maintain discrete lineages? *Development* **100**, 685-698.

Eckert, B. S. (1985). Alteration of intermediate filament distribution in PtK_1 cells by acrylamide. *Eur. J. Cell Biol.* **37**, 169-174.

Eckert, B. S., Daley, R. A. & Parysek, L. M. (1982). In vivo disruption of the cytokeratin cytoskeleton in cultured epithelial cells by microinjection of antikeratin: evidence for the presence of an intermediate-filament-organizing center. *Cold Spring Harb. Symp. quant. Biol.* **46**, 403-412.

Eckert, R. L. (1988). Sequence of the human 40-kDa keratin reveals an unusual structure with very high sequence identity to the corresponding bovine keratin. *Proc. natn. Acad. Sci. U.S.A.* **85**, 1114-1118.

Eichner, R., Bonitz, P. & Sun, T.-T. (1984). Classification of epidermal keratins according to their immunoreactivity, isoelectric point, and mode of expression. *J. Cell Biol.* **98**, 1388-1396.

Eichner, R., Sun, T.-T. & Aebi, U. (1986). The role of keratin subfamilies and keratin pairs in the formation of human epidermal intermediate filaments. *J. Cell Biol.* **102**, 1767-1777.

Enders, A. C. (1971). The fine structure of the blastocyst. In *The Biology of the Blastocyst.* (ed. R. J. Blandau), pp. 71-94. Chicago: The University of Chicago Press.

Ey, P. L. & Ashman, L. K. (1986). The use of alkaline phosphatase-conjugated anti-immunoglobulin with immunoblots for determining the specificity of monoclonal antibodies to protein mixtures. *Meth. Enzymol.* **121**, 497-509.

Fisher, D. Z., Chaudhary, N. & Blobel, G. (1986). cDNA sequencing of nuclear lamins A and C reveals primary and secondary structural homology to intermediate filament proteins. *Proc. natn. Acad. Sci. U.S.A.* **83**, 6450-6454.

Fleming, T. P. (1987). A quantitative analysis of cell allocation to trophectoderm and inner cell mass in the mouse blastocyst. *Devl Biol.* **119**, 520-531.

Fleming, T. P., Warren, P. D., Chisholm, J. C. & Johnson, M. H. (1984). Trophectodermal processes regulate the expression of totipotency within the inner cell mass of the mouse expanding blastocyst. *J. Embryol. exp. Morph.* **84**, 63-90.

Franke, W. W. (1987). Nuclear lamins and cytoplasmic intermediate filament proteins: a growing multigene family. *Cell* **48**, 3-4.

Franke, W. W., Denk, H., Kalt, R. & Schmid, E. (1981a). Biochemical and immunological identification of cytokeratin proteins present in hepatocytes of mammalian liver tissue. *Expl Cell Res.* **131**, 299-318.

Franke, W. W., Hergt, M. & Grund, C. (1987). Rearrangement of the vimentin cytoskeleton during adipose conversion: formation of an intermediate filament cage around lipid globules. *Cell* **49**, 131-141.

Franke, W. W., Mayer, Doris, Schmid, E., Denk, H. & Borenfreund, E. (1981b). Differences of expression of cytoskeletal proteins in cultured rat hepatocytes and hepatoma cells. *Expl Cell Res.* **134**, 345-365.

Franke, W. W., Schiller, D. L., Hatzfeld, M. & Winter, S. (1983). Protein complexes of intermediate-sized filaments: melting of cytokeratin complexes in urea reveals different polypeptide separation characteristics. *Proc. natn. Acad. Sci. U.S.A.* **80**, 7113-7117.

Franke, W. W., Schmid, E., Grund, C. & Geiger, B. (1982a). Intermediate filament proteins in nonfilamentous structures: transient disintegration and inclusion of subunit proteins in granular aggregates. *Cell* **30**, 103-113.

Franke, W. W., Schmid, E., Mittnacht, S., Grund, C. & Jorcano, J. L. (1984). Integration of different keratins into the same filament system after microinjection of mRNA for epidermal keratins into kidney epithelial cells. *Cell* **36**, 813-825.

Franke, W. W., Schmid, E., Schiller, D. L., Winter, S., Jarasch, E. D., Moll, R., Denk, H.,

Jackson, B. W. & Illmensee, K. (1982b). Differentiation-related patterns of expression of proteins of intermediate-size filaments in tissues and cultured cells. *Cold Spring Harb. Symp. quant. Biol.* **46**, 431-453.

Franz, J. K. & Franke, W. W. (1986). Cloning of cDNA and amino acid sequence of a cytokeratin expressed in oocytes of *Xenopus laevis*. *Proc. natn. Acad. Sci. U.S.A.* **83**, 6475-6479.

Franz, J. K., Gall, L., Williams, M. A., Picheral, B. & Franke, W. W. (1983). Intermediate-size filaments in a germ cell: expression of cytokeratins in oocytes and eggs of the frog *Xenopus*. *Proc. natn. Acad. Sci. U.S.A.* **80**, 6254-6258.

Fraser, R. D. B., MacRae, T. P., Suzuki, E. & Parry, D. A. D. (1985). Intermediate filament structure: 2. Molecular interactions in the filament. *Intl J. Biol. Macromol.* **7**, 258-274.

Fraser, S. E., Green, C. R., Bode, H. R. & Gilula, N. B. (1987). Selective disruption of gap junctional communication interferes with a patterning process in Hydra. *Science* **237**, 49-55.

Fuchs, E. V., Coppock, S. M., Green, H. & Cleveland, D. W. (1981). Two distinct classes of keratin genes and their evolutionary significance. *Cell* **27**, 75-84.

Fuchs, E., Grace, M. P., Kim, K. H. & Marchuk, D. (1984). Differential expression of two classes of keratins in normal and malignant epithelial cells and their evolutionary conservation. In *Cancer Cells: The Transformed Phenotype.* (eds. A. J. Levine, G. F. Vande Woude, W. C. Topp & J. D. Watson), pp. 161-167. New York: Cold Spring Harbor Laboratory.

Fuchs, E., Tyner, A. L., Giudice, G. J., Marchuk, D., RayChaudhury, A. & Rosenberg, M. (1987). The human keratin genes and their differential expression. *Curr. Top. devl Biol* **22**, 5-34.

Gall, L., Picheral, B. & Gounon, P. (1983). Cytochemical evidence for the presence of intermediate filaments and microfilaments in the egg of *Xenopus laevis*. *Biol Cell* **47**, 331-342.

Garbutt, C. L., Johnson, M. H. & George, M. A. (1987). When and how does cell division order influence cell allocation to the inner cell mass of the mouse blastocyst? *Development* **100**, 325-332.

Gard, D. L. & Lazarides, E. (1980). The synthesis and distribution of desmin and vimentin during myogenesis in vitro. *Cell* **19**, 263-275.

Gawlitta, W., Osborn, M. & Weber, K. (1981). Coiling of intermediate filaments induced by microinjection of a vimentin-specific antibody does not interfere with locomotion and mitosis. *Eur. J. Cell Biol.* **26**, 83-90.

Geiger, B. & Singer, S. J. (1979). The participation of α-actinin in the capping of cell membrane components. *Cell* **16**, 213-222.

Geisler, N., Fischer, S., Vandekerckhove, J., Plessmann, U. & Weber, K. (1984). Hybrid character of a large neurofilament protein (NF-M): intermediate filament type sequence followed by a long and acidic carboxy-terminal extension. *EMBO J.* **3**, 2701-2706.

Geisler, N., Fischer, S., Vandekerckhove, J., Van Damme, J., Plessmann, U. & Weber, K. (1985a). Protein-chemical characterization of NF-H, the largest mammalian neurofilament component; intermediate filament-type sequences followed by a unique carboxy-terminal extension. *EMBO J.* **4**, 57-63.

Geisler, N., Kaufmann, E., Fischer, S., Plessmann, U. & Weber, K. (1983). Neurofilament architecture combines structural principles of intermediate filaments with carboxy-terminal extensions increasing in size between triplet proteins. *EMBO J.* **2**, 1295-1302.

Geisler, N., Kaufmann, E. & Weber, K. (1982). Proteinchemical characterization of three structurally distinct domains along the protofilament unit of desmin 10 nm filaments. *Cell* **30**, 277-286.

Geisler, N., Kaufmann, E. & Weber, K. (1985b). Antiparallel orientation of the two double-stranded coiled-coils in the tetrametric protofilament unit of intermediate filaments. *J. Mol. Biol.* **182**, 173-177.

Geisler, N. & Weber, K. (1982). The amino acid sequence of chicken muscle desmin provides a common structural model for intermediate filament proteins. *EMBO J.* **1**, 1649-1656.

Georgatos, S. D. & Blobel, G. (1987a). Two distinct attachment sites for vimentin along the plasma membrane and the nuclear envelope in avian erythrocytes: a basis for a vectorial assembly of intermediate filaments. *J. Cell Biol.* **105**, 105-115.

Georgatos, S. D. & Blobel, G. (1987b). Lamin B constitutes an intermediate filament attachment site at the nuclear envelope. *J. Cell Biol.* **105**, 117-125.

Georgatos, S. D. & Marchesi, V. T. (1985). The binding of vimentin to human erythrocyte membranes: a model system for the study of intermediate filament-membrane interactions. *J. Cell Biol.* **100**, 1955-1961.

Giloh, H. & Sedat, J. W. (1982). Fluorescence microscopy: reduced photobleaching of rhodamine and fluorescein protein conjugates by *n*-propyl gallate. *Science* **217**, 1252-1255.

Gimlich, R. L. & Braun, J. (1985). Improved fluorescent compounds for tracing cell lineage. *Devl Biol.* **109**, 509-514.

Giudice, G. J. & Fuchs, E. (1987). The transfection of epidermal keratin genes into fibroblasts and simple epithelial cells: evidence for inducing a Type I keratin by a Type II gene. *Cell* **48**, 453-463.

Glass, C., Kim, K. H. & Fuchs, E. (1985). Sequence and expression of a human Type II mesothelial keratin. *J. Cell Biol.* **101**, 2366-2373.

Godsave, S. F., Wylie, C. C., Lane, E. B. & Anderton, B. H. (1984). Intermediate filaments in the *Xenopus* oocyte: the appearance and distribution of cytokeratin-containing filaments. *J. Embryol. exp. Morph.* **83**, 157-167.

Granger, B. L. & Lazarides, E. (1979). Desmin and vimentin coexist at the periphery of the myofibril Z disc. *Cell* **18**, 1053-1063.

Handyside, A. H. (1978). Time of commitment of inside cells isolated from preimplantation mouse embryos. *J. Embryol. exp. Morph.* **45**, 37-53.

Hanukoglu, I. & Fuchs, E. (1982). The cDNA sequence of a human epidermal keratin: divergence of sequence but conservation of structure among intermediate filament proteins. *Cell* **31**, 243-252.

Hanukoglu, I. & Fuchs, E. (1983). The cDNA sequence of a Type II cytoskeletal keratin reveals constant and variable structural domains among keratins. *Cell* **33**, 915-924.

Hatzfeld, M. & Franke, W. W. (1985). Pair formation and promiscuity of cytokeratins: formation in vitro of heterotypic complexes and intermediate-sized filaments by homologous and heterologous recombinations of purified polypeptides. *J. Cell Biol.* **101**, 1826-1841.

Hatzfeld, M., Maier, G. & Franke, W. W. (1987). Cytokeratin domains involved in heterotypic complex formation determined by *in-vitro* binding assays. *J. Mol. Biol.* **197**, 237-255.

Hawkes, R. (1986). The dot immunobinding assay. *Meth. Enzymol.* **121**, 484-491.

Hedberg, K. K. & Chen, L. B. (1986). Absence of intermediate filaments in a human adrenal cortex carcinoma-derived cell line. *Expl Cell Res.* **163**, 509-517.

Henderson, D., Geisler, N. & Weber, K. (1982). A periodic ultrastructure in intermediate filaments. *J. Mol. Biol.* **155**, 173-176.

Herskowitz, I. (1987). Functional inactivation of genes by dominant negative mutations. *Nature, Lond.* **329**, 219-222.

Hoffman, P. N., Cleveland, D. W., Griffin, J. W., Landes, P. W., Cowan, N. J. & Price, D. L. (1987). Neurofilament gene expression: a major determinant of axonal caliber. *Proc. natn. Acad. Sci. U.S.A.* **84**, 3472-3476.

Hoffmann, W. & Franz, J. K. (1984). Amino acid sequence of the carboxy-terminal part of an acidic type I cytokeratin of molecular weight 51,000 from *Xenopus laevis* epidermis as predicted from the cDNA sequence. *EMBO J.* **3**, 1301-1306.

Hoffmann, W., Franz, J. K. & Franke, W. W. (1985). Amino acid sequence microheterogeneities of basic (Type II) cytokeratins of *Xenopus laevis* epidermis and evolutionary conservativity of helical and non-helical domains. *J. Mol. Biol.* **184**, 713-724.

Hogan, B. & Tilly, R. (1978). *In vitro* development of inner cell masses isolated immunosurgically from mouse blastocysts. II. Inner cell masses from 3.5- to 4.0-day *p.c.* blastocysts. *J. Embryol. exp. Morph.* **45**, 107-121.

Ip, W. (1988). Modulation of desmin intermediate filament assembly by a monoclonal antibody. *J. Cell Biol.* **106**, 735-745.

Ip, W., Hartzer, M. K., Pang, Y.-Y. S. & Robson, R. M. (1985). Assembly of vimentin *in vitro* and its implications concerning the structure of intermediate filaments. *J. Mol. Biol.* **183**, 365-375.

Jackson, B. W., Grund, C., Schmid, E., Bürki, K., Franke, W. W. & Illmensee, K. (1980). Formation of cytoskeletal elements during mouse embryogenesis. Intermediate filaments of the cytokeratin type and desmosomes in preimplantation embryos. *Differentiation* **17**, 161-179.

Jackson, B. W., Grund, C., Winter, S., Franke, W. W. & Illmensee, K. (1981). Formation of cytoskeletal elements during mouse embryogenesis II. Epithelial differentiation and intermediate-sized filaments in early postimplantation embryos. *Differentiation* **20**, 203-216.

Jeffery, W. R. (1985). The spatial distribution of maternal mRNA is determined by a cortical cytoskeletal domain in *Chaetopterus* eggs. *Devl Biol.* **110**, 217-229.

Jeffery, W. R. & Wilson, L. J. (1983). Localization of messenger RNA in the cortex of *Chaetopterus* eggs and early embryos. *J. Embryol. exp. Morph.* **75**, 225-239.

Johnson, D. A., Gautsch, J. W., Sportsman, J. R. & Elder, J. H. (1984). Improved technique utilizing nonfat dry milk for analysis of proteins and nucleic acids transferred to nitrocellulose. *Gene Anal. Techn.* **1**, 3-8.

Johnson, L. D., Idler, W. W., Zhou, X.-M., Roop, D. R. & Steinert, P. M. (1985). Structure of a gene for the human epidermal 67-kDa keratin. *Proc. natn. Acad. Sci. U.S.A.* **82**, 1896-1900.

Johnson, M. H. (1979). Molecular differentiation of inside cells and inner cell masses isolated from the preimplantation mouse embryo. *J. Embryol. exp. Morph.* **53**, 335-344.

Jonas, E., Sargent, T. D. & Dawid, I. B. (1985). Epidermal keratin gene expressed in embryos of *Xenopus laevis*. *Proc. natn. Acad. Sci. U.S.A.* **82**, 5413-5417.

Jones, J. C. R., Goldman, A. E., Steinert, P. M., Yuspa, S. & Goldman, R. G. (1982). Dynamic aspects of the supramolecular organization of intermediate filament networks in cultured epidermal cells. *Cell Motility* **2**, 197-213.

Jones, J. C. R. & Goldman, R. D. (1985). Intermediate filaments and the initiation of desmosome assembly. *J. Cell Biol.* **101**, 506-517.

Jorcano, J. L., Franz, J. K. & Franke, W. W. (1984a). Amino acid sequence diversity between bovine epidermal cytokeratin polypeptides of the basic (type II) subfamily as

determined from cDNA clones. *Differentiation* **28**, 155-163.

Jorcano, J. L., Rieger, M., Franz, J. K., Schiller, D. L., Moll, R. & Franke, W. W. (1984b). Identification of two types of keratin polypeptides within the acidic cytokeratin subfamily I. *J. Mol. Biol.* **179**, 257-281.

Kaufmann, E., Weber, K. & Geisler, N. (1985). Intermediate filament forming ability of desmin derivatives lacking either the amino-terminal 67 or the carboxy-terminal 27 residues. *J. Mol. Biol.* **185**, 733-742.

Kelly, S. J., Mulnard, J. G. & Graham, C. F. (1978). Cell division and cell allocation in early mouse development. *J. Embryol. exp. Morph.* **48**, 37-51.

Kemler, R., Brûlet, P., Schnebelen, M.-T., Gaillard, J. & Jacob, F. (1981). Reactivity of monoclonal antibodies against intermediate filament proteins during embryonic development. *J. Embryol. exp. Morph.* **64**, 45-60.

Kim, K. H., Rheinwald, J. G. & Fuchs, E. V. (1983). Tissue specificity of epithelial keratins: differential expression of mRNAs from two multigene families. *Mol. Cell. Biol.* **3**, 495-502.

Kim, K. H., Stellmach, V., Javors, J. & Fuchs, E. (1987). Regulation of human mesothelial cell differentiation: opposing roles of retinoids and epidermal growth factor in the expression of intermediate filament proteins. *J. Cell Biol.* **105**, 3039-3051.

Klymkowsky, M. W. (1981). Intermediate filaments in 3T3 cells collapse after intracellular injection of a monoclonal anti-intermediate filament antibody. *Nature, Lond.* **291**, 249-251.

Klymkowsky, M. W. (1982). Vimentin and keratin intermediate filament systems in cultured PtK_2 epithelial cells are interrelated. *EMBO J.* **1**, 161-165.

Klymkowsky, M. W. (1988). Metabolic inhibitors and intermediate filament organization in human fibroblasts. *Expl Cell Res.* **174**, 282-290.

Klymkowsky, M. W., Maynell, L. A. & Polson, A. G. (1987). Polar asymmetry in the organization of the cortical cytokeratin system of *Xenopus laevis* oocytes and embryos. *Development* **100**, 543-557.

Klymkowsky, M. W., Miller, R. H. & Lane, E. B. (1983). Morphology, behavior, and interaction of cultured epithelial cells after the antibody-induced disruption of keratin filament organization. *J. Cell Biol.* **96**, 494-509.

Knapp, B., Rentrop, M., Schweizer, J. & Winter, H. (1986). Nonepidermal members of the keratin multigene family: cDNA sequences and in situ localization of the mRNAs. *Nucl. Acids Res.* **14**, 751-763.

Kreis, T. E., Geiger, B., Schmid, E., Jorcano, J. L. & Franke, W. W. (1983). De novo synthesis and specific assembly of keratin filaments in nonepithelial cells after microinjection of mRNA for epidermal keratin. *Cell* **32**, 1125-1137.

Krieg, T. M., Schafer, M. P., Cheng, C. K., Filpula, D., Flaherty, P., Steinert, P. M. & Roop, D. R. (1985). Organization of a Type I keratin gene. *J. biol. Chem.* **260**, 5867-5870.

Krimpenfort, P. J., Schaart, G., Pieper, F. R., Ramaekers, F. C., Cuypers, H. T., van den Heuvel, R. M., Vree Egberts, W. T., van Eys, G. J., Berns, A. & Bloemendal, H. (1988). Tissue-specific expression of a vimentin-desmin hybrid gene in transgenic mice. *EMBO J.* **7**, 941-947.

Kulesh, D. A. & Oshima, R. G. (1988). Cloning of the human keratin 18 gene and its expression in nonepithelial mouse cells. *Mol. Cell. Biol.* **8**, 1540-1550.

Laemmli, U. K. (1970). Cleavage of structural proteins during the assembly of the head of bacteriophage T4. *Nature, Lond.* **227**, 680-685.

Lane, E. B., Goodman, S. L. & Trejdosiewicz, L. K. (1982). Disruption of the keratin filament network during epithelial cell division. *EMBO J.* **1**, 1365-1372.

Lane, E. B., Hogan, B. L. M., Kurkinen, M. & Garrels, J. I. (1983). Co-expression of vimentin and cytokeratins in parietal endoderm cells of early mouse embryo. *Nature, Lond.* **303**, 701-704.

Lane, E. B. & Klymkowsky, M. W. (1982). Epithelial tonofilaments: investigating their form and function using monoclonal antibodies. *Cold Spring Harb. Symp. quant. Biol.* **46**, 387-402.

Lasek, R. J., Oblinger, M. M. & Drake, P. F. (1983). Molecular biology of neuronal geometry: expression of neurofilament genes influences axonal diameter. *Cold Spring Harb. Symp. quant. Biol.* **48**, 731-744.

Lazarides, E. (1980). Intermediate filaments as mechanical integrators of cellular space. *Nature, Lond.* **283**, 249-256.

Lehnert, M. E., Jorcano, J. L., Zentgraf, H., Blessing, M., Franz, J. K. & Franke, W. W. (1984). Characterization of bovine keratin genes: similarities of exon patterns in genes coding for different keratins. *EMBO J.* **3**, 3279-3287.

Lehtonen, E. (1985). A monoclonal antibody against mouse oocyte cytoskeleton recognizing cytokeratin-type filaments. *J. Embryol. exp. Morph.* **90**, 197-209.

Lehtonen, E. (1987). Cytokeratins in oocytes and preimplantation embryos of the mouse. *Curr. Top. devl Biol.* **22**, 153-173.

Lehtonen, E. & Badley, R. A. (1980). Localization of cytoskeletal proteins in preimplantation mouse embryos. *J. Embryol. exp. Morph.* **55**, 211-225.

Lehtonen, E., Lehto, V.-P., Paasivuo, R. & Virtanen, I. (1983a). Parietal and visceral endoderm differ in their expression of intermediate filaments. *EMBO J.* **2**, 1023-1028.

Lehtonen, E., Lehto, V.-P., Vartio, T., Badley, R. A. & Virtanen, I. (1983b). Expression of cytokeratin polypeptides in mouse oocytes and preimplantation embryos. *Devl Biol.*

100, 158-165.

Leube, R. E., Bader, B. L., Bosch, F. X., Zimbelmann, R., Achtstaetter, T. & Franke, W. W. (1988). Molecular characterization and expression of the stratification-related cytokeratins 4 and 15. *J. Cell Biol.* **106**, 1249-1261.

Leube, R. E., Bosch, F. X., Romano, V., Zimbelmann, R., Höfler, H. & Franke, W. W. (1986). Cytokeratin expression in simple epithelia. III. Detection of mRNAs encoding human cytokeratins nos. 8 and 18 in normal and tumor cells by hybridization with cDNA sequences in vitro and in situ. *Differentiation* **33**, 69-85.

Lewis, S. A., Balcarek, J. M., Krek, V., Shelanski, M. & Cowan, N. J. (1984). Sequence of a cDNA clone encoding mouse glial fibrillary acidic protein: structural conservation of intermediate filaments. *Proc. natn. Acad. Sci. U.S.A.* **81**, 2743-2746.

Lewis, S. A. & Cowan, N. J. (1986). Anomalous placement of introns in a member of the intermediate filament multigene family: an evolutionary conundrum. *Mol. Cell. Biol.* **6**, 1529-1534.

Lin, J. J.-C. & Feramisco, J. R. (1981). Disruption of the in vivo distribution of the intermediate filaments in living fibroblasts through the microinjection of a specific monoclonal antibody. *Cell* **24**, 185-193.

Magin, T. M., Hatzfeld, M. & Franke, W. W. (1987). Analysis of cytokeratin domains by cloning and expression of intact and deleted polypeptides in *Escherichia coli*. *EMBO J.* **6**, 2607-2615.

Magin, T. M., Jorcano, J. L. & Franke, W. W. (1986). Cytokeratin expression in simple epithelia. II. cDNA cloning and sequence characteristics of bovine cytokeratin A (no. 8). *Differentiation* **30**, 254-264.

Magnuson, T., Demsey, A. & Stackpole, C. W. (1977). Characterization of intercellular junctions in the preimplantation mouse embryo by freeze-fracture and thin-section electron microscopy. *Devl Biol.* **61**, 252-261.

Marchuk, D., McCrohon, S. & Fuchs, E. (1984). Remarkable conservation of structure among intermediate filament genes. *Cell* **39**, 491-498.

Marchuk, D., McCrohon, S. & Fuchs, E. (1985). Complete sequence of a gene encoding a human type I keratin: sequences homologous to enhancer elements in the regulatory region of the gene. *Proc. natn. Acad. Sci. U.S.A.* **82**, 1609-1613.

Maro, B., Johnson, M. H., Pickering, S. J. & Flach, G. (1984). Changes in actin distribution during fertilization of the mouse egg. *J. Embryol. exp. Morph.* **81**, 211-237.

McKeon, F. D., Kirschner, M. W. & Caput, D. (1986). Homologies in both primary and secondary structure between nuclear envelope and intermediate filament proteins. *Nature, Lond.* **319**, 463-468.

Milam, L. & Erickson, H. P. (1982). Visualization of a 21-nm axial periodicity in shadowed

keratin filaments and neurofilaments. *J. Cell Biol.* **94**, 592-596.

Miller, M. R., Castellot, Jr., J. J. & Pardee, A. B. (1979). A general method for permeabilizing monolayer and suspension cultured animal cells. *Expl Cell Res.* **120**, 421-425.

Miyatani, S., Winkles, J. A., Sargent, T. D. & Dawid, I. B. (1986). Stage-specific keratins in *Xenopus laevis* embryos and tadpoles: the XK81 gene family. *J. Cell Biol.* **103**, 1957-1965.

Moll, R., Franke, W. W., Schiller, D. L., Geiger, B. & Krepler, R. (1982). The catalog of human cytokeratins: patterns of expression in normal epithelia, tumors and cultured cells. *Cell* **31**, 11-24.

Moon, R. T. & Lazarides, E. (1983). Canavanine inhibits vimentin assembly but not its synthesis in chicken embryo erythroid cells. *J. Cell Biol.* **97**, 1309-1314.

Murti, K. G., Goorha, R. & Klymkowsky, M. W. (1988). A functional role for intermediate filaments in the formation of frog virus 3 assembly sites. *Virology* **162**, 264-269.

Myers, M. W., Lazzarini, R. A., Lee, V. M.-Y., Schlaepfer, W. W. & Nelson, D. L. (1987). The human mid-size neurofilament subunit: a repeated protein sequence and the relationship of its gene to the intermediate filament gene family. *EMBO J.* **6**, 1617-1626.

Nelson, W. J. & Traub, P. (1983). Proteolysis of vimentin and desmin by the Ca^{2+}-activated proteinase specific for these intermediate filament proteins. *Mol. Cell. Biol.* **3**, 1146-1156.

Nigg, E. A., Schäfer, G., Hilz, H. & Eppenberger, H. M. (1985). Cycle-AMP-dependent protein kinase Type II is associated with the golgi complex and with centrosomes. *Cell* **41**, 1039-1051.

Nozaki, M., Iwakura, Y. & Matsushiro, A. (1986). Studies of developmental abnormalities at the molecular level of mouse embryos homozygous for the t^{12} lethal mutation. *Devl Biol.* **113**, 17-28.

O'Guin, W. M., Galvin, S., Schermer, A. & Sun, T.-T. (1987). Patterns of keratin expression define distinct pathways of epithelial development and differentatiation. *Curr. Top. devl Biol.* **22**, 97-125.

Olmsted, J. B. (1986). Analysis of cytoskeletal structures using blot-purified monospecific antibodies. *Meth. Enzymol.* **134**, 467-472.

Osborn, M., Franke, W. & Weber, K. (1980). Direct demonstration of the presence of two immunologically distinct intermediate-sized filament systems in the same cell by double immunofluorescence microscopy. *Expl Cell Res.* **125**, 37-46.

Osborn, M., Geisler, N., Shaw, G., Sharp, G. & Weber, K. (1982). Intermediate filaments. *Cold Spring Harb. Symp. quant. Biol.* **46**, 413-429.

Oshima, R. G. (1981). Identification and immunoprecipitation of cytoskeletal proteins from murine extra-embryonic endodermal cells. *J. biol. Chem.* **256**, 8124-8133.

Oshima, R. G. (1982). Developmental expression of murine extra-embryonic endodermal cytoskeletal proteins. *J. biol. Chem.* **257**, 3414-3421.

Oshima, R. G., Howe, W. E., Klier, F. G., Adamson, E. D. & Shevinsky, L. H. (1983). Intermediate filament protein synthesis in preimplantation murine embryos. *Devl Biol.* **99**, 447-455.

Oshima, R. G., Millán, J. L. & Ceceña, G. (1986). Comparison of mouse and human keratin 18: a component of intermediate filaments expressed prior to implantation. *Differentiation* **33**, 61-68.

Oshima, R. G., Trevor, K., Shevinsky, L. H., Ryder, O. A. & Ceceña, G. (1988). Identification of the gene coding for the Endo B murine cytokeratin and its methylated, stable inactive state in mouse nonepithelial cells. *Genes & Devel.*, in press.

Parry, D. A. D., Steven, A. C. & Steinert, P. M. (1985). The coiled-coil molecules of intermediate filaments consist of two parallel chains in exact axial register. *Biochem. biophys. Res. Commun.* **127**, 1012-1018.

Pasdar, M. & Nelson, W. J. (1988a). Kinetics of desmosome assembly in Madin-Darby canine kidney epithelial cells: temporal and spatial regulation of desmoplakin organization and stabilization upon cell-cell contact. I. Biochemical analysis. *J. Cell Biol.* **106**, 677-685.

Pasdar, M. & Nelson, W. J. (1988b). Kinetics of desmosome assembly in Madin-Darby canine kidney epithelial cells: temporal and spatial regulation of desmoplakin organization and stabilization upon cell-cell contact. II. Morphological analysis. *J. Cell Biol.* **106**, 687-695.

Paulin, D., Babinet, C., Weber, K. & Osborn, M. (1980). Antibodies as probes of cellular differentiation and cytoskeletal organization in the mouse blastocyst. *Expl Cell Res.* **130**, 297-304.

Pedersen, R. A., Wu, K. & Balakier, H. (1986). Origin of the inner cell mass in mouse embryos: cell lineage analysis by microinjection. *Devl Biol.* **117**, 581-595.

Penn, E. J., Burdett, I. D. J., Hobson, C., Magee, A. I. & Rees, D. A. (1987). Structure and assembly of desmosome junctions: biosynthesis and turnover of the major desmosome components of Madin-Darby canine kidney cells in low calcium medium. *J. Cell Biol.* **105**, 2327-2334.

Pruss, R. M., Mirsky, R., Raff, M. C., Thorpe, R., Dowding, A. J. & Anderton, B. H. (1981). All classes of intermediate filaments share a common antigenic determinant defined by a monoclonal antibody. *Cell* **27**, 419-428.

Quax, W., van den Broek, L., Vree Egberts, W., Ramaekers, F. & Bloemendal, H. (1985). Characterization of the hamster desmin gene: expression and formation of desmin

filaments in nonmuscle cells after gene transfer. *Cell* **43**, 327-338.

Quax, W., Vree Egberts, W., Hendriks, W., Quax-Jeuken, Y. & Bloemendal, H. (1983). The structure of the vimentin gene. *Cell* **35**, 215-223.

Quax-Jeuken, Y. E. F. M., Quax, W. J. & Bloemendal, H. (1983). Primary and secondary structure of hamster vimentin predicted from the nucleotide sequence. *Proc. natn. Acad. Sci. U.S.A.* **80**, 3548-3552.

Quinlan, R. A., Cohlberg, J. A., Schiller, D. L., Hatzfeld, M. & Franke, W. W. (1984). Heterotypic tetramer (A_2D_2) complexes of non-epidermal keratins isolated from cytoskeletons of rat hepatocytes and hepatoma cells. *J. Mol. Biol.* **178**, 365-388.

Quinlan, R. A. & Franke, W. W. (1982). Heteropolymer filaments of vimentin and desmin in vascular smooth muscle tissue and cultured baby hamster kidney cells demonstrated by chemical crosslinking. *Proc. natn. Acad. Sci. U.S.A.* **79**, 3452-3456.

Quinlan, R. A. & Franke, W. W. (1983). Molecular interactions in intermediate-sized filaments revealed by chemical cross-linking: heteropolymers of vimentin and glial filament protein in cultured human glioma cells. *Eur. J. Biochem.* **132**, 477-484.

Quinlan, R. A., Hatzfeld, M., Franke, W. W., Lustig, A., Schulthess, T. & Engel, J. (1986). Characterization of dimer subunits of intermediate filament proteins. *J. Mol. Biol.* **192**, 337-349.

Quinlan, R. A., Schiller, D. L., Hatzfeld, M., Achtstätter, T., Moll, R., Jorcano, J. L., Magin, T. M. & Franke, W. W. (1985). Patterns of expression and organization of cytokeratin intermediate filaments. In *Intermediate Filaments, Ann. N. Y. Acad. Sci.* **455**, 282-306.

RayChaudhury, A., Marchuk, D., Lindhurst, M. & Fuchs, E. (1986). Three tightly linked genes encoding human Type I keratins: conservation of seqeunce in the 5′-untranslated leader and 5′-upstream regions of coexpressed keratin genes. *Mol. Cell. Biol.* **6**, 539-548.

Reima, I. & Lehtonen, E. (1985). Localization of nonerythroid spectrin and actin in mouse oocytes and preimplantation embryos. *Differentiation* **30**, 68-75.

Rieger, M., Jorcano, J. L. & Franke, W. W. (1985). Complete sequence of a bovine type I cytokeratin gene: conserved and variable intron positions in genes of polypeptides of the same cytokeratin subfamily. *EMBO J.* **4**, 2261-2267.

Romano, V., Hatzfeld, M., Magin, T. M., Zimbelmann, R., Franke, W. W., Maier, G. & Ponstingl, H. (1986). Cytokeratin expression in simple epithelia. I. Identification of mRNA coding for human cytokeratin no. 18 by a cDNA clone. *Differentiation* **30**, 244-253.

Sauk, J. J., Krumweide, M., Cocking-Johnson, D. & White, J. G. (1984). Reconstitution of cytokeratin filaments in vitro: futher evidence for the role of nonhelical peptides in filament assembly. *J. Cell Biol.* **99**, 1590-1597.

Schiller, D. L., Franke, W. W. & Geiger, B. (1982). A subfamily of relatively large and basic cytokeratin polypeptides as defined by peptide mapping is represented by one or several polypeptides in epithelial cells. *EMBO J.* **6**, 761-769.

Schmid, E., Osborn, M., Rungger-Brändle, E., Gabbiani, G., Weber, K. & Franke, W. W. (1982). Distribution of vimentin and desmin filaments in smooth muscle tissue of mammlian and avian aorta. *Expl Cell Res.* **137**, 329-340.

Sharp, G., Osborn, M. & Weber, K. (1982). Occurrence of two different intermediate filament proteins in the same filament in situ within a human glioma cell line. *Expl Cell Res.* **141**, 385-395.

Shaw, G. (1986). Neurofilaments: abundant but mysterious neuronal structures. *BioEssays* **4**, 161-166.

Singer, P. A., Trevor, K. & Oshima, R. G. (1986). Molecular cloning and characterization of the Endo B cytokeratin expressed in preimplantation mouse embryos. *J. biol. Chem.* **261**, 538-547.

Sobel, J. S. (1983). Localization of myosin in the preimplantation mouse embryo. *Devl Biol.* **95**, 227-231.

Sobel, J. S. & Alliegro, M. A. (1985). Changes in the distribution of a spectrin-like protein during development of the preimplantation mouse embryo. *J. Cell Biol.* **100**, 333-336.

Soellner, P., Quinlan, R. A. & Franke, W. W. (1985). Identification of a distinct soluble subunit of an intermediate filament protein: tetrameric vimentin from living cells. *Proc. natn. Acad. Sci. U.S.A.* **82**, 7929-7933.

Solter, D. & Knowles, B. B. (1975). Immunosurgery of mouse blastocyst. *Proc. natn. Acad. Sci. U.S.A.* **72**, 5099-5102.

Soltyñska, M. S. (1985). Ultrastructure of mouse blastocysts during blastocoele expansion. *Roux's Arch. devl Biol.* **194**, 425-428.

Spindle, A. I. (1978). Trophoblast regeneration by inner cell masses isolated from cultured mouse embryos. *J. exp. Zool.* **203**, 483-489.

Spindle, A. (1980). An improved culture medium for mouse blastocysts. *In Vitro* **16**, 669-674.

Steinberg, M. S., Shida, H., Giudice, G. J., Shida, M., Patel, N. H. & Blaschuk, O. W. (1987). On the molecular organization, diversity and functions of desmosomal proteins. In *Junctional Complexes of Epithelial Cells.* (Ciba Found. Symp. 125), pp. 3-25. Chichester: John Wiley & Sons.

Steinert, P., Idler, W., Aynardi-Whitman, M., Zackroff, R. & Goldman, R. D. (1982a). Heterogeneity of intermediate filaments assembled in vitro. *Cold Spring Harb. Symp. quant. Biol.* **46**, 465-474.

Steinert, P. M., Idler, W. W., Cabral, F., Gottesman, M. M. & Goldman, R. D. (1981). *In*

vitro assembly of homopolymer and copolymer filaments from intermediate filament subunits of muscle and fibroblastic cells. *Proc. natn. Acad. Sci. U.S.A.* **78**, 3692-3696.

Steinert, P. M., Jones, J. C. R. & Goldman, R. D. (1984a). Intermediate filaments. *J. Cell Biol.* **99**, 22s-27s.

Steinert, P. M. & Parry, D. A. D. (1985). Intermediate filaments: conformity and diversity of expression and structure. *Ann. Rev. Cell Biol.* **1**, 41-65.

Steinert, P. M., Parry, D. A. D., Idler, W. W., Johnson, L. D., Steven, A. C. & Roop, D. R. (1985a). Amino acid sequences of mouse and human epidermal Type II keratins of M_r 67,000 provide a systematic basis for the structural and functional diversity of the end domains of keratin intermediate filament subunits. *J. biol. Chem.* **260**, 7142-7149.

Steinert, P. M., Parry, D. A. D., Racoosin, E. L., Idler, W. W., Steven, A. C., Trus, B. L. & Roop, D. R. (1984b). The complete cDNA and deduced amino acid sequence of a type II mouse epidermal keratin of 60,000 Da: analysis of sequence differences between type I and type II keratins. *Proc. natn. Acad. Sci. U.S.A.* **81**, 5709-5713.

Steinert, P. M., Rice, R. H., Roop, D. R., Trus, B. L. & Steven, A. C. (1983). Complete amino acid sequence of a mouse epidermal keratin subunit and implications for the structure of intermediate filaments. *Nature, Lond.* **302**, 794-800.

Steinert, P. M., Steven, A. C. & Roop, D. R. (1985b). The molecular biology of intermediate filaments. *Cell* **42**, 411-419.

Steinert, P., Zackroff, R., Aynardi-Whitman, M. & Goldman, R. D. (1982b). Isolation and characterization of intermediate filaments. *Meth. Cell Biol.* **24**, 399-419.

Sun, T.-T., Eichner, R., Nelson, W. G., Tseng, S. C. G., Weiss, R. A., Jarvinen, M. & Woodcock-Mitchell, J. (1983). Keratin classes: molecular markers for different types of epithelial differentiation. *J. invest. Derm.* **81**, 109s-115s.

Sun, T.-T., Eichner, R., Schermer, A., Cooper, D., Nelson, W. G. & Weiss, R. A. (1984). Classification, expression, and possible mechanisms of evolution of mammalian epithelial keratins: a unifying model. In *Cancer Cells: The Transformed Phenotype.* (eds. A. J. Levine, G. F. Vande Woude, W. C. Topp & J. D. Watson), pp. 169-176. New York: Cold Spring Harbor Laboratory.

Sun, T.-T., Tseng, S. C. G., Huang, A. J.-W., Cooper, D., Schermer, A., Lynch, M. H., Weiss, R. & Eichner, R. (1985). Monoclonal antibody studies of mammalian epithelial keratins: a review. In *Intermediate Filaments, Ann. N. Y. Acad. Sci.* **455**, 307-329.

Surani, M. A. H. & Barton, S. C. (1984). Spatial distribution of blastomeres is dependent on cell division order and interactions in mouse morulae. *Devl Biol.* **102**, 335-343.

Thomas, J. O. & Kornberg, R. D. (1975). An octamer of histones in chromatin and free in solution. *Proc. natn. Acad. Sci. U.S.A.* **72**, 2626-2630.

Tokuyasu, K. T., Maher, P. A. & Singer, S. J. (1985). Distributions of vimentin and desmin in

developing chick myotubes in vivo. II. Immunoelectron microscopic study. *J. Cell Biol.* **100**, 1157-1166.

Tölle, H.-G., Weber, K. & Osborn, M. (1985). Microinjection of monoclonal antibodies specific for one intermediate filament protein in cells containing multiple keratins allow insight into the composition of particular 10 nm filaments. *Eur. J. Cell Biol.* **38**, 234-244.

Tölle, H.-G., Weber, K. & Osborn, M. (1986). Microinjection of monoclonal antibodies to vimentin, desmin, and GFA in cells which contain more than one IF type. *Expl Cell Res.* **162**, 462-474.

Traub, P. & Vorgias, C. E. (1983). Involvement of the N-terminal polypeptide of vimentin in the formation of intermediate filaments. *J. Cell Sci.* **63**, 43-67.

Traub, U. E., Nelson, W. J. & Traub, P. (1983). Polyacrylamide gel electrophoretic screening of mammalian cells cultured *in vitro* for the presence of the intermediate filament protein vimentin. *J. Cell Sci.* **62** 129-147.

Tseng, S. C. G., Jarvinen, M. J., Nelson, W. G., Huang, J.-W., Woodcock-Mitchell, J. & Sun, T.-T. (1982). Correlation of specific keratins with different types of epithelial differentiation: monoclonal antibody studies. *Cell* **30**, 361-372.

Tyner, A. L., Eichman, M. J. & Fuchs, E. (1985). The sequence of a type II keratin gene expressed in human skin: conservation of structure among all intermediate filament genes. *Proc. natn. Acad. Sci. U.S.A.* **82**, 4683-4687.

Van Blerkom, J., Barton, S. C. & Johnson, M. H. (1976). Molecular differentiation in the preimplantation mouse embryo. *Nature, Lond.* **259**, 319-321.

Vasseur, M., Duprey, P., Brûlet, P. & Jacob, F. (1985). One gene and one pseudogene for the cytokeratin endo A. *Proc. natn. Acad. Sci. U.S.A.* **82**, 1155-1159.

Venetianer, A., Schiller, D. L., Magin, T. & Franke, W. W. (1983). Cessation of cytokeratin expression in a rat hepatoma cell line lacking differentiated functions. *Nature, Lond.* **305**, 730-733.

Venuti, J. M., Swalla, B. J. & Jeffery, W. R. (1987). Characterization of potential mRNA binding sites in the cortical cytoskeletal domain of *Chaetopterus* eggs. *J. Cell Biol.* **105**, 172a.

Watson, A. J. & Kidder, G. M. (1988) Immunofluorescence assessment of the timing of appearance and cellular distribution of Na/K-ATPase during mouse embryogenesis. *Dev. Biol.* **126**, 80-90.

Weber, K. & Geisler, N. (1985). Intermediate filaments: structural conservation and divergence. In *Intermediate Filaments, Ann. N. Y. Acad. Sci.* **455**, 126-143.

Winkles, J. A., Sargent, T. D., Parry, D. A. D., Jonas, E. & Dawid, I. B. (1985). Developmentally regulated cytokeratin gene in *Xenopus laevis*. *Mol. Cell. Biol.* **5**, 2575-2581.

Wolosewick, J. & De Mey, J. (1982). Localization of tubulin and actin in polyethylene glycol embedded rat seminiferous epithelium. *Biol. Cell* **44**, 85-88.

Yarosh, D. B. & Setlow, R. B. (1981). Permeabilization of ultraviolet-irradiated Chinese hamster cells with polyethylene glycol and introduction of ultraviolet endonuclease from *Micrococcus luteus*. *Mol. Cell. Biol.* **1**, 237-244.

Zimmermann, H.-P., Plagens, U., Vorgias, C. E. & Traub, P. (1986). Changes in the organization of non-epithelial intermediate filaments induced by triethyl lead chloride. *Expl Cell Res.* **167**, 360-368.

Appendix

Detailed Step-By-Step Laboratory Protocols

CULTURE OF PFHR9 CELLS

1. Remove provial from liquid nitrogen (Revelation tank) and immediately thaw cell suspension in 37°C water bath with gentle agitation; swab outside of vial with 70% EtOH.

2. Transfer cell suspension to a 15 ml conical tissue culture tube and add 10 ml warm Complete Medium; centrifuge at 1200 rpm for 4 min.

3. Aspirate supernate, resuspend cells in 6 ml medium, and transfer cell suspension to a 25 cm^2 tissue culture flask (alternatively, the cells can be cultured in 10 ml medium in a 100 mm tissue culture dish).

4. Culture at 7% CO_2 and 37°C until cells are confluent. To passage cells, warm Ca^{2+}/Mg^{2+}-free Dulbecco's PBS, 0.05% Trypsin Solution (Cell Culture Facility), and Complete Medium to 37°C.

5. Aspirate medium from flask, rinse cell monolayer with 3-5 ml of PBS, and remove PBS.

6. Add 3-5 ml of Trypsin Solution to the flask and incubate at 37°C until the cells start to detach (~ 4 min). Tap the flask to detach all cells from the bottom (if cells are in tissue culture dishes, dissociate them by pipetting medium up and down over the dish surface).

7. Remove cell suspension to a conical centrifuge tube that contains an equal volume of complete medium. Spin at 1200 rpm for 4 min.

8. Aspirate supernate and resuspend cells in Complete Medium. For early splits, resuspend cells in 3 ml of medium and distribute to three 25 cm^2 tissue culture flasks that each contain 5 ml Complete Medium (the final density should be about 5×10^5 cells/ml). After 3 or 4 passages, the cells grow faster and can be split 1:6 for confluency at 4 days.

9. Replenish frozen stock as needed: resuspend cell pellet in Freezing Medium at a concentration of $3\text{-}5 \times 10^6$ cells/ml; add 0.5-1 ml of the cell suspension to each provial **Freezing Medium** (10 ml) = 8 ml Complete Medium + 1 ml FCS + 1 ml DMSO.

10. Place the provials in a styrofoam test tube rack and wrap with 3-4 layers of bench cote.

11. Place at -80°C overnight and put in liquid nitrogen the next day; test thaw a vial after a few days in liquid nitrogen.

Complete Medium

Base medium = Dulbecco's Modified Eagle's Medium that contains 4.5 g glucose/L and 3.7 g $NaHCO_3$/L (DME H-21, Cell Culture Facility).

To a 450 ml bottle of DME H-21, add the following:
- 50 ml fetal calf serum (10% final concentration)
- 5 ml 100X sodium pyruvate (0.11 g/L final concentration)
- 5 ml 100X L-glutamine (0.292 g/L final concentration) (add fresh every 6 weeks)
- 5 ml 100X Pen-Strep (100 U/ml final activity) (optional).

INTERMEDIATE FILAMENT ISOLATION FROM PFHR9 CELLS

(adapted from Franke's group: *J. Mol. Biol.* **153**: 933, 1981; *PNAS* **80**: 7113, 1983; *Meth. Enzymol.* **134**: 355, 1986)

1. Three days prior to harvesting, seed log phase HR9 cells into several 75 cm^2 tissue culture flasks (approx. $9x10^5$ cells in 16 ml complete medium); proceed when cells form a confluent monolayer.

2. Wash flasks 3X with 10 ml Ca^{2+}/Mg^{2+}-free Dulbecco's PBS (CMF D-PBS).

3. Add 10 ml Lysis Buffer to each flask - incubate 4 min.

4. Remove Lysis Buffer and add 10 ml High Salt Lysis Buffer - incubate 25-30 min.

5. Remove High Salt Lysis Buffer and gently rinse with 10 ml CMF D-PBS.

6. Add 8 ml CMF D-PBS and scrape off cytoskeletal residue with rubber policeman.

7. Remove solution into 30 ml siliconized Corex tubes (on ice).

8. Spin in high speed centrifuge for 10 min at 10,000 rpm, 4°C.

9. Aspirate supernates and combine pellets into one Corex tube with 20 ml CMF D-PBS.

10. Spin 10 min, 10,000 rpm, 4°C.

11. Remove supernate and add 5 ml Nuclease Lysis Buffer - incubate 2 min, vortexing occasionally.

12. Stop reaction by adding 0.1 ml of 250 mM EDTA (5mM final concentration).

13. Add 15 ml Post-Nuclease Buffer and spin for 15 min, 10,000 rpm, 4°C.

14. Remove supernate and resuspend pellet in 1.4 ml Post-Nuclease Buffer; transfer solution to microfuge tube using a siliconized pasteur pipette.

15. Spin 10 min in cold microfuge.

16. Remove supernate, add 0.5-1.0 ml fresh Post-Nuclease Buffer, and store at -80°C.

17. For Lowry or gel analysis, pellet can be dissolved by boiling in PBS + 2.3% SDS.

18. To concentrate solution, dialyze against PBS + 0.1% SDS and concentrate with Centricon unit per manufacturer's directions.

SOLUTIONS

(all filtered through Whatman #1 paper)

Buffer	*Final Concentration*	*Stock Conc.*	*Stock Vol.*
Lysis Buffer (200 ml)	10 mM Tris-HCl, pH 7.6	100 mM	20 ml
	140 mM NaCl	1 M	28 ml
	5 mM EDTA	250 mM	4 ml
	1% Triton X-100	10%	20 ml
	0.5 mM PMSF	100 mM	1 ml
	dH_2O	-	127 ml
High Salt Lysis Buffer (200 ml)	10 mM Tris-HCl, pH 7.6	100 mM	20 ml
	140 mM NaCl	1 M	28 ml
	5 mM EDTA	250 mM	4 ml
	0.5% Triton X-100	10%	10 ml
	1.5 M KCl	3 M	100 ml
	0.5 mM PMSF	100 mM	1 ml
	dH_2O	-	37 ml
Nuclease Lysis Buffer (5 ml)	10 mM Tris-HCl, pH 8.0	100 mM	0.5 ml
	140 mM NaCl	1 M	0.7 ml
	5 mM $CaCl_2$	10 mM	2.5 ml
	10 μg/ml Micrococcal Nuclease (Sigma #N-3755)	1 mg/ml	0.05 ml
	dH_2O	-	1.25 ml
Post-Nuclease Buffer (100 ml)	5 mM Tris-HCl, pH 8.0	100 mM	5 ml
	140 mM NaCl	1 M	14 ml
	5 mM EDTA	250 mM	2 ml
	dH_2O	-	79 ml

LOWRY PROTEIN ASSAY

(adapted from Lowry *et al., J. Biol. Chem.* **193**: 265, 1951)

1. Reagents:
   a. 3% Na_2CO_3 in 0.1 N NaOH (3 g Na_2CO_3 + 10 ml 1 N NaOH + 90 ml dH_2O)
   4% Sodium tartrate (Fisher #S-435)
   2% Cupric sulfate ($CuSO_4 \cdot H_2O$)

   b. **Protein Detection Solution**: add 1 ml of Sodium tartrate solution to 100 ml of Na_2CO_3 solution and mix well; next, add 1 ml of Cupric sulfate solution to tartrate/Na_2CO_3 solution and mix well.

   c. dilute Phenol Reagent Solution 2N (Fisher #SO-P-24) to 1 N in dH_2O.

2. Prepare protein standards as follows:
   a. 0.1 g BSA in 10 ml dH_2O → 10 mg/ml BSA;
   b. make a 1:10 dilution of 10 mg/ml BSA in same buffer as samples → 1 mg/ml BSA (2.3% SDS does not interfere with the asssay);
   c. make a 1:10 dilution of 1 mg/ml BSA in sample buffer → 0.1 mg/ml BSA.

3. Aliquot 1 ml each of the Protein Detection Solution to several 12 x 75 mm dispo glass tubes; add appropriate volumes of sample buffer to each tube and vortex (each tube should receive the same total volume of buffer and protein solution).

4. Add appropriate volumes of protein standard to each tube and vortex immediately, allowing 30 sec between each sample for vortexing, adjusting pipetman, etc.

5. Sample volumes that are used to generate the standard curve are as follows:

Buffer Vol.	**Protein Std. Vol.**	**Amt. Protein**
50 µl	0	0
40 µl	10 µl (0.1 mg/ml stock)	1 µg
20 µl	30 µl (" " ")	3 µg
0	50 µl (" " ")	5 µg
40 µl	10 µl (1.0 mg/ml stock)	10 µg
35 µl	15 µl (" " ")	15 µg
20 µl	30 µl (" " ")	20 µg
vol. to total 50 µl	exp. vol.	from standard curve

6. After 10 min, add 0.1 ml of 1 N Phenol Reagent Solution to each tube and vortex immediately, once again leaving 30 sec between each sample.

7. After 10 min, read samples at A670.

8. Plot standard curve (µg protein on horizontal axis and OD on vertical axis); determine amount of protein in experimental samples from standard curve.

BLOT PURIFICATION OF ANTI-ENDO B ANTIBODY

(adapted from Nigg *et al.*, *Cell* **41**: 1039-1051, 1985 &
Olmsted, *Meth. Enzymol.* **134**: 467-472, 1986)

1. Separate PFHR9 cytoskeletal fraction on a 10% preparative polyacrylamide gel (use 16.5x17.5 cm notched plates).

2. Gently shake gel in 100 ml Transfer Buffer for at least 20 min (to remove excess SDS and to equilibrate gel); soak nitrocellulose in Transfer Buffer (to remove air bubbles).
   Transfer Buffer = 25 mM sodium phosphate, monobasic (20.7 g $NaH_2PO_4 \cdot H_2O$ in 6 L H_2O, pH to 6.5 with 10N NaOH).

3. Place nitrocellulose/gel sandwich into transfer apparatus (Hoefer TE 42); run overnight at 100 mAmp.

4. Remove nitrocellulose; draw lines across top and bottom for later alignment.

5. Cut out narrow marker strips - stain with India Ink (the cytoskeletal fraction has a reproducible pattern with only a few abundant proteins; if sample is complex, marker strips will have to be immunoblotted to identify the desired protein).

6. Align marker strips with unstained blot; cut out nitrocellulose bands containing Endo B.

7. Block nitrocellulose strip with 2-3 ml PBS + 5% Carnation non-fat dry milk*, 60 min, 37°C, shaking (in 12x75 mm polypropylene snap cap tube).

8. Incubate strip overnight, room temperature, shaking with antibody (2 ml of anti-Endo B, IgG fraction, in PBS, 0.1 g (5%) milk added).

9. Place strip into clean tube and wash 6X with PBS, 3-4 ml, 5 min, shaking (save antibody solution - test for activity).

10. Elute bound antibody with 0.4 ml 0.2 M glycine-HCl, pH 2.2; agitate by hand for 2 min exactly.

11. Add 0.2 ml 1 M K_2HPO_4 to neutralize pH; remove nitrocellulose strip.

12. Dialyze antibody against PBS, 4°C, several 500 ml changes.

13. Add azide to 0.02%.

*Reference for nonfat milk as blocking agent: Johnson et al., *Gene Anal. Techn.* **1**: 3-8, 1984.

CULTURE OF TROMA-1 HYBRIDOMA

1. Remove provial from liquid nitrogen (Revelation tank) and immediately thaw cell suspension in 37°C water bath with gentle agitation; swab outside of vial with 70% EtOH.

2. Transfer cell suspension to a 15 ml conical tissue culture tube and add 10 ml warm Complete Medium; spin at 1200 rpm for 4 min.

3. Remove supernate, gently resuspend pellet in 5 ml medium, and transfer cell suspension to a 75 cm^2 tissue culture flask containing 1 x 10^6 peritoneal macrophages* in 20 ml medium.

4. Grow hybridoma at 7% CO_2 and 37°C; healthy cells are big and round and grow in suspension, although most will settle to the bottom of the flask. When the bottom is fairly crowded, it is time to pass the cells (if the cells are growing well, this must be done every other day).

5. Loosen cells by pipetting medium up and down over bottom surface of the flask, being careful not to foam the medium; remove cell suspension into 50 cc conical tissue culture tube(s) and spin at 1200 rpm for 4 min.

6. Remove supernate, filter through 0.45 μm Millex filter unit to remove debris, and store at -20°C.

7. Resuspend cell pellet in 5-10 ml complete medium and split into four or five 75 cm^2 tissue culture flasks containing 25 ml medium (final concentration approx. 1-5 x 10^5 cells/ml).

8. Replenish frozen stock as needed: resuspend cell pellet in 90% FCS/10% DMSO at a concentration of 1 x 10^7 cells/ml; add 1 ml each to individual provials.

9. Place provials in styrofoam test tube rack and wrap with 3-4 layers of bench cote.

10. Place at -80°C overnight and put in liquid nitrogen the next day; test thaw a vial after a few days in liquid nitrogen.

*Grow hybridoma cells in presence of macrophages when first thawed or at any time when they look very sparse or like they are not going to make it (i.e. are dented/less refractile).

Complete Medium

Base medium = Dulbecco's Modified Eagle's Medium that contains 4.5 g glucose/L and 3.7 g $NaHCO_3$/L (DME H-21, Cell Culture Facility).

To a 450 ml bottle of DME H-21, add the following:
- 50 ml fetal calf serum (10% final concentration)
- 5 ml 100X sodium pyruvate (0.11 g/L final concentration)
- 5 ml 100X L-glutamine (0.292 g/L final concentration) (add fresh every 6 weeks)
- 5 ml 100X Pen-Strep (100 U/ml final activity) (optional).

COLLECTION OF PERITONEAL MACROPHAGES

1. Etherize a CF_1 adult female mouse and pin shoulders to cork board.

2. Wet abdomen with 70% EtOH and peel skin away from the peritoneum, being careful not to puncture the peritoneum; wet peritoneum with 70% EtOH.

3. Using a 20 guage needle, inject 5 ml Dulbecco's PBS into the peritoneal cavity; gently swirl the PBS around the cavity.

4. Insert pasteur pipette into peritoneal cavity (use point of small scissors to enlarge needle hole); add two squirts of air to lift up peritoneum.

5. Being careful not to touch the spleen or liver, remove PBS containing macrophages and put into 15 ml conical tissue culture tube; spin at 1200 rpm for 10 min.

6. Remove supernate, resuspend cell pellet in 2 ml complete medium, and remove 10 μl aliquot for cell count; yield usually 1-3x10^6 macrophages/mouse.

IN VITRO PRODUCTION OF TROMA-1 IgG

(adapted from Bodeus *et al.*, *J. Immunol. Meth.* **79**: 1-6, 1985)

1. Harvest exponentially growing hybridoma cells from one to two 75 cm^2 tissue culture flasks.

2. Resuspend cell pellet in complete medium at a concentration of 5x10^6 cells/ml.

3. Add 2 ml (10x10^6 cells) to an 850 cm^2 tissue culture roller bottle (Corning #25140) containing 300 ml complete medium; tighten cap.

4. Incubate for two weeks at 37°C on a roller apparatus set at 0.5 rpm (during this time there is some cell growth followed by cell death, and the medium will turn from purple to orange/red to yellow).

5. Harvest roller bottle by pouring off suspension into six 50 ml conical tissue culture tubes; spin at 1500 rpm for 15 min.

6. Pour off supernates and filter through 0.45 μm Millex units into sterile bottles; place at -20°C if not used right away (TROMA-1 IgG concentration will be approx. 15-25 μg/ml).

AFFINITY PURIFICATION OF TROMA-1 IgG

1. Matrix of affinity-purified goat anti-rat IgG-agarose purchased from Zymed Lab (#62-9541), placed in a 2 ml Poly-Prep column (Bio Rad #731-1550), and stored at 4°C in PBS + 0.005% Thimerosal.

2. Let column and all solutions warm up to room temperature to prevent formation of air bubbles in column.

3. Pre-cycle column with 10 ml of Elution Buffer at 2 ml/min; wash column with 20 ml PBS, 2 ml/min.

4. With a 25 guage needle on outport of column, run 30-60 ml of roller bottle supernate through column by gravity flow (approx. 1 ml/5-6 min); pH of supernate is slightly lower than optimum - if it is dialyzed against several changes of PBS to bring the pH up to 7.0, the efficiency of IgG binding to the matrix is increased some (test flow through for activity before discarding).

5. Wash column with 20 ml PBS, first 4-5 ml by gravity flow, rest at 1 ml/min.

6. Elute TROMA-1 IgG with 10 ml Elution Buffer at 0.5-1.0 ml/min; collect 1 ml fractions and immediately add 75 µl 1M Tris-HCl, pH 8.8 to each fraction to neutralize the pH.

7. Read OD 280 (with G-HCl/Tris as blank), pool Ig-containing fractions (IgG usually off in first 3-4 ml), and dialyze at 4°C against several changes of PBS (for standard assays) or PBK (for microinjection).

8. Remove from dialysis, determine protein concentration, and test for TROMA-1 activity by indirect immunofluorescence.

9. For standard assays, add sodium azide to 0.05%, airfuge 15 min, aliquot in 25 µl volumes, and store at -80°C.

10. For microinjection, use Centricon 30 microconcentrator (Amicon #4208) per manufacturer's directions to concentrate IgG to 20^{+} mg/ml; airfuge 15 min, aliquot in 5 µl volumes, and store at -80°C.

SOLUTIONS

Buffer	*Final Concentration*	*Amount*
Elution Buffer	0.1 M Glycine	0.75 g
(100 ml)	0.15 M NaCl	0.88 g

pH to 2.4 with concentrated HCl; filter through Whatman #1 paper.

PBK	10 mM KH_2PO_4	8.16 g
(6 L)	0.12 M KCl	53.7 g

pH to 7.4 with 5 N KOH.

INDIRECT IMMUNOFLUORESCENT STAINING FOR PFHR9 CELL INTERMEDIATE FILAMENTS

(parts adapted from Geiger & Singer, *Cell* **16**: 213-222, 1979)

1. Two days prior to assay, place cleaned and sterilized 9 mm square glass coverslips* (Bellco Glass) into individual wells of a 24-well culture plate; incubate with 0.5 ml of 0.1% gelatin in dH_2O (filtered and sterilized) for 30-60 minutes; rinse wells one time with Complete Medium before adding cells.

2. Plate log phase HR9 cells at $1x10^4$ cells/ml/well in Complete Medium.

3. Aspirate media and rinse cells two times with 1 ml Dulbecco's PBS (D-PBS); wash cells one well at a time, so they do not dry out.

4. Fix with 0.5 ml of 2% paraformaldehyde# in D-PBS for 30 minutes at room temperature.

5. Wash 2X with D-PBS + 0.1 M glycine (keep sterile) to quench free aldehydes of fixative, 0.5 ml, 3 min each; wash 2X with D-PBS, 1 ml, 3 min each.

6. Permeabilize with 0.1% Triton X-100 in D-PBS, 0.5 ml, 4 min.

7. Wash 3X with D-PBS, 1 ml, 3 min; incubate 30 min with 0.5 ml D-PBS + 1 mg/ml ovalbumin (keep sterile).

8. Aspirate solution and center coverslips in wells (make sure all fluid is aspirated from area surrounding coverslips and corners of coverslip do not touch edges of well, otherwise antibody will drain off the coverslip); add 10-15 µl primary antibody solution, put damp kimwipe over top of plate, replace lid, and incubate at 37°C in a humid chamber for 60 min.
    a. anti-Endo B IgG at 0.05 mg/ml in D-PBS + 1% BSA.
    b. TROMA-1 culture supernate used straight, without dilution.

9. Wash 2X with D-PBS + 0.1% Tween-20, then 2X with D-PBS, 1 ml, 7 min each.

10. Incubate 5-10 min in 0.5 ml D-PBS + ovalbumin.

11. Aspirate solution as above and add 10-15 µl secondary antibody; incubate as above for 30 min.
    a. 1:40 A.P. FITC-conjugated goat anti-rabbit IgG (Cappel #1612-3151) in D-PBS + 1% BSA.
    b. 1:40 A.P. FITC-conjugated goat anti-rat IgG (Cappel #1613-3151) in D-PBS + 1% BSA. (Alternatively, a biotin-conjugated secondary antibody followed by Texas Red-conjugated streptavidin [1:200 of each] may be used to visualize the filaments.)

12. Wash 2X with D-PBS + 0.1% Tween and 3X with D-PBS, 1 ml, 10 min each, in the dark.

13. Dip coverslips 2X into beaker of distilled water, drain on a kimwipe, and invert onto 0.9

μl of 2% n-propyl gallate (in 70% glycerol, 30% 0.1 M Tris-HCl, pH 9.0; has to be heated to get it into solution); four coverslips can be mounted onto one slide.

14. Gently seal with nail polish, being careful not to move the coverslip around.

15. Observe with plan neofluor 40X and 63X objectives; store at 4°C in the dark.

*coverslips cleaned as follows:
a. soak in concentrated nitric acid for 30 min with occasional stirring;
b. boil 10 min in dH_2O;
c. rinse in running dH_2O;
d. drain on kimwipe, airdry on lens paper;
e. place in small beakers, cover with foil, and autoclave.

#2% paraformaldehyde prepared as follows:
a. mix 0.2 gm paraformaldehyde in 5 ml dH_2O and heat at 70°C for 20 min;
b. add one drop 1N NaOH and heat an additional 10 min at 70°C;
c. mix with 5 ml of 2X D-PBS and filter through 0.45μm;
d. use within 24 hours.

Dulbecco's PBS

Compound	*1 L.*	*2 L.*
KCl	0.2 g	0.4 g
KH_2PO_4	0.2 g	0.4 g
NaCl	8.0 g	16.0 g
$Na_2HPO_4 \cdot 7H_2O$	2.16 g	4.32 g

Bring up to volume with dH_2O (minus 10 ml/L.), pH to 7.2, filter through Whatman #1 paper, put 495 ml/bottle, and autoclave. When cool, add 5 ml 100X C-M Stock to each bottle and mix well.

100X C-M Stock 1 g $CaCl_2$ and 1 g $MgCl_2 \cdot 6H_2O$ in 100 ml dH_2O
(filter sterilize through 0.22 μm into sterile 100 ml bottle)

Note: all commercial secondary antibody and streptavidin solutions should be microfuged after arrival/reconstitution and before aliquoting into small volumes for long term storage in freezer.

EMBRYO RECOVERY AND CULTURE

1. Superovulate 6-10 week old female CF_1 mice (random bred, Charles River Lab, Boston) by intraperitoneal injection of 0.1 ml pregnant mare's serum (PMS, Teikoku Zoki Co., Tokyo, 1000 units/2 ml, diluted 1:10 in saline); 46-50 hours later, inject 0.1 ml of human chorionic gonadotropin (HCG, Carter-Glogau Laboratories, Inc., Glendale, AZ, 5000 USP units/10 ml, diluted 1:10 in saline) and place females singly with males overnight.

2. Check for presence of vaginal plug; day 1 of embryogenesis is taken as day of plug.

3. Recover zygotes early on day 1 by rupturing the oviductal ampulla and allowing the cumulus mass to flow out into a small drop of flushing medium I (Spindle, *In Vitro* 16: 669-674, 1980); incubate a few minutes in an excess of hyaluronidase (Sigma Type IV, #H-2376, 0.1% in CMF-D-PBS + 10 mg/ml PVP) until the follicle cells are dispersed; remove zygotes and wash 4X in flushing medium I.

4. Culture zygotes and cleavage-stage embryos in egg culture medium (ECM, Spindle, 1980) at 37°C and 5% CO_2 in a humid chamber.

5. Flush cleavage-stage embryos from oviducts with flushing medium I:
   a. harvest 2-cell embryos on morning of day 2;
   b. harvest 8-cell embryos early on day 3;
   c. for morulae, either flush directly from both oviducts and uteri late on day 3 (or very early on day 4) or else culture 8-cell embryos in 0.8 ml of ECM in organ tissue culture dish (Falcon #3037) for 12-24 hours, depending on desired cell number.

6. Flush blastocysts from uteri on day 4 with flushing medium II (contains amino acids and fetal calf serum); culture in modified Eagle's medium containing 10% FCS (Spindle, 1980).

IMMUNOSURGERY FOR INNER CELL MASS (ICM) ISOLATION

1. Wash blastocysts 4X in flushing medium I and place into a 60 μl drop of rabbit anti-mouse L cell antibody (diluted 1:5 in flushing medium); incubate 20 min at 37°C in a humid chamber.

2. Wash the blastocysts 3X in flushing medium, then incubate for 20 min at 37°C in 60 μl of guinea pig complement (Gibco #640-9190, diluted 1:5 in flushing medium).

3. Wash the blastocysts 3X and incubate an additional 30 minutes in fresh medium at 37°C, during which time the outer layer of dead TE cells loosens up.

4. Strip off the dead TE cells by pipetting the blastocysts up and down repeatedly through a polished, drawn-out pipette with tip diameter approximately equal to that of the ICM.

5. Collect the ICMs and culture in modified Eagles medium containing 10% FCS.

DETECTION OF ENDO B AND ENDO A IN PREIMPLANTATION MOUSE EMBRYOS BY IMMUNOBLOTTING

(parts adapted from Burnette, *Anal. Biochem.* **112**: 195-203, 1981)

1. Harvest embryos by rinsing them through 3-4 changes of D-PBS + 3 mg/ml PVP (to remove BSA) and pipetting them into the bottom of a 0.5 ml microfuge tube, in as little PBS as possible.

2. Add approximately 20 µl of SDS-Sample Buffer (SDS-SB) to the tube, vortex, spin briefly in the microfuge, and store at -80°C. Approximately 100 blastocysts are necessary to obtain a detectable signal for cytokeratins on immunoblots. To increase the number of embryos per sample, embryos recovered at later times can be pooled with an earlier sample, as long as the SDS-SB is not diluted out. However, as many embryos as possible should be harvested at any one time to avoid repeated freeze-thawing of the sample.

3. Pour a 10% lower acrylamide gel, using the 14 cm notched plates and 1 mm spacers (leave space for the comb and at least 1-1 1/2 cm between bottom of the comb and lower gel). Gently overlay gel with 0.5 ml of dH_2O and allow gel to polymerize for at least two hours before pouring the stacking gel (the lower gel can be poured the night before and stored overnight with an overlay of 1/4-lower gel buffer).

4. Pour upper gel, insert comb with 8 mm-wide teeth, and allow gel to polymerize for 30-90 minutes.

5. While upper gel is polymerizing, prepare samples. To each embryo sample, add 1 µl of bromophenol blue (0.1% in 25% glycerol, tracking dye) and 3 µl of methylene blue (0.04% in SDS-SB, transfer dye). For cytokeratin markers, use 1-2 µl of the HR9 cytoskeletal fraction (stock is 1 mg/ml in PBS + 2.3% SDS) mixed with 18 µl SDS-SB, 1 µl bromophenol blue, and 3 µl methylene blue per lane.

6. Place gel apparatus into gel box, remove comb, add running buffer, and pipette all air bubbles away from the bottom of the gel.

7. Boil samples 2-3 min, spin briefly in microfuge, and load into wells with the 100 µl Hamilton syringe, rinsing the syringe between each sample.

8. Run gel at 15 mAmp constant current until the dye solutions reach the bottom of the gel, which usually takes about 3 hr if gel buffers are made properly; the methylene blue separates away from the bromophenol blue near the end of the run.

9. Remove lower gel and equilibrate it in 100 ml Transfer Buffer for 30 min. Cut nitrocellulose paper (0.45 µm, Schleicher & Schuell #BA-85) to size of gel and soak in Transfer Buffer to remove air bubbles. (See Results for a discussion of technical modifications that may increase the detectability of cytokeratins on blots.)

10. Make sandwich as follows: bottom grid (with tab)→scotch pad→filter paper (Bio-Rad #165-0921)→nitrocellulose paper→gel→2 sheets filter paper→top grid. Assemble sandwich in tray, keeping all elements submerged in Transfer Buffer and making sure that no air bubbles are trapped between any of the layers.

11. Fill transfer apparatus (Hoefer Transphor Unit #TE-42) with Transfer Buffer and quickly place sandwich in a center slot of the unit. Put lid on unit such that the bottom grid of the sandwich (with tab) is next to the anode (red, positive pole). Because the negatively-charged proteins will migrate towards the anode, this orientation will ensure that the proteins move out of the gel into the nitrocellulose paper. Run transphor overnight at 100 mAmp constant current.

12. Remove nitrocellulose, number lanes (methylene blue staining of the nitrocellulose indicates a successful transfer and demarcates the lanes), and draw lines across the top and bottom for later alignment, if paper is to be cut into individual strips.

13. Block unbound sites of nitrocellulose with 20-30 ml of 3% Carnation non-fat dry milk in PBS for 1 hr at 37°C on a shaking platform (incubations are done in small tupperware containers, Linbro microtiter plate lids, or lids of pipette tip racks that are kept covered to minimize evaporation; individual strips are incubated in screw-top Kimax tubes).

14. Incubate in 10-20 ml of primary antibody solution for 2 hr at room temperature:
    a. 1:500 dilution of anti-Endo B IgG (#1588, 3 mg/ml stock) in PBS/milk;
    b. TROMA-1 culture supernate, used straight.

15. Wash nitrocellulose 5X for 6 min each with 10-20 ml of PBS; re-block with 10-20 ml PBS/milk for 15 min at room temperature.

16. Incubate in 10-20 ml of secondary antibody solution for 1 hr at room temperature:
    a. 1:750 dilution in PBS/milk of A.P. biotin-conjugated goat anti-rabbit IgG (Cappel #0612-3151, biotinylated with biotinyl N-hydroxy succinimide ester [E-Y Lab #BA-106] per manufacturer's directions, final concentration ~ 1 μg/ml);
    b. 1:750 dilution in PBS/milk of A.P. biotin-conjugated goat anti-rat IgG (Zymed Lab #62-9640, 1 μg/ml final concentration).

17. Wash 5X for 6 min each with 10-20 ml of PBS; re-block 15 min with 10-20 ml of PBS/milk.

18. Incubate 45-60 min with a 1:500 dilution in PBS/milk of peroxidase-conjugated avidin (Cappel #24972, 5 μg/ml final concentration). An enhanced signal may be obtained by use of ^{35}S-StrepAvidin, available from Amersham (see Chisholm & Houliston, *Development* **101**: 565-582, 1987).

19. Wash 5X for 6 min each with 10-20 ml PBS.

20. React for peroxidase as follows (DeBlas & Cherwinski, *Anal. Biochem.* **133**: 214-219, 1983):
    a. pre-incubate 10 min in 10 ml of Substrate Solution;
    b. incubate up to 30 min in 10 ml of Substrate Solution that contains 0.01% H_2O_2;
    c. stop reaction by washing 3-4X with dH_2O
    (discard all DAB-containing solutions in carcinogen waste container).

21. Photograph immediately with Polaroid apparatus, as the nitrocellulose turns brown fairly quickly.

SOLUTIONS AND RECIPES FOR PROTEIN GELS (LAEMMLI)

SDS Sample Buffer (SDS-SB) (100 ml)

0.756 g Tris (Bio-Rad #161-0719)
2.3 g SDS (Bio-Rad #161-0301)
10 g glycerol
5 ml β-mercaptoethanol
pH to 6.8 with conc. HCl

Use triple deionized water for all solutions.
For all buffers except Running Buffer, filter through Whatman #1 paper and store at 4°C.

30% Acrylamide Stock (100 ml)

29.2 g acrylamide (Bio-Rad #161-0100)
0.8 g bisacrylamide (Bio-Rad #161-0200)
30% (w/v) glycerol
(filter w/ 0.45 μm Nalgene unit)
(store in dark at 4°C)

Lower Gel Buffer (LGB) (250 ml)

45.4 g Tris
1 g SDS
pH to 8.8 with conc. HCl

Upper Gel Buffer (UGB) (250 ml)

15.12 g Tris
1 g SDS
pH to 6.8 with conc. HCl

Running Buffer (4 L)

12.1 g Tris
4 g SDS
57.65 g glycine (Bio-Rad #161-0718)

Lower Gels	**10%**	**12.5%**	**14%**	**16%**	**18%**
LGB	5 ml	5	5	5	5
30% Acrylamide Stock	6.66 ml	8.33	9.34	10.66	12
dH_2O	8.34 ml	6.66	5.66	4.34	3
10% ammonium persulfate*	29 μl	29	29	29	29
TEMED (Bio-Rad #161-0800)	10 μl	10	10	10	10

*Make up fresh ammonium persulfate (Bio-Rad #161-0700, 0.1 g in 1 ml dH_2O) every few days. Before adding ammonium persulfate, degas gel solutions to remove air bubbles.

Upper Gel

UGB	3 ml
30% Acrylamide Stock	1.8 ml
dH_2O	7.2 ml
10% ammonium persulfate*	36 μl
TEMED	12 μl

SOLUTIONS FOR IMMUNOBLOTTING

Buffer	*Final Conc.*	*Stock Amt.*
Transfer Buffer (6 L)	25 mM Sodium phosphate dH_2O pH to 6.5 with 10N NaOH	20.7 g $NaH_2PO_4 \cdot H_2O$ 6 L
PBS (1 L)	0.9% NaCl 10 mM Sodium phosphate dH_2O pH to 7.4 with conc. NaOH	9 g 1.38 g $NaH_2PO_4 \cdot H_2O$ 1 L

	Final Conc.	*Stock Conc.*	*Stock Amt.*
Substrate Solution (Peroxidase) (40 ml)	0.5 mg/ml DAB (Sigma #D-5637) (3,3´-Diaminobenzidine)	-	20 mg
	0.03% $CoCl_2$ (Sigma #C-2644)	3%	0.4 ml
	0.04% $NiCl_2$ (Sigma #N-5756)	8%	0.2 ml
	PBS, pH 7.4	-	40 ml

Substrate Solution containing 0.01% H_2O_2 — add 0.2 ml of a 1% H_2O_2 solution (0.1 ml of 30% stock in 2.9 ml dH_2O) to 20 ml of **Substrate Solution.**

INDIRECT IMMUNOFLUORESCENT STAINING FOR CYTOKERATINS IN PREIMPLANTATION MOUSE EMBRYOS (WHOLE MOUNT)

(parts adapted from Maro *et al.*, *J. Embryol. Exp. Morph.* **81**: 211-237, 1984)

1. Wash embryos 4X in D-PBS + 3 mg/ml polyvinyl pyrrolidone (PVP, Calbiochem #5295, 40,000 MW).

2. Fix embryos for 30 min at room temperature in 0.5 ml of 2% paraformaldehyde in D-PBS.

3. Wash 2X in D-PBS + PVP + 0.1 M glycine (keep sterile) to quench free aldehydes of fixative, 0.2 ml, 3 min each; wash 2X in D-PBS + PVP, 0.2 ml, 3 min each.

4. Permeabilize in 0.25% Triton X-100 in D-PBS, 1-2 ml, 4 min, room temperature.

5. Wash 3X in D-PBS + PVP, 0.2 ml, 3 min; incubate 30 min with 0.2 ml D-PBS + 1 mg/ml ovalbumin (keep sterile).

6. Incubate in 20-50 μl of primary antibody solution for 60 min at 37°C in 35 mm petri dish in humid chamber:
   a. rabbit anti-Endo B IgG at 0.05 mg/ml in D-PBS + 3% BSA + 0.1% Tween 20.
   b. TROMA-1 (rat monoclonal) culture supernate used straight, without dilution.
   c. for control antibody, use non-immune rabbit IgG (Cappel #6012-0080) or rat IgG (Cappel #6013-0080), respectively, at 5-10 μg/ml in PBS + BSA + Tween or hybridoma culture medium, respectively.

7. Wash 2X with D-PBS + 0.1% Tween-20, then 3X with D-PBS + PVP, 0.2 ml, 10 min each.

8. Incubate in 20-50 μl of secondary antibody as above for 30-60 min:
   a. 1:40 A.P. FITC-conjugated goat anti-rabbit IgG (Cappel #1612-3151, stock = 1 mg/ml) in D-PBS + BSA + Tween.
   b. 1:40 A.P. FITC-conjugated goat anti-rat IgG (Cappel #1613-3151, stock = 1 mg/ml) in D-PBS + BSA + Tween.
   (Alternatively, a biotin-conjugated secondary antibody followed by Texas Red-conjugated streptavidin may be used to visualize the filaments.)

9. Wash 2X in D-PBS + 0.1% Tween and 3X in D-PBS + PVP, 0.2 ml, 10 min each, in the dark.

10. To determine the number of nuclei in each embryo, stain with Hoechst (Bisbenzimid H 33258, Riedel-de Haën Ag) as follows (in the dark):
    a. incubate 5 min in 100 μl drop of a 1:100 dilution of Hoechst in D-PBS + PVP (stock = 0.5 mg/ml in EtOH);
    b. wash 4X in 0.2 ml PBS + PVP for 2 min each.

11. Quickly rinse the embryos in a drop of dH_2O and pipette them into a small drop of 2% n-propyl gallate (in 70% glycerol, 30% 0.1M Tris, pH 9.0; has to be heated to get it into solution) on a clean glass slide; gently lower an 18 mm round coverslip over the drop (2 coverslips can be mounted onto one slide) and seal with nail polish, being careful not to

move the coverslip around.

12. Observe with plan neofluor 40X and 63X objectives on a Zeiss compound microscope equipped with epifluorescent optics and a 100W DC mercury lamp; store at 4°C in the dark.

D-PBS = Dulbecco's phosphate-buffered saline; A.P. = Affinity-purified

PREPARATION OF [^{35}S]METHIONINE-LABELED CYTOSKELETONS FROM MOUSE BLASTOCYSTS

(adapted from Jackson *et al., Differentiation* **17**: 161-179, 1980 & Oshima *et al., Dev. Biol.* **99**: 447-455, 1983)

1. [^{35}S]methionine stock (#NEG-009T, New England Nuclear) is at 9.1 mCi/ml; 10 µl is dried down using the Speed Vac and resuspended in 91 µl of modified Eagle's medium (without methionine) containing 1% dialyzed fetal calf serum, for a final concentration of 1 mCi/ml.

2. A 25 µl drop of the labeling medium is placed in the center of a 35 mm petri dish and equilibrated at 37°C and 5% CO_2 for 15 min before the dish is flooded with mineral oil.

3. Approximately 100 blastocysts (Oshima *et al.* used as few as 25 blastocysts) are rinsed through 3-4 drops of methionine-free Eagle's medium and placed into the label drop.

4. After a 4 hr incubation at 37°C and 5% CO_2, the blastocysts are washed 4X in flushing medium I (without methionine) and placed in a 1.5 µl microfuge tube for extraction.

5. Add 100 µl of Lysis Buffer to the tube and incubate for 2-3 min at room temperature with frequent vortexing (Oshima *et al.* added 10 µg of unlabeled HR9 cytoskeletal proteins per 25 blastocysts as carrier; I did not do this, but it could be done in the future to increase the recovery of embryonic material).

6. Recover the embryo residue by a 5 min spin in a microfuge (12,000g) at 4°C; remove supernate.

7. Wash pellet one time with 100 µl of Lysis Buffer, spin 5 min in microfuge, and remove supernate.

8. Add 100 µl of Digestion Buffer, vortex, and incubate 5 min on ice; spin 5 min at 4°C in the microfuge and remove supernate.

9. Extract residue 2X for 5 min each with 0.5 ml of Extraction Buffer.

10. Recover cytoskeletal material by a 5 min spin in the microfuge at 4°C, and dissolve pellet in 25 µl of SDS-Sample Buffer.

11. Remove 2 µl for determination of [^{35}S]methionine incorporation into protein by trichloroacetic acid (TCA) precipitation; store rest of sample at -80°C.

12. Add sample for TCA precipitation to 100 µl of dH_2O in a 12 x 75 mm glass tube, seal tube with parafilm, and store at -20°C.

SOLUTIONS

Buffer	*Final Concentration*	*Stock Conc.*	*Stock Amt.*
Lysis Buffer (1 ml)	10 mM Tris-HCl, pH 7.4	100 mM	0.1 ml
	140 mM NaCl	1 M	0.14 ml
	1% Triton X-100	10%	0.1 ml
	0.5 mM PMSF	50 mM	0.01 ml
	dH_2O	-	0.65 ml
Digestion Buffer (0.5 ml)	10 mM Tris-HCl, pH 7.4	100 mM	50 µl
	5 mM $MgCl_2$	300 mM	8.33 µl
	0.1 mM $CaCl_2$	10 mM	5 µl
	50 µg/ml micrococcal nuclease (Sigma #N-3755)	1 mg/ml	25 µl
	dH_2O	-	412 µl
Extraction Buffer (5 ml)	10 mM Tris-HCl, pH 7.4	100 mM	0.5 ml
	1.5 M KCl	3 M	2.5 ml
	140 mM NaCl	1 M	0.7 ml
	0.5% Triton X-100	10%	0.25 ml
	0.5 mM PMSF	50 mM	0.05 ml
	dH_2O	-	1 ml

TCA PRECIPITATION

1. Thaw sample and add 50 µg of BSA (50 µl of 1 mg/ml stock) as carrier protein.

2. Add equal volume (152 µl) of 15% TCA + 0.01 M methionine.

3. Vortex and boil 15 min (breaks down charged tRNA's), with cork loosely placed in tube opening.

4. Collect TCA precipitate on 2.5 cm GF/C filter disc (Whatman #8574).

5. Rinse tube and filter disc 2X with 3 ml of 5% TCA.

6. Dry filter disc by pinning above a styrofoam rack (infrared heat lamp can be used to speed the drying).

7. Place disc in liquid scintillation minivial, add 5 ml Omnifluor scintillation cocktail, and count samples using the ^{14}C window specifications.

ANALYSIS OF [^{35}S]-LABELED CYTOSKELETAL FRACTION BY SDS-PAGE

1. Thaw samples, add 1 μl of bromophenol blue solution (0.1% in 25% glycerol) to each sample, boil for 2-3 min, and spin briefly in microfuge. Prepare MW markers for at least one lane.

2. Load samples into individual wells and separate on a 10% polyacrylamide gel (details in immunoblotting method).

3. Fix and stain lower gel for 20 min in Gel Staining Solution. Destain in 2-3 changes (overnight or until MW markers are visible). Kimwipes or other absorbent material can be added to the destain to sop up the stain and speed the destaining process.

4. Dry gel, mark corner of gel and/or MW markers with radioactive ink, and place in film cassette with a sheet of pre-flashed Kodak X-Omat AR film.

5. Expose for a week at -80°C. If a small amount of material is used, an enhanced signal may be obtained by fluorography (described by Bonner, *Meth. Enzymol.* **104**: 460-465, 1984).

6. Develop film and set up a second film for a longer exposure.

SOLUTIONS

Solution	*Final Concentration*	*Stock Conc.*	*Stock Amt.*
Gel Staining Solution	0.2% Coomassie Blue	-	2.2 g
(1.1 L)	45.4% Methanol	100%	500 ml
	9.1% Acetic acid	100%	100 ml
	dH_2O	-	500 ml
	(filter through Whatman #1 paper)		
Destain	5% Methanol	100%	100 ml
(2 L)	7.5% Acetic acid	100%	150 ml
	dH_2O	-	1750 ml

MW Markers Stock → 1 mg/ml in SDS-Sample Buffer of each of the following:

a. bovine serum albumin M_r 66,000
b. ovalbumin M_r 45,000 (Sigma #A-5503)
c. trypsinogen (+ PMSF) M_r 24,000
d. β-lactoglobulin M_r 18,400 (Sigma #L-7880)

(Despite the PMSF, the trypsinogen appears to degrade the other proteins. Therefore, it should be replaced with carbonic anhydrase [Sigma #C-2273], M_r 29,000).

For Coomassie blue stained gels, use 25 μl stock (25 μg each marker) per lane.

For silver stained gels or India ink stained blots, dilute stock 1:20 in SDS-Sample Buffer to 0.05 mg/ml and use 10 μl of diluted markers (0.5 μg each marker) per lane.

SILVER STAINING POLYACRYLAMIDE GELS

(from Merril *et al.*, *Meth. Enzymol.* **104**: 441, 1984)

Pre-staining precautions

1. After detergent washing, soak glass plates in 1:1 70% nitric acid:deionized H_2O; rinse well with dH_2O and dry.

2. Use deionized H_2O (3X at least) for all solutions.

Staining (in glass baking dish on rotary shaker)

1. Fix gel in 50% methanol, 12% acetic acid, from 20 min to overnight.

2. Rinse gel 3X with 200 ml 10% ethanol, 5% acetic acid, 10 min each (I find this step unnecessary).

3. Soak gel 5 min in 200 ml 0.0034 M potassium dichromate, 0.0032 N nitric acid (0.2 g $K_2Cr_2O_7$ & 41 µl 70% HNO_3 in 200 ml H_2O).

4. Wash gel 4X with 200 ml H_2O, 30 sec each.

5. Leave for 30 min in 250 ml 0.012 M silver nitrate (0.51 g $AgNO_3$/250 ml H_2O).

6. Rinse gel for 2 min with 200 ml H_2O (eliminates swirling on gel).

7. Rinse rapidly 2X with approx. 300 ml of Developer and then add fresh Developer until bands appear (5-10 min). When satisfied with development, stop by discarding Developer and adding 1% acetic acid. Gel can be stored in this.

   Developer = 0.28 M Na_2CO_3 (30 g/L)
   0.5 ml 37% formaldehyde/L

INDIA INK STAINING OF PROTEINS ON NITROCELLULOSE PAPER

(from Hancock & Tsang, *Anal. Biochem.* **133**: 157-162, 1983)

1. Wash blot 4X with 50 ml PBS + 0.3% Tween 20 - 10 min ea, 37°C, shaking; rinse with dH_2O after each wash.

2. Incubate blot in 50 ml of a 1 µl ink/ml PBS-Tween solution, shaking, room temperature, few hours to overnight (bands appear within an hour, but get darker and more defined with time) (India Ink = Pelikan Fount India Drawing Ink for Fountain Pens - Black).

3. Rinse blot 2-3X with dH_2O and dry.

DETECTION OF ENDO B SYNTHESIS IN PREIMPLANTATION MOUSE EMBRYOS

(adapted from Oshima *et al., Dev. Biol.* **99**: 447-455, 1983)

A. Lysate Preparation

1. Prepare a 25 μl culture drop under oil of modified Eagle's medium (without methionine) containing 1% dialyzed FCS and 1 mCi/ml of [^{35}S]methionine.

2. Wash embryos 3X with flushing medium I (methionine-free) and incubate in the culture drop for 3 hr at 37°C and 5% CO_2.

3. Wash embryos 4X with flushing medium I and transfer to a 12 x 75 mm dispo glass tube.

4. Add 0.5 ml of Lysis Buffer, mix well, and incubate 3-5 min on ice (for ICMs or small numbers of embryos, use 1/4 to 1/2 the volumes).

5. Add EDTA, pH 7.2 and SDS to obtain final concentrations of 10 mM and 0.5%, respectively (add 61 μl of 0.1 M EDTA, pH 7.2 and 50 μl of 5% SDS).

6. Heat samples at 100°C for 2 min; cool and add a tenth volume of 10% NP-40 stock (61 μl).

7. Transfer 10 μl of each sample to a 12 x 75 mm glass tube containing 100 μl dH_2O for determination of radioactivity incorporation into protein by TCA precipitation. Transfer the rest of the sample to a 1.5 ml microfuge tube and store at -80°C.

B. Immunoprecipitation

1. Reconstitute a vial of Staph A (Zysorbin, Zymed #10-1051-1) with 10 ml sterile dH_2O; store at 4°C.

2. Using a 3 ml syringe and a sterile needle, remove 2.6 ml of the Staph A solution and divide it into two 1.5 ml microfuge tubes.

3. Centrifuge in the microfuge for 2.5 min, remove supernates, and resuspend pellets in 1 ml each of Buffer B. Repeat 2X.

4. After final wash, resuspend each pellet in 1.3 ml Buffer A to make a 10% Staph A Solution.

5. Thaw lysate(s) and divide into two equal volumes. A detectable signal is obtained from as few as 30,000 cpm of starting blastocyst lysate (approx. 30 embryos) after a week exposure of the autorad. For earlier stages or ICMs, a greater number of starting cpm ($\geq$ 50,000) is required to detect a signal after a 1 month exposure. If necessary, cleavage-stage or ICM lysates from separate days should be pooled to obtain an adequate number of starting cpm. The volume of antibody added for immunoprecipitation should be adjusted accordingly.

6. Preabsorb lysates with 15 μl of normal rabbit serum (NRS) and 150 μl of the 10% Staph A Solution; incubate 15 min on ice.

7. Spin in microfuge for 2.5 min, transfer supernates to fresh tubes, and discard pellets.

8. For immunoprecipitation, add 12 μl of NRS to one sample (nonimmune control) and 12 μl of anti-Endo B IgG (1 mg/ml stock, final concentration ~ 25 μg/ml) to its duplicate. Incubate at least two hours on ice (or overnight at 4°C).

9. Add 150 μl of 10% Staph A Solution to each tube, mix well, and incubate 15-30 min on ice.

10. Spin 2.5 min in microfuge and save supernates. The recovery of Endo B is not quantitative, and significant amounts of Endo B are recovered with subsequent rounds of immunoprecipitation.

11. Wash pelleted bacteria 2X with 1 ml each of Buffer B, 2X with 1 ml each of Buffer C, and 1X with 1 ml each of Buffer D. Carefully remove all buffer with a drawn-out pasteur pipette after last wash.

12. Add 30-40 μl of SDS-Sample Buffer, mix vigorously, heat at 100°C for 3-4 min, mix again, and spin for 2.5 min in microfuge.

13. Carefully remove the supernates containing the eluted proteins with a drawn-out pasteur pipette, transfer to fresh microfuge tubes, and store at -80°C.

14. Separate the eluted proteins on a 10% SDS-polyacrylamide gel, stain, destain, and dry the gel, and set it up for autoradiography (described in the method for the analysis of the cytoskeleton).

SOLUTIONS

Buffer	*Final Concentration*	*Stock Conc.*	*Stock Amt.*
Lysis Buffer (5 ml)	10 mM Tris-HCl, pH 7.4	100 mM	0.5 ml
	3 mM $MgCl_2$	300 mM	0.05 ml
	0.1 mM $CaCl_2$	10 mM	0.05 ml
	0.1% SDS	5%	0.1 ml
	1 mM N-ethylmaleimide (Sigma #E-3876)	100 mM	0.05 ml
	0.5 mM PMSF (Sigma #P-7626)	50 mM	0.05 ml
	0.19 Trypsin Inhibitor Unit (TIU) (Aprotinin, Sigma #A-4529)	19 TIU/ml	0.05 ml
	dH_2O	-	4.15 ml
	Add 5 µl of DNase I* (1 mg/ml) to 0.5 ml of Lysis Buffer, for a final conc. of 10 µg/ml.		
Buffer A (10 ml)	10 mM Tris-HCl, pH 7.4	100 mM	1 ml
	0.5% SDS	5%	1 ml
	1% NP-40	10%	1 ml
	1 mg/ml ovalbumin	10 mg/ml	1 ml
	0.19 TIU Aprotinin	19 TIU/ml	0.1 ml
	dH_2O	-	5.9 ml
Buffer B (50 ml)	10 mM Tris-HCl, pH 7.4	100 mM	5 ml
	0.5% SDS	5%	5 ml
	1% NP-40	10%	5 ml
	dH_2O	-	35 ml
Buffer C (10 ml)	10 mM Tris-HCl, pH 7.4	100 mM	1 ml
	0.5 M NaCl	1 M	5 ml
	5 mM EDTA	100 mM	0.5 ml
	0.05% NP-40	0.5%	1 ml
	1 mg/ml ovalbumin	10 mg/ml	1 ml
	dH_2O	-	1.5 ml
Buffer D (10 ml)	50 mM Tris-HCl, pH 7.4	100 mM	5 ml
	0.15 M NaCl	1 M	1.5 ml
	5 mM EDTA	100 mM	0.5 ml
	0.05% NP-40	0.5%	1 ml
	dH_2O	-	2 ml

*PREPARATION OF PROTEASE-FREE DNASE I

(adapted from Otsuka & Price, *Anal. Biochem.* **62**: 180-187, 1974)

1. Place 1 ml of lima bean trypsin inhibitor III-conjugated agarose (P-L Biochemicals #5592) in a 2 ml Poly-Prep column.. Wash matrix with at least 10 volumes of 20 mM Tris-HCl, pH 8.0 + 5 mM $CaCl_2$.

2. Dissolve 6-7 mg of DNase I (Worthington #2139) in 0.2 ml of 15 mM Tris-HCl, pH 8.0 + 5 mM $CaCl_2$ and apply to top of matrix.

3. Allow sample to flow into the column and wash with 20 ml of 20 mM Tris, pH 8.0 + 5 mM $CaCl_2$ at a flow speed of 1 ml/6 min. Collect fifteen 0.5 ml fractions.

4. Determine the protein content of each fraction by a fluorescent-based protein assay:
   a. add 40 µl of each fraction to 1.5 ml of 0.2 M Borate Buffer, pH 9.0 and mix well;
   b. add 0.5 ml of 20 mg% Fluram (fluorescamine, Roche Diagnostics #43023) in acetone and mix well;
   c. read samples on spectrofluorometer (390 nm excitation, 480 nm emission).

5. Combine fractions that contain DNase I, dialyze at 4°C against 4 changes of dH_2O, and lyophilize. Store dessicated at -20°C.

6. Regenerate column by eluting with 10 volumes of 1 mM HCl + 1 M NaCl at 1 ml/3 min.

7. Wash column with 5 volumes of 20 mM Tris-HCl, pH 8.0 + 5 mM $CaCl_2$ + 0.02% sodium azide. Store at 4°C.

POLYETHYLENE GLYCOL EMBEDDING OF PREIMPLANTATION MOUSE EMBRYOS FOR INDIRECT IMMUNOFLUORESCENCE MICROSCOPY

(adapted from Wolosewick, *Meth. Enzymol.* **134**: 580-591, 1986, Wolosewick & De May *Biol. Cell* **44**: 85-88, 1982, and Watson & Kidder, *Dev. Biol.* **126**: 80-90, 1988)

1. Wash embryos 4X in 0.2 ml D-PBS + 3 mg/ml PVP (Calbiochem #5295, 80,000 MW).

2. Fix embryos 30 min in 0.5 ml of 2% paraformaldehyde in D-PBS.

3. Wash 2X for 3 min each in 0.2 ml D-PBS + PVP + 0.1 M glycine (to quench free aldehydes); wash 2X for 3 min each in 0.2 ml PBS + PVP (embryos can be stored in this at 4°C).

4. Dehydrate embryos as follows:
   a. incubate 5 min at -20°C in 1-2 ml of 70% EtOH (in 35 mm petri dish);
   b. pipette embryos into bottom of square bottom micromold (Polysciences #8408), fill halfway with 70% EtOH, cover with parafilm, and stick embryos to bottom of mold by spinning 5-10 min at 3,000 rpm in Beckman microfuge;
   c. being careful not to disturb the embryos, pipette off most of the 70% EtOH, re-fill the mold with 80% EtOH, and incubate 5 min at -20°C;
   d. remove most of the 80% EtOH, re-fill mold with 95% EtOH, and incubate 1 hr at -20°C.

5. Prepare PEG as follows:
   a. add PEG 1450 (Sigma #P-5402) and PEG 3350 (Sigma #P-3640) to separate 100 ml glass bottles and melt the PEG (the PEG 1450 will melt at 55-60°C, but it is necessary to put the PEG 3350 in a 65-70°C water bath to melt it);
   b. pour 9 ml PEG 1450 (18%) and 41 ml PEG 3350 (82%) into a prewarmed graduated cylinder, drain into a warm glass beaker or flask, mix well with a glass rod, and keep at 55-60°C (PEG solution can be stored in oven).

6. Heat vacuum oven to 55-60°C; break off pasteur pipette tip and warm in oven (to use for transferring PEG solution to mold).

7. Remove 95% EtOH, leaving approx. 10-20 µl at bottom (if too much is removed, the embryos will loosen and start to swirl around, due to the convection caused by the evaporating EtOH).

8. After making sure that the embryos are still stuck to the bottom of the mold, place it in the vacuum oven and immediately fill the mold with the warm PEG solution; vacuum infiltrate for two hours at 55-60°C.

9. Remove micromold from the oven and allow the PEG to cool and harden.

10. Prepare poly-L-lysine-coated coverslips as follows:
    a. place acid-cleaned 9 mm glass coverslips into individual wells of a 24-well culture plate;
    b. spread 50-100 µl of poly-lysine (150,000-300,000 MW, Sigma #P-1399, 1 mg/ml in

dH_2O, pH 8.5) over each coverslip and incubate 5 min;
c. wash coverslips 3X with 0.5 ml dH_2O, air dry on paper towel, and return to wells of culture plate, poly-lysine side up.

11. Make two cuts on opposite sides of micromold with razor blade, carefully remove the PEG block, and mount onto Sorval JB-4A microtome.

12. Position glass knife relatively vertical and section block at 1 μm thickness; ribbons should start to form almost immediately (the knife angle and speed of sectioning may have to be adjusted to obtain full, relatively wrinkle-free sections).

13. When the ribbon length reaches approximately 9 mm, pick up the ribbon with watchmaker's forceps and transfer it to a poly-lysine-coated coverslip (the PEG will stick to the forceps, so that section will be lost); tack ribbon down with a fine hair and melt sections onto coverslip by placing it on a 55-60°C heat block for a few seconds.

14. Repeat steps 12 & 13 until approximately 150 sections have been cut (all the embryos should be sectioned by this point); place coverslips back into 24-well culture plate, section side up.

15. Remove PEG and rehydrate sections by 10 min changes, 1 ml each of 95% EtOH, 80% EtOH, 70% EtOH, D-PBS, and D-PBS (can be rehydrated directly into PBS).

16. Observe coverslips with inverted phase microscope to identify the ones which have embryo sections.

17. Process for indirect immunofluorescence as with PFHR9 cells (starting at step 7.5); for signal enhancement, use biotin-conjugated secondary antibody (Zymed #62-9640, 1:200 dilution) followed by Texas Red-conjugated streptavidin (Zymed #43-4317, 1:200 dilution).

MICROINJECTION OF TROMA-1 ANTIBODIES INTO MURAL TROPHECTODERM CELLS

(adapted from Cruz & Pedersen, *Dev. Biol.* **112**: 73-83, 1985)

1. Using 1 mm (o.d.) thin-walled glass capillary tubing (Omega Dot, Frederick Haer #30-30-0), pull micropipettes with the Model P-77 Brown-Flaming Micropipette Puller (Sutter Instrument Co.) set at pull strength = 1246 and heat index = 190.

2. Mix 5 μl of TROMA-1 IgG (10-20 mg/ml) with 1.25 μl of 4% rhodamine-conjugated dextran (RDX - Gimlich & Braun, *Dev. Biol.* 115: 340-352, 1986), spin in microfuge for 10 minutes, and back fill a micropipette with approximately 0.2 μl of the antibody solution.

3. Leaving a small air bubble behind the antibody solution, fill the remainder of the micropipette with 0.05M KCl and place into an electrode holder (W-P Instruments #MEH-2S) attached to a Leitz micromanipulator; fill a holding pipette (flame-polish with the De Fonbrune Series A #323 microforge to o.d. approx. 100 μm) with flushing medium II and place into electrode holder on the other micromanipulator (both electrode holders are filled with 0.05 M KCl).

4. Place a 5 x 50 mm coverslip strip lengthwise across the center of a 1-chamber tissue culture slide (Lab-Tek #4801) with the chamber removed, fill the area under the coverslip with flushing media II, and flood the remainder of the chamber with mineral oil (Sigma #400-5).

5. Place 10-20 blastocysts in the media under the coverslip and place the slide on the stage of the Zeiss compound microscope equipped with epifluorescence optics and iontophoresis electronics (Model 1090 Micro-Electrode Pre-Amplifier, BR-1 Bridge, and Tektronix D10 Single Beam Oscilloscope, Winston Electronics Co.).

6. Immerse both the needle and holding pipette into the media and check for adequate current as follows:
   a. set oscilloscope to 0.1 volts/div and 10 μm sec/div - center trace with position knob;
   b. flip output switch of pre-amplifier to normal - center trace on oscilloscope with zero knob;
   c. flip input switch of pre-amplifier to normal - center trace on oscilloscope with zero knob (if the trace goes off the screen, the circuit is incomplete, usually due to a bad needle or an air bubble somewhere - switch needles if this happens, being careful to flip the input and output switches back to ground before removing the needle);
   d. with meter on +, switch on bridge: if current meter deflects to $>0.9\text{x}10^{-8}$ Amp, then the needle is fine and the system is ready for injection; if meter will not deflect, even with turning the D.C. stim. current knob clockwise, then needle is clogged - switch needles and repeat above steps.

7. Align blastocyst with holding pipette at 200X magnification such that a cross-sectional view of the perinuclear area of a mural trophectoderm cell is in focus.

8. Making sure that the oscilloscope trace is centered, insert needle into the perinuclear region of the cytoplasm (a very slight touch); turn the negative capacity knob rapidly

clockwise (until the oscilloscope trace disappears), then back counterclockwise (until trace reappears) - the needle has penetrated the membrane if the trace has dropped below the center line.

9. Iontophorese the antibody/RDX solution into the cell by turning the bridge on (the oscilloscope trace will disappear) - adjust the current to 0.9×10^{-8} Amp with D.C. stim. current knob and inject for 15-20 seconds (very little antibody will be iontophoresed into the cell if the current is <7-8 nAmp); there will be some swelling of the cell with injection; turn off the bridge and remove the needle (the trace should reappear).

10. Score for a successful injection by viewing under fluorescence with the rhodamine filter (#BP 546).

11. Inject other MTE cells of the same and different blastocysts; fix and process the injected blastocysts for double-label indirect immunfluorescence within 30-60 minutes of injection.

MICROINJECTION OF TROMA-1 ANTIBODY INTO 2-CELL EMBRYOS

1. Using 1 mm (o.d.) thin-walled glass capillary tubing (Omega Dot, Frederick Haer #30-30-0), pull microinjection needles with the Model P-77 Brown-Flaming Micropipette Puller (Sutter Instrument Co.) set at pull strength = 1246 and heat index = 190.

2. Fill needles halfway with oil (polydimethylsiloxane, 20 centistokes, Petrarch Systems, Inc. #PS 039.5); leave vertical for at least 20 min to allow needle tips to fill.

3. Mix 5 μl of TROMA-1 IgG (20 mg/ml) with 1.25 μl of 4% rhodamine-conjugated dextran (RDX - Gimlich & Braun, *Dev. Biol.* 115: 340-352, 1986) and spin in microfuge for 10 minutes.

4. Fill a holding pipette (flame-polish with the De Fonbrune Series A #323 microforge to o.d. approx. 100 μm) with flushing medium I and place into microelectrode holder (W.P. Instruments, Inc. #MPH-310) attached to a Leitz micromanipulator; fill the remainder of an injection needle with oil and place into electrode holder of the other micromanipulator (needle holder filled with oil, while holding pipette holder is filled with media flush with oil interface; make sure there are no air bubbles anywhere i n the system).

5. Remove the chamber from a 2-chamber tissue culture slide (Lab-Tek #4802) and spread an 8 μl drop of flushing medium I in the center of one chamber; place a 1.5 μl drop of the TROMA-1/RDX solution next to the media drop and flood the chamber with mineral oil (Sigma #400-5).

6. Transfer 30-40 2-cell embryos into the media drop and place the slide on the stage of the Zeiss compound microscope equipped with epifluorescence optics, silicon intensified target (SIT) camera (Dage-MTI, Inc.), and an oil-filled pressure injection system (composed of Gilmont micrometer syringes (VWR #60381-037), Lancer Lab Bubble Tubing, and W.P. Instruments microelectrode holders).

7. Immerse both the needle and holding pipette into the media drop; at 200X magnification, lightly touch the needle to end of holding pipette (media should move into the needle).

8. Remove holding pipette from media drop and slightly raise the injection needle; move microscope stage so the antibody drop is in focus (make sure that the needle travels through the oil between drops - there is less chance of clogging versus traveling through the air); lower injection needle into antibody drop and fill the needle, watching the oil/antibody interface.

9. Raise filled needle slightly, move stage back to media drop, and lower both needle and holding pipette into drop.

10. At 200X magnification, align embryo on holding pipette with one cell above the other (condenser may have to be lowered to get adequate optics); using SIT camera and fluorescence, adjust pressure on injection needle such that the antibody solution is slowly flowing from the tip.

11. Move injection needle into cell relatively quickly - plasma membrane should rebound when it is pierced; inject antibody solution into cell, watching for cytoplasmic swirling and cell swelling; remove needle just as cell starts to swell.

12. Score for a successful injection by briefly viewing under fluorescence with the rhodamine filter (#BP 546), 50% neutral density filter, and the SIT camera.

13. Repeat process for second blastomere, then put injected embryo on opposite side of media drop as the uninjected embryos.

14. Repeat steps 10-13; when all of the antibody solution is expelled from an injection needle, change needles and repeat steps 7-9.

15. Place injected embryos and uninjected controls into separate 30 μl drops of equilibrated egg culture medium in 35 mm petri dish under oil; incubate at 37°C and 5% CO_2 for two days.

16. When embryos reach the late morula/early blasytocyst stage, transfer them to 30 μl drops of equilibrated Eagle's culture medium containing 10% FCS under oil; culture at 37°C and 5% CO_2 until embryos reach the blastocyst stage.

17. Remove from culture and process the blastocysts for double-label indirect immunfluorescence:
    a. Primary incubation = 1:100 A.P. biotin-conjugated goat anti-rat IgG (Zymed #62-9640, 0.75 mg/ml stock) + 1:40 anti-Endo B IgG (#1588, 3 mg/ml stock) in D-PBS + 3% BSA + 0.1% Tween 20; incubate in 30 μl drops in 35 mm petri dishes contained in glass petri dish with moist Whatman #1 filter circle in bottom at 37°C for 1 hour in humid chamber;
    b. Secondary incubation = 1:100 Texas Red-conjugated streptavidin (Zymed #43-4317, 0.5 mg/ml stock) + 1:40 A.P. FITC-conjugated goat anti-rabbit IgG (Cappel #1612-3151, 1 mg/ml stock) in D-PBS + BSA + Tween; incubate as above for 45-60 minutes;
    c. wash 4X with 0.2 ml of D-PBS + PVP, 10 min each;
    d. Tertiary labeling = 1:100 Hoechst (Bisbenzimid H 33258, Riedel-de Haën Ag, 0.5 mg/ml stock in EtOH) in D-PBS + PVP, 100 μl drops, 5 min at room temp.;
    e. wash 4X in 0.2 ml PBS + PVP, 2 min each, mount in small drop of mounting medium, and observe with a Zeiss compound microscope equipped with epifluorescence optics and a 100W DC mercury lamp.

18. Using the plan neofluor 40X objective, observe with FITC filter to examine the status of the cytokeratin filament network, with rhodamine filter to examine the distribution and state of the injected TROMA-1 IgG, and with Hoechst filter to determine the nuclear number.

IMMUNOBLOT QUANTITATION OF RAT IgG INJECTED INTO 2-CELL EMBRYOS*

(parts adapted from Ey & Ashman, *Meth. Enzymol.* **121**: 497-509, 1986)

1. After injection, wash embryos 3-4X in PBS + 3 mg/ml PVP and store at -80°C in 10-20 μl dH_2O + 0.5 mM PMSF.

2. Prepare lysates by thawing samples and freeze-thawing 3X in dry ice/acetone bath; add appropriate volume of 10X PBS, vortex, and spin briefly in microfuge.

3. To generate standard curve, prepare serial dilutions of Rat IgG in PBS + PMSF as follows:
   a. dilute Rat IgG (Cappel #6013-0080, 15 mg/ml) 1:1500 to 10 μg/ml;
   b. starting with the 10 μg/ml solution, make 10 serial doubling dilutions (final dilution = 0.0098 μg/ml);
   c. add 10 μl of each dilution (#1 = 100 ng, #11 = 0.098 ng, #12 = no IgG) to 10 μl uninjected embryo lysate (generate the standard curve with the same stage and approximately the same amount of embryo lysate as in the experimental samples; blastocysts and morulae contain relatively high, endogenous levels of alkaline phosphatase, and an alternative enzyme, such as horse radish peroxidase, should be used to analyze these stages.).
   d. vortex and spin briefly in microfuge.

4. Cut nitrocellulose paper (S&S #BA-85) to Hybriblot (BRL) size and wash 10 min with PBS.

5. Blot dry on Whatman #1 paper, place onto Hybriblot apparatus, and clamp down with vacuum on; wash wells 2X with 100 μl PBS + PMSF; release vacuum.

6. Load samples (standard curve in one row, experimental samples in other), making sure that the solution spreads evenly in bottom of each well (place 20 μl PBS + PMSF in any empty wells); let sit for 15 min, then apply vacuum and wash wells 2X with 100 μl PBS.

7. Unbolt apparatus, remove nitrocellulose, and let air dry for 1-2 min.

8. Wash 10 min with 20 ml PBS (all washes and incubations done at room temperature on a rotary shaker in covered microtiter lid).

9. Block unbound sites with 20 ml PBS + 3% Carnation non-fat dry milk, 30 min.

10. Incubate 2 hours with a 1:750 dilution (1 μg/ml) of affinity-purified biotin-conjugated goat anti-rat IgG (Zymed #62-9640) in PBS + milk (20 μl 0.75 mg/ml stock in 15 ml PBS + milk).

11. Wash 5X, 6 min each with 20 ml PBS.

12. Incubate 45 min with a 1:200 dilution of DETEK I-*alk* Signal Generating Complex (Enzo #EBP-822) (50 μl in 10 ml PBS + milk).

13. Wash 3X, 6 min each with 20 ml PBS; place nitrocellulose in clean microtiter lid and

wash 2X, 6 min each with 20 ml Pre-Detection Buffer.

14. Add Substrate Solution and let develop in the dark until suitable signal is reached; wash 4X with dH_2O, photograph (f4.5, 1/30), and dry between several sheets of Whatman #1 paper.

15. Scan blot with Bio Rad densitometer in reflectance mode, quantitate area of peaks with H-P integrator, plot standard curve, and determine experimental protein quantities.

SOLUTIONS

Buffer	*Final Concentration*	*Stock Conc.*	*Stock Amt.*
Pre-Detection Buffer (50 ml)	25 mM Tris-HCl, pH 7.5	100 mM	12.5 ml
	0.15 M NaCl	1 M	7.5 ml
	0.1 mM $MgCl_2$	1 M	5 µl
	0.4 µM $ZnCl_2$	1 mM	20 µl
	dH_2O	-	30 ml
Substrate Buffer (100 ml)	0.1 M Tris-HCl	-	1.21 g
	25 mM diethanolamine	9.324 M	0.269 ml
	0.1 M NaCl	1 M	10 ml
	2 mM $MgCl_2$	1 M	0.2 ml
	1 µM $ZnCl_2$	1 mM	0.1 ml
	dH_2O	-	89.4 ml
		pH to 9.55 with conc. HCl	

BCIP Stock 40 mg/ml 5-Bromo-4-chloro-3-indolyl phosphate (Sigma #B-8503) in dimethyl formamide (store in dark glass bottle, 4°C, make fresh every 4-6 weeks)

Phenazine Methosulfate 2 mg/ml in dH_2O (make up fresh in dark glass vial)

Substrate Solution
3.3 mg Nitroblue Tetrazolium
10 ml Substrate Buffer
67 µl Phenazine Methosulfate
34 µl BCIP Stock

*This method may be adapted for any protein for which there is an antibody or for any enzyme which can be detected with an insoluble substrate.

BRODART CAT. NO. 23 012 PRINTED IN U.S.A.